WWW.OEAW.AC.AT

ÖAW ÖSTERREICHISCHE AKADEMIE DER WISSENSCHAFTEN

50+

ANNUAL REPORT 2022

IWF INSTITUT FÜR WELTRAUMFORSCHUNG

WWW.OEAW.AC.AT/IWF

COVER IMAGE

Logo of IWF's 50th anniversary.

TABLE OF CONTENTS

THE DIRECTOR'S PAGE 2022

2022 held many achievements and highlights based on hard work, perseverance and collegiality at our institute. The following pages record the activities of the Space Research Institute (Institut für Weltraumforschung, IWF) of the Austrian Academy of Sciences (OeAW) during this year.

Scientifically, the IWF placed "Nature" papers based on *BepiColombo* instrument data and on the super-hot exoplanet KELT-9b. The IWF's total h-index is 93, that of 2022 is 12. The distribution of citations shows how well our research is recognized within the solar system community as well as in the astrophysics / exoplanet community. From our space instrumentation and technology groups, two flight models were delivered to China and a Satellite Laser Ranging (SLR) station in Tenerife based on IWF SLR technology joined the International Laser Ranging Service. Our *JUICE* contributions passed all tests, ready for launch in April 2023. Despite all challenges of the past two years, all instrument developments for *SMILE*, *PLATO*, *Comet Interceptor* are well on schedule.

On 28 June 2022, guests including the Nobel Price 2022 winner Prof. Anton Zeilinger in his then capacity of the OeAW president, the Rectors and Vice-Rectors of the Graz University of Technology and the University of Graz, Prof. Harald Kainz, Prof. Peter Riedler and Prof. Horst Bischof as well as the Graz Mayor Elke Kahr and Austrian and Styrian government representatives showed their appreciation for the achievements of the IWF by joining the IWF's 50th anniversary celebration. Part of the celebration was the inauguration of the Young Researcher Program in Interdisciplinary Space Science and Planetary Research, YRP@Graz. The PhD pillar of the program is rooted in the collaboration between the local universities and the IWF. Later in the year, we had the honor to welcome Minister Martin Polaschek and the new OeAW President Heinz Faßmann at the IWF.

Prof. Anton Zeilinger won the Physics Nobel Prize 2022, which is given with the universal ambition to serve the benefit of humankind. This is a strong support for fundamental research in general, and hence, for research as we conduct it at the IWF in tandem with dedicated technology development. Prof. Zeilinger shared the stage in Stockholm with Prof. Reinhard Genzel, member of the OeAW's Research Board, who received the 2020 Nobel Prize in Physics. Prof. Zeilinger's Nobel Prize lecture held some heureka moments for our SLR colleagues who found their names rightfully listed as contributors!

IWF Director Prof. Dr. Christiane Helling (© OeAW/IWF/Scherr).

Not all is happiness, and the institute in particular moans the far too early loss of Christian Hagen, a highly valued member and friend from our Magnetometer group. With great respect we bid our final farewell to the late Peter Pesec who was instrumental for the planning of our SLR station at the Lustbühel Observatory and who developed the Austrian GPS Geodynamics Network, amongst other pioneering projects. A great worry for many is also the war that yet again has reached European soil. The European Union, one of the biggest research funders, has its roots in the desire to prevent such sufferings. Members of the IWF hold or are part of EU-funded large-scale projects: the Marie Curie Innovative Training Network for European Joint Doctorates CHAMELEON, the Twinning project ExoHost, and the CoPhyLab. Space research has always facilitated international collaborations and it requires to see beyond cultural differences. The IWF itself has members of 20 different nationalities.

Space research requires and inspires. The IWF is therefore very active in its outreach in order to share our knowledge with the wider public. One example is the anniversary exhibition MISSION POSSIBLE!, which was visited by more than 15,000 people. Since the end of 2022, the comic drawn by Chris Scheuer for this exhibition decorates our institute's atrium over a length of six meters and attracts admiring glances.

With the best of wishes,

Christiane Helling

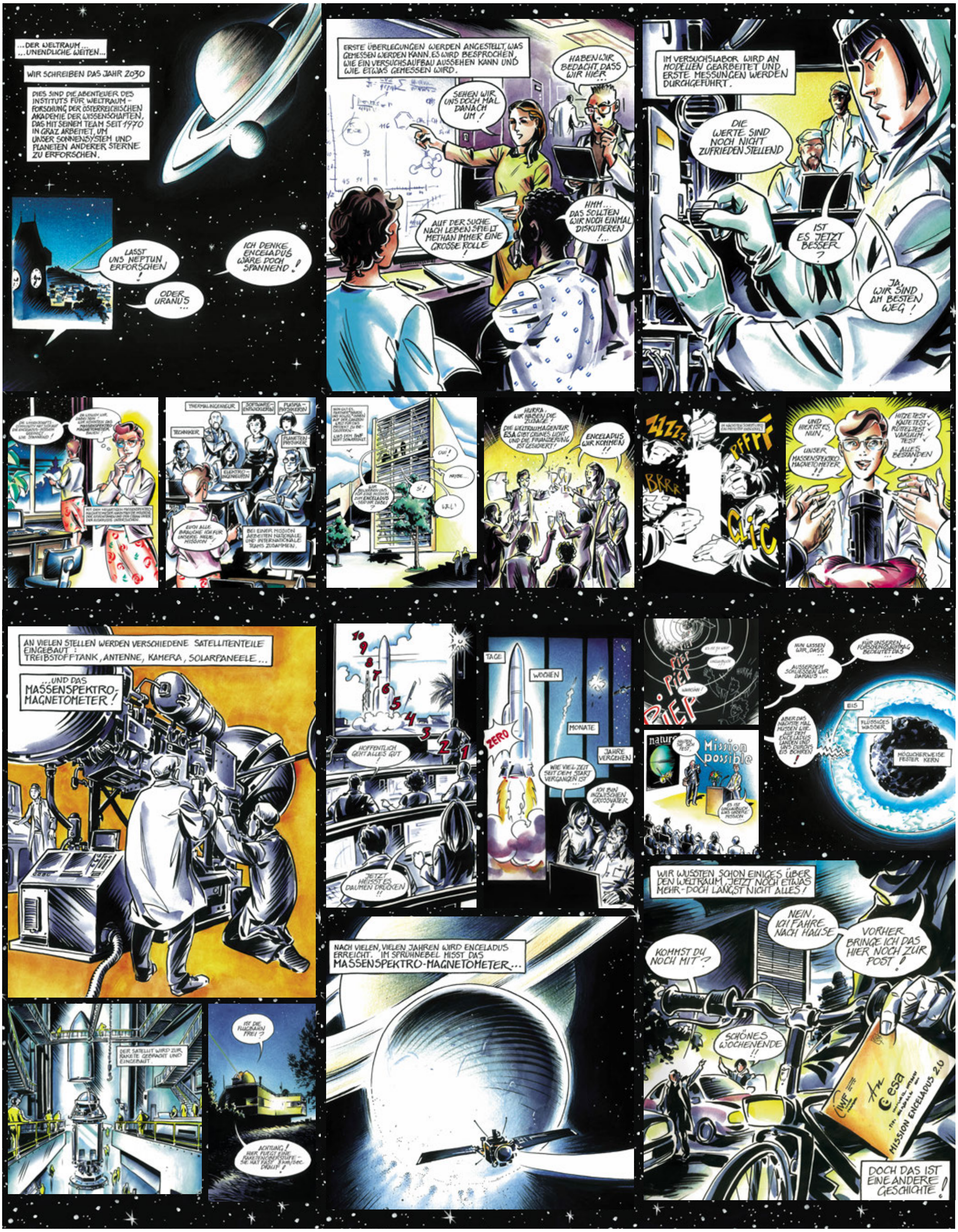

This comic tells the story of the development of a space mission. It was drawn by the Graz artist Chris Scheuer as part of the special exhibition MISSION POSSIBLE!, developed and curated by the Graz Children's Museum FRida & freD for the IWF's 50th anniversary.

INTRODUCTION

The Space Research Institute in Graz focuses on the physics of our solar system and the diversity of exoplanets. With about 100 staff members from 20 nations it is one of the largest institutes of the Austrian Academy of Sciences (Österreichische Akademie der Wissenschaften, OeAW).

The IWF develops and builds space-qualified instruments and analyzes and interprets the data returned by the space missions. Its core engineering expertise is in building magnetometers and on-board computers, as well as in satellite laser ranging, which is performed at a station operated by the IWF at the Lustbühel Observatory. In terms of science, the institute concentrates on the physics of solar and extrasolar planets, planet-forming disks, and space plasmas.

The IWF cooperates closely with international space agencies and with numerous other national and international research institutions. Tight cooperations exist with the European Space Agency (ESA).

In 2022, the IWF was involved in 23 active and future international space missions; among these:

- The *Cluster* mission continues to provide unique data to better understand plasma processes in near-Earth space.
- The four *Magnetospheric MulitScale (MMS)*spacecraft perform multi-point measurements to study the dynamics of the Earth's magnetosphere.
- The first *China Seismo-Electromagnetic Satellite (CSES-1)* is studying the Earth's ionosphere. *CSES-2* will follow in 2023.
- On the halfway point of the journey to its destination, *BepiColombo* had its second Mercury flyby in June.
- *CHEOPS (CHaracterizing ExOPlanets Satellite)* continued nominal science operations, characterizing exoplanets around bright stars.
- ESA's *Solar Orbiter* saw a giant solar eruption in February, was hit by a CME before its third Venus flyby in September and approached the Sun in October at a distance of about 0.29 AU.
- The NASA CubeSat *CUTE (Colorado Ultraviolet Transit Experiment)* delivered its first science data.
- ESA's *JUpiter ICy moons Explorer (JUICE*, launch: April 2023) will investigate Jupiter and three of its largest moons, Ganymede, Callisto, and Europa.
- *SMILE* (launch: 2025) is designed to study the interaction between the solar wind and Earth's magnetosphere.

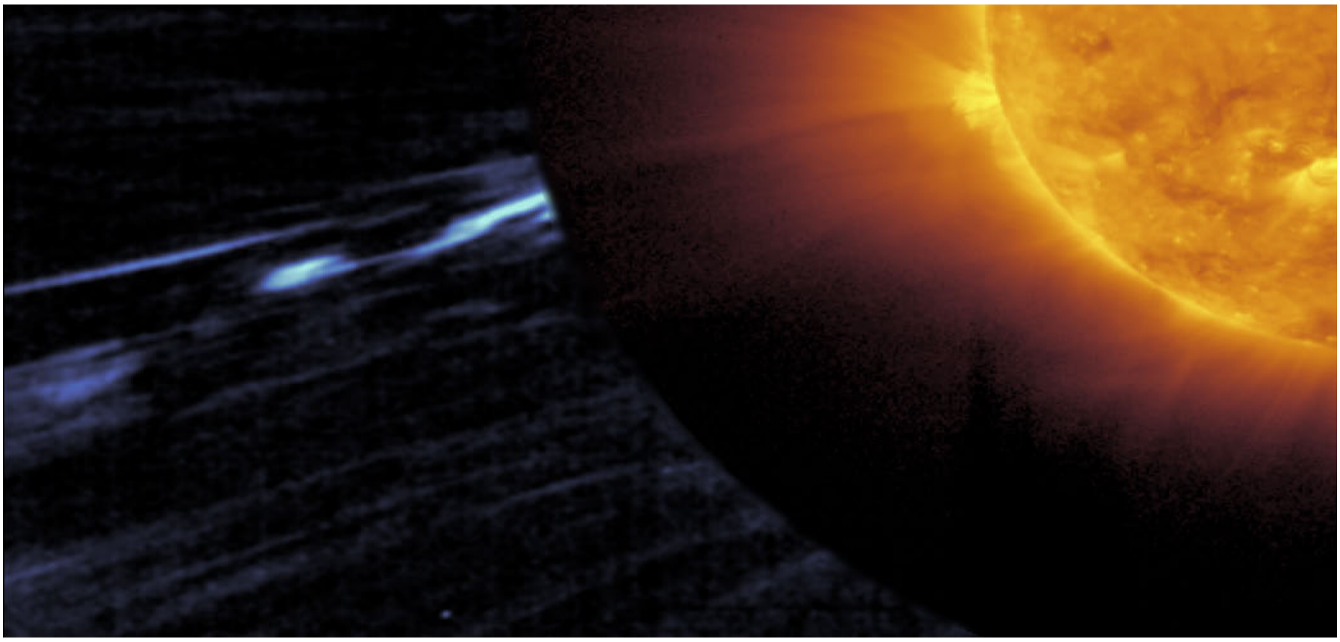

A magnetic phenomenon known as solar switchbacks has been imaged by the *Solar Orbiter* spacecraft for the first time. The image zooms in on the switchback (blue/white feature extending towards the left) as captured in the solar corona by the *Metis* instrument on 25 March 2022. The switchback appears to be linked to the active region seen in the central *Extreme Ultraviolet Imager* image (right; © ESA & NASA/*Solar Orbiter*/*EUI* & *Metis* Teams and D. Telloni et al., 2022).

- The *FORESAIL-2* (launch: 2025) CubeSat will characterize the variability of ultra-low frequency waves in the inner magnetosphere.
- *PLATO* (launch: 2026) is a space-based observatory to search for planets orbiting alien stars.
- *HelioSwarm* (launch: 2028) was selected as NASA's new Medium-Class Explorers (MIDEX) mission in February 2022. The multi-satellite mission will help to better understand the interaction between the solar wind and Earth.
- *Comet Interceptor* (launch: 2029) will characterize in detail, for the first time, a dynamically-new comet or interstellar object.

HIGHLIGHTS IN 2022

- In "Physics of Plasmas" K. Blasl et al. presented the first kinetic scale observations of the Kelvin-Helmholtz instability under southward interplanetary magnetic field conditions using high-resolution *MMS* data. These observations were complemented by fully kinetic Particle-In-Cell simulations and have led to the detection of space plasma processes such as magnetic reconnection and wave instabilities at different temporal and spatial scales.
- In the "Journal of Geophysical Research: Planets" D. Schmid et al. shared findings about the tenuous exosphere surrounding Mercury. Through on-site detection of plasma waves by magnetic field measurements it was possible to obtain the hydrogen density profile at various altitudes around the planet. This new information has provided valuable insights into the complex dynamics of Mercury's exosphere and contributed to our understanding of the physical processes in the inner solar system.
- In "Nature Astronomy" F. Borsa et al. reported the results of observations carried out with the CARMENES high-resolution spectrograph that have led to the detection of neutral oxygen in the atmosphere of the ultra-hot Jupiter KELT-9b. This detection has been guided by new models produced by members of the institute and opened a new way to detect oxygen in exoplanetary atmospheres.
- In "Astronomy & Astrophysics" D. Kubyshkina and L. Fossati presented the results of atmospheric evolution modeling for planets in the 1-108 $M_{\oplus}$ mass range and its further comparison with the mass-radius distribution of the currently known exoplanets. The predictions reproduced the observed mass-radius distribution well. The simulations led to the conclusion that the observed characteristics of low-mass planets (≤10-15 $M_{\oplus}$) strongly depend on the impact of atmospheric mass loss, while the parameters at formation play the dominant role for more massive planets.
- In "Astronomy & Astrophysics" P. Woitke et al. presented a model for vertical turbulent mixing in thermo-chemical models for planet-forming disks. It was shown that vertical mixing enriches the mixture of ions, atoms, molecules and ice species which creates a more active chemistry and opens new chemical pathways. Icy grains were shown to reach the visible disc surface where they cause mid-IR ice emission features that will be observable with the *James Webb Space Telescope.*

THE YEAR 2022 IN NUMBERS

Members of the institute published 158 papers in refereed international journals, of which 32 were first author publications. During the same period, articles with authors from the institute were cited 8163 times in the international literature. In addition, 89 talks (18 invited) and 37 posters were presented by IWF members at international conferences. Institute members were involved in the organization of 15 international meetings, e.g. EGU General Assembly, EPSC, the 22nd International Workshop on Laser Ranging (ILRS), European Astrobiology Institute (EAI) Academy, and the CHAMELEON Network Retreat.

IWF STRUCTURE AND FUNDING

The institute is led by Christiane Helling, who simultaneously holds a university professorship in space science at the Graz University of Technology. In April, Luca Fossati followed Werner Magnes as Deputy Director.

The IWF hosts eight research groups:

- Exoplanet Weather and Climate
  (Lead: Christiane Helling)
- Exoplanet Characterization and Evolution
  (Lead: Luca Fossati)
- Planet-Forming Disks and Astrochemistry
  (Lead: Peter Woitke)
- Solar System Planetary Physics
  (Lead: Helmut Lammer)
- Space Plasma Physics
  (Lead: Rumi Nakamura)
- On-Board Computers
  (Lead: Manfred Steller)
- Space Magnetometers
  (Lead: Werner Magnes)
- Satellite Laser Ranging
  (Lead: Michael Steindorfer)

The IWF is mainly financed by the OeAW and to a lesser extent through competitive grants from the Austrian Research Promotion Agency (FFG), the Austrian Science Fund (FWF), the European Union, and ESA.

NEAR-EARTH SPACE

Near-Earth space is a natural plasma laboratory with different types of boundaries and regions that are created as a consequence of the interaction between the solar wind and the Earth's intrinsic magnetic field and plasmas. It allows us to study fundamental plasma physical processes such as acceleration or heating as well as geo/planetary sciences, i.e., how the Sun and solar wind affect the Earth/planetary plasma environment, called, in a more general term, space weather phenomena. The IWF has been participating in a number of near-Earth space missions from the planning and proposal phase, to the development and building of new hardware and finally the operation and calibration of the instruments. Data taken from these missions have been extensively analyzed at the IWF by applying different methods and by theoretical modeling to compare with the observations.

Among the different space plasma missions, the *Magnetospheric MultiScale (MMS)* mission is designed to study the Earth's magnetosphere on the electron scales with high-cadence multi-point measurements. This year new studies on the Kelvin-Helmholtz instability (KHI), which is an important instability to explain the solar wind plasma entry process at the flank of the magnetosphere, have been reported. By combining the detailed particle and electric and magnetic field observations from *MMS* and an advanced computer simulation, these studies succeeded to show the structures and the evolution of secondary instabilities within the K-H waves that lead to deformations of the vortices and mixing of the plasma across the boundary layer. These studies highlighted the importance of multi-scale and multi-processes that take place within the KHI and the complex nature of the interaction processes between the solar wind and the Earth/planetary magnetosphere.

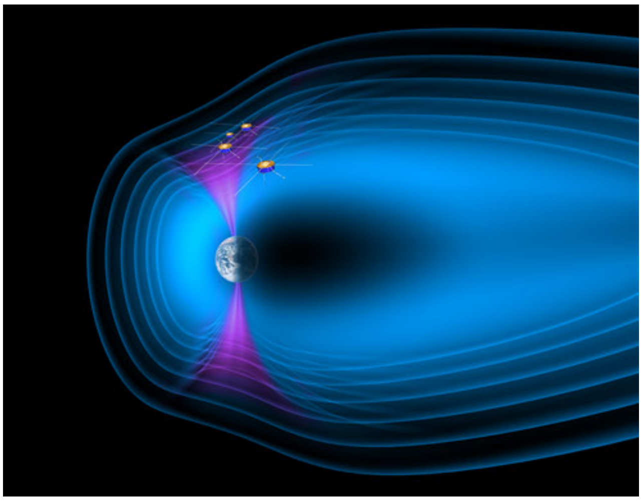

CLUSTER

ESA's *Cluster* mission is designed to study different plasma processes due to the interaction between the solar wind and the Earth's magnetosphere. *Cluster*, launched in July and August 2000, is the first four-spacecraft mission that can differentiate between temporal and spatial changes of the different plasma processes. Request from the scientific community for the *Cluster* mission extension during the time interval 2023-2025 has been submitted. The IWF is Principal and/or Co-Investigator (PI/Co-I) on five instruments and has contributed to data archiving activities at the *Cluster Science Archives (CSA)* in addition to the science data analysis.

Celebrating the successful 22 years in space, the *Cluster* 22nd Anniversary Symposium was held at the European Space Operations Centre (ESOC) in early November. The talks covered not only the newest scientific results, but also comprehensive reviews on the missions, instruments and science relevant to *Cluster*. Several IWF members gave invited talks at the symposium.

MMS

NASA's *Magnetospheric Multi-Scale (MMS)* mission, launched in 2015, explores the dynamics of the Earth's magnetosphere and its underlying energy transfer processes. Four identically equipped spacecraft carry out highest temporal and spatial measurements in the Earth's magnetosphere. *MMS* investigates the small-scale basic plasma processes, which transport, accelerate and energize plasmas in thin boundary and current layers. Extension of *MMS* until 2025 is under discussion.

The IWF has taken the lead for the *Active Spacecraft POtential Control (ASPOC)* of the satellites and is participating in the *Electron Drift Instrument (EDI)* and the *Digital FluxGate magnetometer (DFG)*. In addition to the operation of these instruments and the scientific data analysis, the IWF is contributing to inflight calibration activities and also deriving a new data product such as the density determined from the controlled spacecraft potential.

Artist's impression of the four *Cluster* spacecraft crossing the northern cusp of Earth's magnetosphere (© ESA/AOES Medialab).

THEMIS/ARTEMIS

NASA's five-spacecraft mission *THEMIS (Time History of Events and Macroscale Interactions during Substorms)*, was launched in 2007. In 2010, the two outer spacecraft were sent to an orbit around the Moon and renamed *ARTEMIS (Acceleration, Reconnection, Turbulence and Electrodynamics MISsion)*. The inner three probes remained in their near-Earth orbits.

THEMIS studies dynamical processes, such as substorms, that cause aurora and different plasma processes in the magnetosphere and solar wind up to lunar distance. An extension of both missions until 2025 is under discussion. As Co-I of the magnetometer, the IWF is participating in processing and analyzing data.

GEO-KOMPSAT-2A

GEO-KOMPSAT-2A (GEOstationary KOrea Multi-Purpose SATellite-2A) is a South Korean meteorological and environmental satellite in geostationary orbit at 128.2° East, which also hosts a space weather environment monitoring system. The Korean Meteorological Administration managed the implementation of the satellite, launched in 2018, and the necessary ground segment. The space weather observations aboard *GEO-KOMPSAT-2A* are performed by the Korean Space Environment Monitor (KSEM), which was developed under the lead of the Kyung Hee University. It consists of a set of particle detectors, a charging monitor and a four-sensor *Service Oriented Spacecraft MAGnetometer (SOSMAG)*.

The *SOSMAG* development was initiated and conducted by ESA as part of the Space Situational Awareness program and built by the *SOSMAG* consortium: IWF, Magson GmbH, Technische Universität Braunschweig, and Imperial College London. The *SOSMAG* instrument is a "ready-to-use" magnetometer avoiding the need of imposing magnetic cleanliness requirements onto the hosting spacecraft. This is achieved through the use of two high quality fluxgate sensors on a one-meter-long boom and two additional magneto-resistive sensors mounted within the spacecraft body. The measurements of the two inner-spacecraft sensors together with the inner boom sensor enable an automated correction of the outer boom sensor measurement for the dynamic stray fields from the spacecraft.

Flight data verification, in-flight calibration and operation support were continued also during the fourth year of operation. In addition, a concept for a further improved data cleaning was elaborated and proposed to ESA. It includes the correction of temperature induced offset drifts of the fluxgate sensors which face a temperature change of more than 100°C every 24 hours.

SOSMAG data are publicly available via the Space Weather Service Network of ESA's Space Safety program at swe.ssa.esa.int.

CSES

The *China Seismo-Electromagnetic Satellites (CSES)* are scientific missions dedicated to investigate and monitor varying electromagnetic fields and waves as well as plasma parameters and particle fluxes in near-Earth space, which are induced by natural sources on ground like seismic and volcanic events.

After the successful launch of the first satellite *CSES-1* in February 2018, the second satellite *CSES-2* is scheduled for launch in the second half of 2023. It will be in the same Sun-synchronous circular low Earth orbit as *CSES-1*, with a local time of the descending node at 2 pm, but with a phase difference of 180 degrees. The combined observations of both satellites will double the detection probability of natural hazard-related events and will help to separate seismic from non-seismic events.

The *CSES* magnetometers, which are nearly identical on both spacecraft, have been developed in cooperation between the Chinese National Space Science Center (NSSC), the Institute of Experimental Physics of Graz University of Technology (TUG), and the IWF. NSSC is responsible for the dual sensor fluxgate magnetometer, the instrument processor and the power supply unit, while the IWF and TUG participate with the newly developed absolute scalar magnetometer, called *Coupled Dark State Magnetometer (CDSM).*

In 2022, the testing of the flight instrument for *CSES-2* was completed in Austria and it was subsequently delivered to China. Remote support for a successful integration and testing of the *CDSM* with the Chinese magnetometer hardware took place throughout the year.

Like in the years before, the magnetometer sensors of *CSES-1* operated continuously in good health. Based on a cross comparison analysis between the *CDSM* of *CSES-1* and the *Absolute Scalar Magnetometer (ASM)* of the *Swarm Alpha* and *Bravo* satellites it has been possible to demonstrate that the *CDSM* has maintained long-term stability and accuracy.

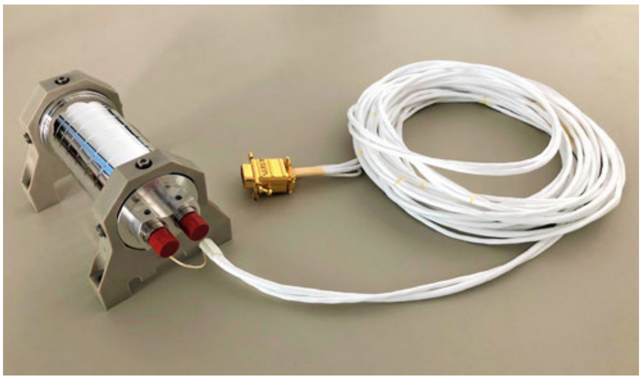

CDSM flight model sensor for *CSES-2* (© OeAW/IWF).

FORESAIL-2

FORESAIL is a CubeSat program conducted by Aalto University in the frame of the Finnish Centre of Excellence in Research of Sustainable Space. *FORESAIL-1*, was launched in May 2022, but contact was lost after a short time of in-orbit operation. A replacement satellite, *FORESAIL-1-PRIME* is therefore planned to be launched in 2023. The construction and launch of this additional CubeSat delayed the plans for *FORESAIL-2*, which contains an IWF-provided magnetometer. This CubeSat is now planned for launch into geostationary transfer orbit (GTO) in 2025, although finding a CubeSat launch provider for this orbit turned out to be a challenge that is currently not resolved. The technology demonstration goal of this mission is to survive the harsh radiation of the Van Allen belts using low-cost components and a fault-tolerant software approach. In addition, a Coulomb-drag experiment shall demonstrate safe de-orbiting from orbits with high apogee.

The characterization of the variability of ultra-low frequency waves and their role in energizing particles in the inner magnetosphere are the core scientific objectives of *FORESAIL-2*. This shall be achieved by in-situ measurements of the magnetic field as well as relativistic electrons and protons.

In cooperation with the Institute of Electronics of Graz University of Technology, the IWF contributes a miniaturized magnetometer, which will be based on a newly developed microchip for the readout of the triaxial magnetic field sensor.

In 2022, the first prototype microchip was received from XFAB Silicon Foundries and extensively tested. The knowledge gained was incorporated into the design of the second prototype microchip, which was delivered to XFAB for production in October 2022. Furthermore, the development of an Engineering as well as an Interface-Verification Model of the *FORESAIL-2* magnetometer was continued.

MACAO SCIENCE SATELLITE

Macao Science Satellite 1 was initiated by the State Key Laboratory of Lunar and Planetary Science at the Macau University of Science and Technology and is being implemented with support from the China National Space Administration and the local government. It is the world's first and only scientific satellite to be placed in a near-equatorial orbit to study the geomagnetic field, and specifically the South Atlantic Anomaly, from space. The launch is scheduled for mid 2023.

The South Atlantic Anomaly is an area with a significantly weakened geomagnetic field and associated increased radiation activity. Its center lies over Brazil and its eastern coast. The inner of the two Van Allen radiation belts extends to about 700 kilometers from the Earth at the equator. In the region of the South Atlantic Anomaly, it comes much closer to Earth. Currently, this magnetic anomaly is increasing its spatial extension and the field strength is further decreasing. Together with ESA's *Swarm* mission, launched in 2013, it will be explored and measured in greater detail than ever before.

The scientific payload consists of a high-energy particle detector, a star tracker, a fluxgate magnetometer, and a scalar magnetometer. The sensor and sensor-related electronics of the scalar magnetometer are contributed by the IWF in cooperation with the Institute of Experimental Physics of Graz University of Technology. The flight instrument is a replica of the instrument for the *CSES-2* satellite. The development of the processor and power supply electronics for the scalar magnetometer as well as its overall integration and testing are carried out by the Harbin Institute of Technology, Shenzhen.

In 2022, the flight model of the scalar magnetometer was integrated with the Chinese magnetometer hardware followed by a set of environmental and calibration tests. In November 2002, the magnetometer was installed on the spacecraft.

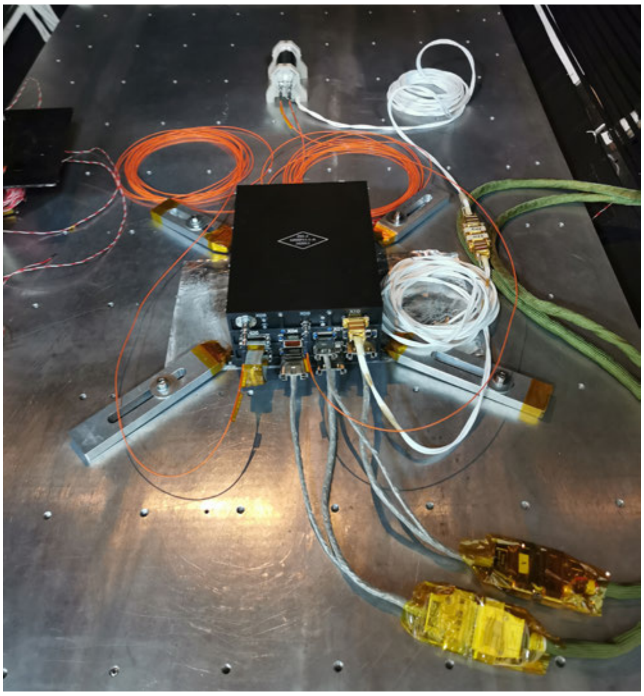

Flight model of the scalar magnetometer mounted in the thermal vacuum chamber of the National Space Science Center (NSSC) of the Chinese Academy of Sciences (© NSSC).

SMILE

The *Solar wind Magnetosphere Ionosphere Link Explorer (SMILE)* is a joint mission of ESA and the Chinese Academy of Sciences (CAS), scheduled for launch in 2025. It aims to complete our understanding of the Sun-Earth connection by measuring the solar wind and its dynamic interaction with the magnetosphere. The IWF participates in two instruments: the *Soft X-ray Imager (SXI)*, led by the University of Leicester, and the magnetometer *(MAG)*, led by CAS.

The institute, in close cooperation with international partners, contributes the instrument's control and power unit *EBox* for *SXI*. The IWF is coordinating the development and design of the Digital Processing Unit (DPU) and is responsible for the mechanical design and the tests at box level.

In addition to hardware activities, the IWF is participating in the preparation of the science working group activities such as modeling and in-situ measurements.

In 2022, the team concentrated on the qualification model of the DPU and the *EBox*. Extensive board level tests of the DPU were followed by the electrical integration of the power supply with the DPU and the radiation shutter electronics. In parallel the mechanical structure of the *EBox* was prepared for the installation of the electronics. The environmental tests have been completed with only minor issues, thus the model was delivered to University of Leicester in Q3 2022. In addition to the hardware activities, the thermal and structural analysis has been updated in accordance with results from the environmental tests. Finally, the manufacturing of the components for the flight model has been initiated. The delivery of the flight model is planned for Q3 2023.

Qualification model of the *SMILE SXI EBox* (© OeAW/IWF/Steller).

SPACE WEATHER FOLLOW-ON

The *Space Weather Follow-On (SWFO)* mission is a joint undertaking by NASA and the National Oceanic and Atmospheric Administration (NOAA). The satellite will collect solar wind data and coronal imagery to support NOAA's mission to monitor and forecast space weather events.

The *SWFO* satellite will orbit the Sun at approximately 1.5 million kilometers from Earth in Lagrange point L1. At this point the gravitational and centrifugal forces of Sun and Earth balance each other, which makes it an ideal place for observing the Sun.

The Southwest Research Institute together with two sub-contractors at the University of New Hampshire, Durham, and the IWF design, develop, integrate, and calibrate the magnetometer instrument *SWFO-MAG*. It includes two three-axis magnetometers and associated electronics to measure the vector of the interplanetary magnetic field. The IWF has the lead for the Sensor Controller Board, which hosts the front-end electronics for the two fluxgate sensors. A microchip, which has originally been developed for the *Magnetospheric Multi-Scale* mission, is the central component of the front-end electronics.

The main activities at the IWF in 2022 included the completion of the parts engineering, the finalization of the layout for the sensor controller board, and the start-up, testing and pre-calibration of the flight model.

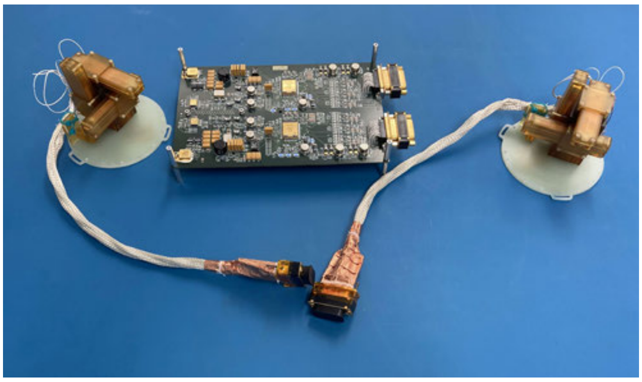

Flight model of *SWFO-MAG* with the two fluxgate sensors and the sensor control board (© OeAW/IWF/Valavanoglou).

HELIOSWARM

HelioSwarm is NASA's new Medium-Class Explorers (MIDEX) mission to be launched in 2028. The IWF is a member of the science team contributing to the multi-point analysis. *HelioSwarm* consists of nine spacecraft (1 hub and 8 nodes). The *HelioSwarm* constellation makes multipoint measurements of magnetic fields, density and velocity as well as single point measurements of the velocity distribution function. The instruments on board consist of fluxgate and search coil magnetometers, Faraday Cups and an ion electrostatic analyzer.

MULTI-SCALE EVOLUTION OF THE MAGNETOPAUSE KELVIN-HELMHOLTZ WAVES DURING SOUTHWARD IMF

When the fast-flowing solar wind encounters the magnetic obstacle of Earth's magnetosphere, it is deflected and streams around the boundary layer called the magnetopause. The large velocity shear between this fast-flowing plasma and the relatively stagnant magnetosphere can lead to indentations in the magnetopause forming wavy structures. These surface waves can develop into large-scale vortices that can effectively transport solar wind plasma into the magnetosphere when they decay. Previous numerical simulations suggested that this process involves multiple scales, eventually down to the electron scale.

This study reports the first observations of the Kelvin-Helmholtz instability (KHI) during southward interplanetary magnetic field (IMF) conditions from *MMS* data on the dusk flank of Earth's magnetopause. This instability is studied using high-resolution data on the electron scales for the first time. The results showed irregular structures and the multi-scale evolution of secondary instabilities, leading to deformations of the vortices, and mixing across the boundary layer, highlighting the importance of a multi-scale and multi-process approach in the study of the KHI.

Blasl et al., Phys. Plasmas, 29, 012105, 2022.

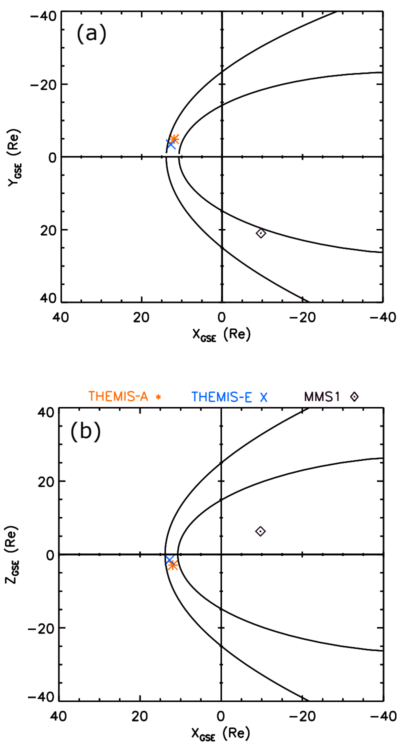

Locations of *THEMIS-A*, *THEMIS-E* and *MMS1* spacecraft at the time of observations of the KHI during southward IMF. The *MMS* spacecraft was located on the dusk flank (a) of the Earth's magnetopause, while the *THEMIS* spacecraft observed the deflected solar wind near the equator (a, b), enabling multi-point measurements and a relation between these observations.

These findings were further studied using numerical simulations of the *MMS* event. Considering the observations made during this event, the simulation setup closely followed the plasma parameters and magnetic field configuration during this time interval. Indeed, the simulations showed how instabilities grow from the linear stage of KHI (a) and predicted similar plasma and magnetic field signatures as were observed by the *MMS* spacecraft crossing the KHI structure (b). Furthermore, the 2D and 3D fully kinetic PIC simulations showed the evolution of secondary instabilities as observed in in-situ data leading to a multi-scale character and irregular structures. Southward IMF conditions might be unique to the strong evolution of these secondary instabilities due to the magnetic field configuration across the boundary layer. This might explain the much lower observational probability of the KHI during these periods and enable future multi-scale and multi-process studies of the KHI at Earth's magnetopause.

Nakamura T.K.M. et al., Phys. Plasmas, 29, 012901, 2022.

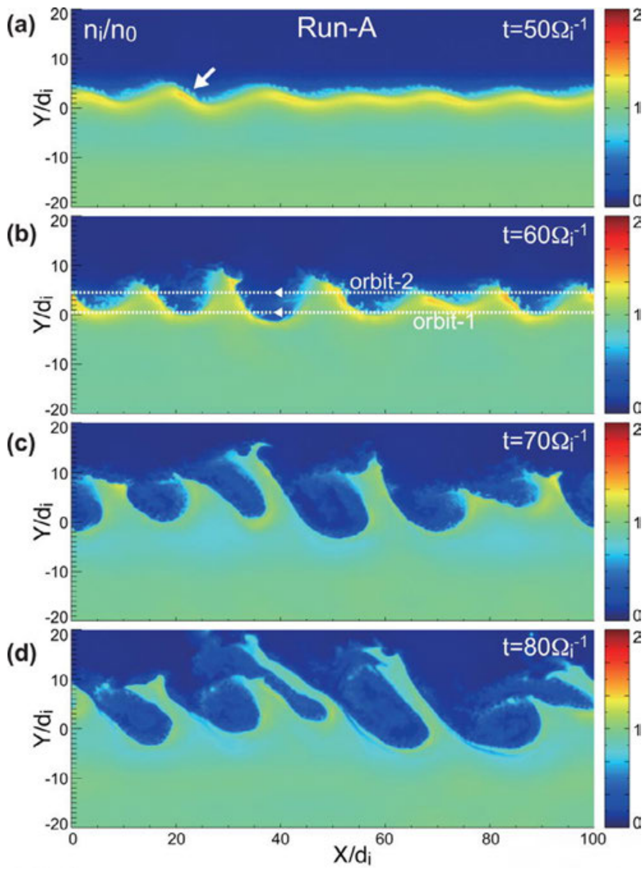

Color contours of ion density for different time steps of the numerical simulations studying the development of the KHI during the *MMS* observations. The KH waves develop into irregular structures due to the effect of secondary instabilities on their evolution. Plasma mixing can be observed along the boundary layer indicated by the white arrow in panel (a).

E-FIELD FLUCTUATIONS AROUND THE LOWER-HYBRID FREQUENCY AT DIPOLARIZATION FRONTS

Dipolarization fronts (DFs) are thin magnetic boundary structures, embedded in short-duration, fast earthward-moving plasma flows, so-called bursty bulk flows. Due to the density gradient present across the front, the lower-hybrid drift instability (LHDI) and resulting kinetic-scale waves can be excited. These waves feature strong electric field fluctuations and associated particle acceleration/heating. Electric field fluctuations in the lower-hybrid (LH) frequency range are statistically examined, using data from the *MMS* mission during 2017 and 2018 when its apogee was in the magnetotail.

All electric field fluctuations in this frequency range perpendicular to the background magnetic field exhibited enhanced power, varying by several orders of magnitude. Although the correlation between the absolute values of the density gradient and the power of the E-field fluctuations is weak, the peak in power mostly occurs at the same time when also the density gradient is the steepest. The results also reveal that the wave power correlates with the magnetic flux transport rate of the DFs; when the large flux transport is responsible for the particle pileup ahead of the DF, strong LHDI-related waves can be excited, which in turn modify the original gradient layer in the course of its propagation.

Hosner et al., Phys. Plasmas, 29, 012111, 2022.

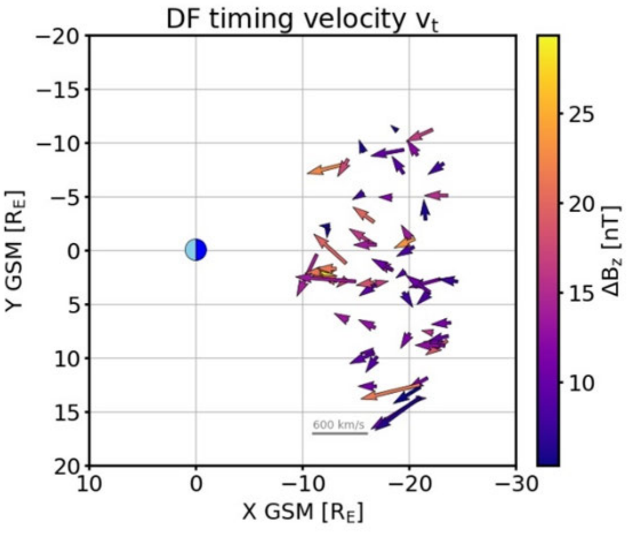

An overview of the 61 DF events in the Earth's magnetotail, examined in this study. The figure shows the X/Y plane in Geocentric Solar Magnetospheric (GSM) coordinates. The arrows represent the DFs propagation direction, with the length as their respective propagation velocity. The color shows the increase of the northward magnetic field component ΔB_z across the DF.

WAVELENGTH ESTIMATION IN SPACE PLASMA OBSERVATIONS

The wave telescope technique is an analysis method based on the adaptive filter theory, and provides a powerful algorithm to determine the wavelengths and propagation directions from the multi-spacecraft data without any assumption of wave modes or plasma model a priori. This technique has been improved and extensively documented by making use of the noise property in the data, studying the sensitivity in the long and short wavelength limit. Unambiguous determination of wavelengths and propagation directions is rare in experimental space plasma physics. Single spacecraft data are obtained as time series along the trajectory, and the frequency information (time variation) and the wavelength information (spatial structure) are mixed here. Even combining various data sets such as electric and magnetic field, one still has to assume certain wave properties (wave modes or number of discrete waves) expected from plasma theory to determine the wavelength. Observations using multiple spacecraft are being applied to various regions of near-Earth space to overcome the problem of identifying the spatial structure from time series data. The technique has successfully been applied to the *Cluster* and *MMS* missions, and is expected to play a leading role in the upcoming *HelioSwarm* mission.

Narita et al., J. Geophys. Res., 127, e2021JA030165, 2022.

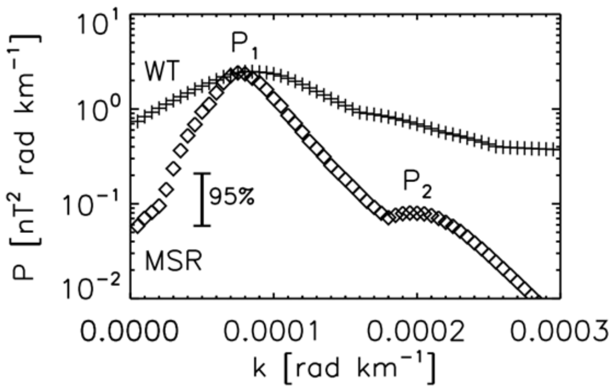

Wavenumber spectrum from the *Cluster* data in the solar wind evaluated by the conventional method with minimum variance projection (WT) and that by the improved method with noise-separating projection (MSR). The latter method is highly sensitive and can detect a wave of smaller power.

MAGNETOTAIL ION STRUCTURING BY KINETIC BALLOONING-INTERCHANGE INSTABILITIES

Ballooning-interchange (BI) heads are fundamental dynamic objects in Earth's nightside magnetosphere, which represent magnetic structures that are similar in shape to atmospheric mushroom clouds resulting from a sudden formation of a volume of lower-density gases. The heads appear in series and drive geomagnetic east-west oriented aurora, which glows like a pearl necklace across the night sky. By combining three-probe *THEMIS* observations and 3-D Particle-in-Cell simulations, key structures on the ion gyroradius scale are identified that occur in connection with ballooning-interchange instability heads in the Earth's magnetotail. The mesoscale structures occur at sites of strong ion velocity shear and vorticity where the thermal ion Larmor radius is about half the width of the head. Magnetospheric ions appear to sense the heads and modify their circular paths perpendicular to the magnetospheric magnetic field, because their gyration radii are on the order of the head's size. Such a modification of the ion motion appears to lead to ion redistribution on the two sides of the head according to the ion energy. Finer structures occur at smaller scales characterizing the wavelength of the electromagnetic ion cyclotron waves generated at the heads. Together with the finer ion structuring, which occurs along the magnetic field lines, these two processes act to erode and thin the current sheet, thereby forming a local magnetotail configuration that is favorable for reconnection, which may lead to severe magnetospheric disturbances and prolonged bright aurora.

Panov et al., Geophys. Res. Lett., 49, e2021GL096796, 2022.

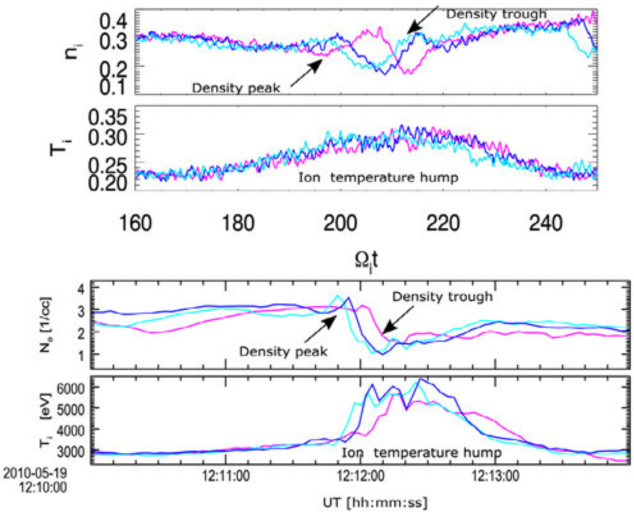

Interplay of different processes during later stage of development of a BI head in 3D PIC simulations and *THEMIS* observations. Top: Ion density and temperature observations by three virtual spacecraft. Bottom: *THEMIS* observations with a similar three-point constellation.

THE KINETIC ALFVÉN-LIKE NATURE OF TURBULENT FLUCTUATIONS IN THE EARTH'S MAGNETOSHEATH

Identifying the nature and the properties of turbulent fluctuations in the Earth's magnetosheath is key to understanding energy transfer and conversion. A new method was used to identify the properties of fluctuations in Earth's magnetosheath with NASA's *MMS* mission. Electron and ion Alfvén ratios were calculated to identify the type of fluctuations present. These are the ratios of the velocity fluctuations to the magnetic fluctuations (normalized to velocity units). The exceptional time resolution of the Fast Plasma Investigation's velocity measurement (0.15 s for ions and 0.03 s for electrons) allows the calculations of these ratios down to kinetic scales.

The Alfvén ratios were calculated for both ion and electron velocities and compared to the theoretical predictions for both kinetic Alfvén waves. The comparison is shown in the figure below. Both ion and electron velocities were found to be consistent with the linear predictions of kinetic Alfvén waves. Furthermore, several other analysis methods were used to confirm the kinetic Alfvén wave nature of the fluctuations. The wave telescope method was used to measure the dispersion relation diagram. The cross-correlation spectra of the magnetic field magnitude and electron data were also calculated, all reinforcing the Alfvén ratio method.

Roberts et al., Phys. Plasmas, 29, 012308, 2022.

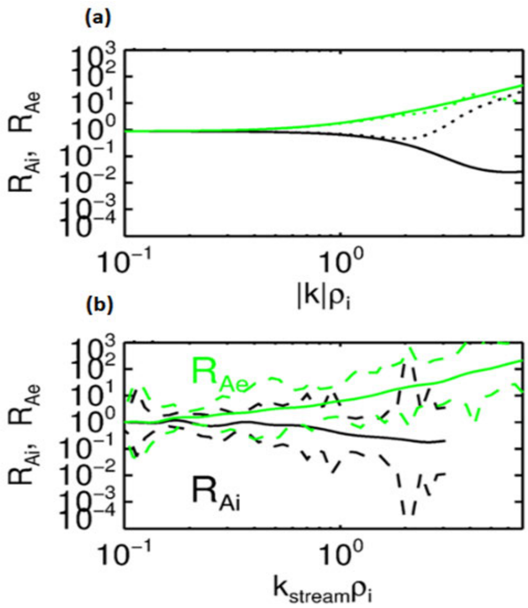

(a) Theoretical prediction of Alfvén ratios for the kinetic Alfvén wave, for ion velocities at 80 (black, dotted) and 89 degrees (black, solid) propagation angles; electrons (green). (b) Measured *MMS* data for the ion velocity (black) and electrons (green). Dashed lines indicate the error.

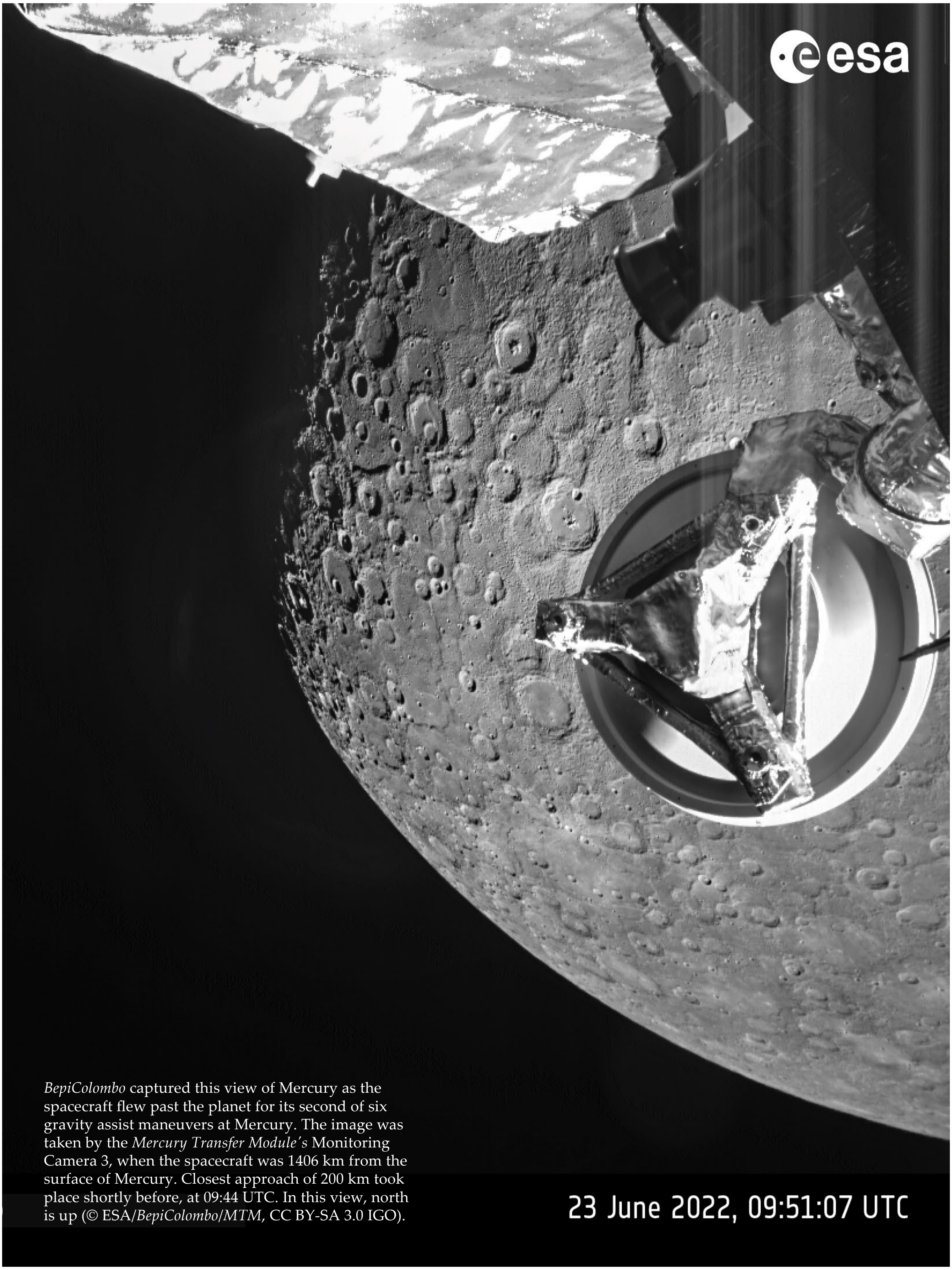

BepiColombo captured this view of Mercury as the spacecraft flew past the planet for its second of six gravity assist maneuvers at Mercury. The image was taken by the *Mercury Transfer Module's* Monitoring Camera 3, when the spacecraft was 1406 km from the surface of Mercury. Closest approach of 200 km took place shortly before, at 09:44 UTC. In this view, north is up (© ESA/*BepiColombo*/*MTM*, CC BY-SA 3.0 IGO).

SOLAR SYSTEM

The IWF is involved in several international space missions and experiments that address solar system phenomena, planetary environments and related data analysis. Solar physics and the solar wind, its interaction with the magnetospheres, upper atmospheres or surfaces of solar system planets and bodies are studied. Moreover, theoretical studies related to comparative planetology, habitability and space plasma physics between solar system planets and exoplanets are also carried out for understanding the early and later evolution of Venus, Earth and Mars.

A highlight occurred on 23 June 2022, when the ESA/JAXA *BepiColombo* spacecraft had its second successful flyby at the Sun's innermost planet, Mercury.

SUN & SOLAR WIND

The Sun's electromagnetic radiation, magnetic activity, and the solar wind are strong drivers for various processes in the solar system.

SOLAR ORBITER

Solar Orbiter is an ESA-led space mission with NASA participation to investigate the Sun. Flying a novel trajectory, with partial Sun-spacecraft corotation, the mission plans to investigate in-situ plasma properties of the inner solar heliosphere and to observe the Sun's magnetized atmosphere and polar regions. Gravity assist from Venus and Earth will be used to reach the operational orbit, a highly elliptical orbit with perihelion at 0.28 au.

The IWF built the Digital Processing Unit (DPU) for the *Radio and Plasma Waves (RPW)* instrument and calibrated the *RPW* antennas, using numerical analysis and anechoic chamber measurements. Furthermore, the institute contributed to the fluxgate magnetometer *(MAG)*. *RPW* will measure the magnetic and electric fields at high time resolution and determine the characteristics of magnetic and electrostatic waves in the solar wind from almost DC to 20 MHz. Besides the 5 m long antennas and the AC magnetic field sensors, the instrument consists of four analyzers: the thermal noise and high frequency receiver, the time domain sampler, the low frequency receiver, and the bias unit for the antennas. The control of all analyzers and the communication will be performed by the DPU.

On 26 March, *Solar Orbiter* encircled the Sun within a distance of approximately 48 million kilometers. This corresponds to less than one third of the distance between Earth and Sun and marks a preliminary highlight of the mission. All instruments have been operating during flyby. The in-situ imaging instruments observed several bursts of energetic particles and solar flares. The flare registered on 31 March 2022 was classified as one of the highest categories. Later in the year, on 4 September, *Solar Orbiter* did its third Venus flyby, at a distance of about 12,500 km. Just shortly before, on 30 August, the probe has been hit by a CME directly. Fortunately, there was no damage to the spacecraft. It is designed to withstand and measure violent outbursts from our Sun.

INTERPLANETARY CORONAL MASS EJECTIONS OBSERVED BY MULTIPLE SPACECRAFT

Based on the data of *Solar Orbiter*, *BepiColombo*, *Parker Solar Probe (PSP)*, *Wind*, and *STEREO-A*, together with coronagraph and heliospheric imaging observations from *STEREO-A/SECCHI* and *SOHO/LASCO*, an exploration analysis was performed including visualizations of the magnetic-field and plasma observations.

Seventeen ICME events could be observed by the *STEREO-A* heliospheric imagers during their interplanetary propagation to their impact at the aforementioned spacecraft. Two events of special interest were highlighted: (1) a small streamer blowout CME on 23 June 2020 (see figure) observed with a triple lineup by *PSP*, *BepiColombo*, and *Wind*, guided by imaging with *STEREO-A*, and (2) the first fast CME of solar cycle 25 on 29 November 2020 observed in situ by *PSP* and *STEREO-A*. These results are useful for modeling the magnetic structure of ICMEs and the interplanetary evolution and global shape of their flux ropes and shocks, and for studying the propagation of solar energetic particles. The combined data from these missions are expected to become even more valuable with an increasing number of ICME events expected during the rise and maximum of solar cycle 25.

Möstl et al., Astrophys. J. Lett., 924, L6, 2022.

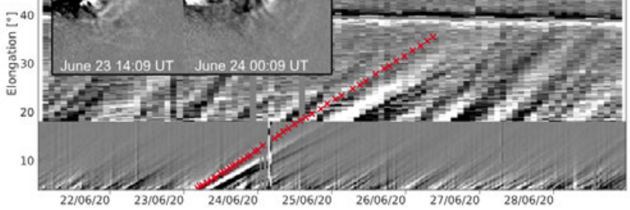

STEREO-A heliospheric imager time-elongation map with HI1 images and track of the CME front overlaid as red crosses.

SMALL-SCALE INTENSITY ENHANCEMENTS IN ACTIVE SOLAR REGIONS

Small-scale moving intensity enhancements remotely observed in extreme ultraviolet (EUV) images of solar active regions, also called active region moving campfires (ARMCs), are related to local plasma temperature and/or density enhancements. They have characteristic velocities near the background sound speed. Their dynamics is driven by physical processes in the entire coronal plasma. To investigate the dynamical and statistical properties of ARMCs, a simultaneous cross-validating analysis of EUV images from two observational missions, SDO/AIA (171Å, 193Å, and 211Å channels) and Hi-C2.1 (172Å channel) has been performed on active region AR12712. The statistical model of intensity centroid convergence and tracking, as well as the Gaussian mixture model, were elaborated and applied to reveal how the observed ARMCs are distributed over the active region and to analyze their possible grouping according to distinct physical characteristics. Several groups of ARMCs with respect to blob intensity and velocity have been identified (see figure below). They all have velocities at the level of the typical sound speed in coronal loops and differ from the well-known fast Alfvénic jets from magnetic reconnection sites. The latter is additionally proven by the fact that ARMCs propagate along the active region magnetic structure (strands). The nature of the discovered statistical grouping of the ARMCs remains unknown, requiring their further theoretical study and modeling.

Shergelashvili, Astron. Astrophys., 662, A30, 2022.

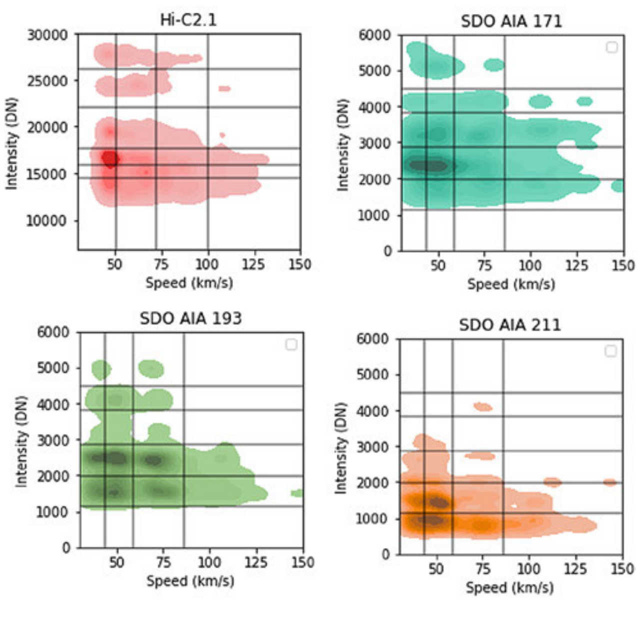

Active region moving campfires' (ARMC) grouping in the intensity-speed maps revealed from Hi-C2.1 (172Å) and the SDO/AIA (171Å, 193Å, 211Å) data. The color density reflects the amount of detected ARMC events.

MERCURY

Mercury is in the center of attention because of the ESA/JAXA *BepiColombo* mission. The planet has a weak intrinsic magnetic field that results in a small magnetosphere, which strongly interacts with the solar wind plasma so that elements can be released from the surface minerals which produces a silicate-rich exosphere.

On 23 June 2022, *BepiColombo* made its second close flyby at Mercury. This was three and a half years after the launch, and it's still three and a half years to go before the spacecraft will finally reach Mercury. Half time! All instruments worked well and produced data that were analyzed. It was also possible to identify various geological features that will be studied in more detail once the spacecraft will be in Mercury's orbit.

BEPICOLOMBO

The European-Japanese spacecraft, launched in 2018, is on its way to Mercury. During its seven-year cruise to the innermost planet of the solar system, *BepiColombo* performed its second gravity assist maneuver at Mercury on 23 June 2022. This flyby was the fifth of nine flybys. The spacecraft flew by Mercury at a distance of just 200 km from the planet's surface. The closest approach, which took place at 09:44 UTC, was on the planet's nightside. As *BepiColombo* flew from the nightside to dayside, the Sun seemingly rose over the cratered surface of the planet, casting shadows along the terminator - the boundary between night and day - and highlighting the topography of the terrain. The three monitoring cameras of the spacecraft shot a number of photos of this dramatic scenery.

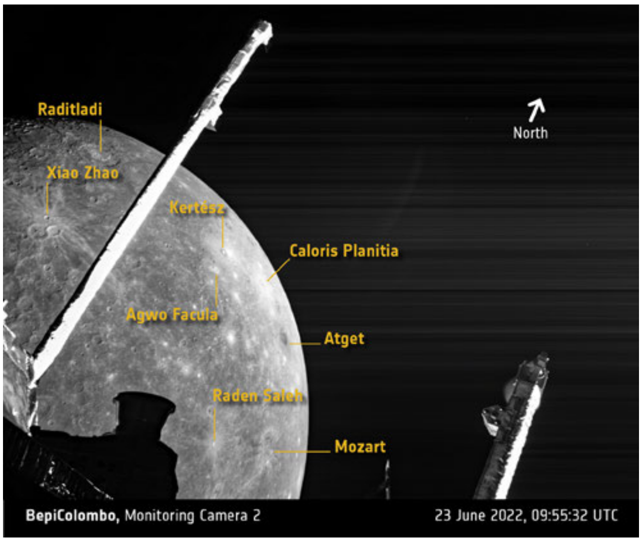

BepiColombo captured this view of Mercury during its second of six gravity assist maneuvers. The image was taken at 09:55:32 UTC by the *Mercury Transfer Module's* Monitoring Camera 2, when the spacecraft was 2862 km from the planet's surface, shortly before closest approach (© ESA/*BepiColombo*/*MTM*, CC BY-SA 3.0 IGO).

Similar to the first Mercury flyby in 2021, most scientific instruments were switched on to investigate Mercury's planetary environment, including the three payloads with IWF hardware contribution on both the European *Mercury Planetary Orbiter (MPO)* and the Japanese *Mercury Magnetospheric Orbiter (Mio)*.

As part of the *SERENA (Search for Exospheric Refilling and Emitted Natural Abundances)* suite, *PICAM (Planetary Ion CAMera*, IWF PI-ship) was operational from one day before, until two days after the closest approach. During this period of time *PICAM* observed the solar wind as well as Mercury's magnetosphere. However, this was the first time that *PICAM* was in high cadence mode, sampling the ion distribution at 250 ms. These high time resolution data are currently being analyzed, providing more details on bow shock and magnetopause crossings, as well as inner-magnetosphere ion dynamics. The observations were mostly aimed at *BepiColombo's* cruise science campaign, but also for the investigation of spacecraft outgassing. Furthermore, *PICAM* was switched on for more than 30 days of 2022 in the interplanetary medium.

In addition, the *BepiColombo* magnetometers *MPO-MAG* (IWF technical management) and *Mio-MGF* (IWF PI-ship) were active during the flyby and (*Mio-MGF* only partially) during the cruise phase, returning valuable scientific measurements of the inner heliosphere. The data from both magnetometers are affected by the spacecraft's magnetic disturbances, as the spacecraft is still in cruise configuration, which is not optimal for magnetic measurements. A dedicated cleaning of the data using measurements of both magnetometers (*MPO-MAG* and *Mio-MGF*) has been initiated to make high quality data available, in order to enable reliable scientific analysis of the highly dynamic magnetosphere of Mercury.

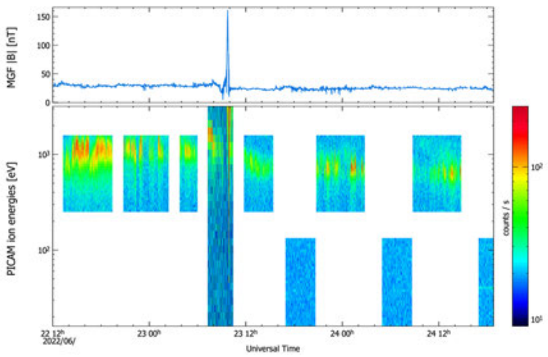

Mio-MGF magnetic field (top) and *PICAM* ion energy spectrogram (bottom) during the second Mercury flyby. The peak in the total magnetic field, together with the observation of high energetic ions, marks the closest approach (C/A). One day before, the magnetic field and ion energy observation show rather quiet solar wind. Two hours before C/A the magnetic field suddenly increases: crossing of the bow shock. After that the magnetic field is highly fluctuating and ion energies increase: the magnetosheath region. The weak magnetic field and low ion energy observations one hour before C/A are characteristic for the magnetotail region. After C/A *BepiColombo* crosses the magnetopause and bow shock, entering the solar wind again.

SOLAR WIND DEPENDENT STREAMLINE MODEL FOR MERCURY'S MAGNETOSHEATH

Mercury's magnetosphere and magnetosheath are unique as they are highly time-dependent, since the planet has only a small-scale magnetosphere originating from the weak intrinsic planetary magnetic field. Yet, it is believed that the plasma therein reaches a quasi-stationary state, i.e., the ground state of magnetospheric dynamics, when the solar wind smoothly passes by the magnetosphere without energy or momentum exchange under quiet conditions. A semi-analytical streamline model for Mercury's magnetosheath was constructed to extend the modeling effort from the magnetospheric plasma to the magnetosheath plasma. The model has the capability of determining the plasma density and the velocity as a function of the radial distance from the planet and the solar wind conditions. It reasonably explains and reproduces the in-situ measurements around Mercury by previous missions. Thus, it provides a good reference point for comparison with observations, also for *BepiColombo*. It has even the potential to estimate the solar wind parameters using the magnetosheath plasma observation of *Mio* during periods in Mercury's orbit, when even *Mio* stays mainly in the magnetosphere and magnetosheath and hardly encounters the solar wind. Moreover with the model one will better understand Mercury's current systems, instabilities, substorms and plasma waves in the planetary environment.

Schmid et al., A&A, 668, A113, 2022.

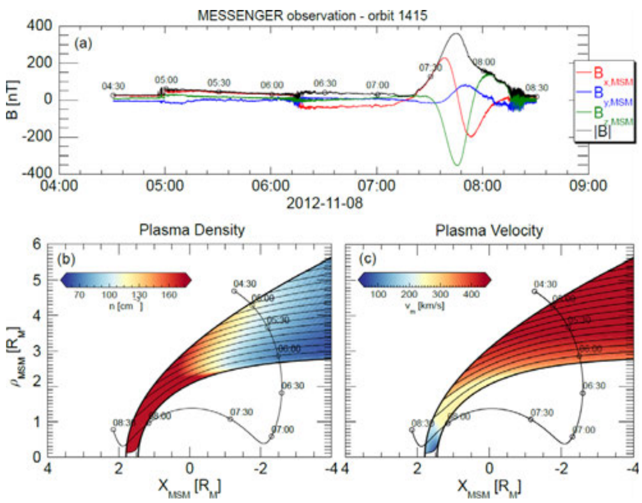

Panel (a) shows the magnetic field observations of *MESSENGER* on 8 November 2012 during orbit 1415. Panel (b) and (c) show the modeled plasma density and velocity distribution within the magnetosheath, respectively. The black line indicates the trajectory of *MESSENGER* for the time interval in panel (a).

MERCURY'S H_2 EXOSPHERE DENSITIES INFERRED BY PLASMA OBSERVATIONS

Mercury possesses an extended exosphere that contains a variety of species. So far, only two spacecraft have probed the space environment around Mercury: *Mariner 10* in 1974 and 1975, and *MESSENGER* four decades later. Optical observations by *Mariner 10* and *MESSENGER* showed that Mercury has an exosphere, which is abundant in hydrogen. To date the hydrogen density at Mercury could only be estimated from models that use optical observations as constraints, since no in-situ measurements of hydrogen are available to determine its exact number density. For the first time an altitude-density profile of Mercury's H- and H_2-exosphere was derived, based on the in-situ magnetic field measurements by *MESSENGER*. From the observations of so-called pick-up ion cyclotron waves in the magnetic field data, it is possible to derive the local H number density, necessary to excite these waves. The results reveal an extended atomic hydrogen exosphere with densities that are 1-2 orders of magnitude larger than previously predicted. It was found that the unexpected large H densities could only be explained by dissociation of H_2, which allowed, for the first time, to constrain the so far unknown H_2 number density profile and surface density in Mercury's environment.

Schmid et al., JGR Planets, 127, e2022JE007462, 2022.

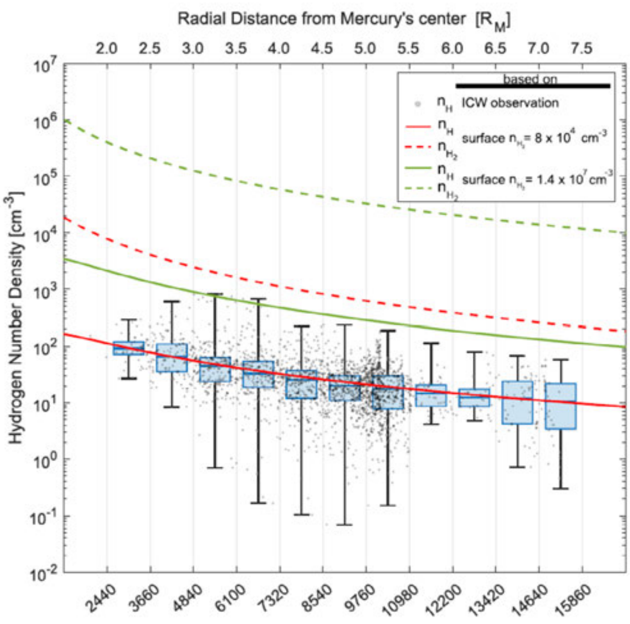

Altitude density profile of obtained H_2 and H profiles at Mercury (red lines best fits). The black error bar indicates the minimum and maximum number density within each 0.5 RM bin. The boxes indicate the lower and upper quartiles and the horizontal blue lines the median number density of each bin.

INNER SOUTHERN MAGNETOSPHERE OBSERVATION OF MERCURY VIA BEPICOLOMBO/SERENA

Mercury's southern inner-magnetosphere has broadly remained an unexplored region to the scientific community. However, during *BepiColombo's* first close encounter with Mercury in October 2021 the ESA/JAXA mission became the first spacecraft to ever fly through this region. Various instruments including the *SERENA* suite operated and captured the plasma properties during this passage. In particular, two of *SERENA's* sensors *PICAM* and *MIPA (Miniature Ion Precipitation Analyser)* focused on the dynamics of ions throughout the flyby. *PICAM's* measurements revealed signatures of an interplanetary flux rope upstream Mercury's bow shock, in the solar wind. *PICAM* and *MIPA* observations showed strong evidence for a ring current-like distribution of plasma being present around Mercury. The data collected by *MIPA* confirmed the presence of an unexpected dayside magnetospheric asymmetry with higher ion density at the dawnside magnetopause, which had also been tentatively reported by the *MESSENGER* mission before.

Orsini et al., Nat. Comm., 13, 7390, 2022.

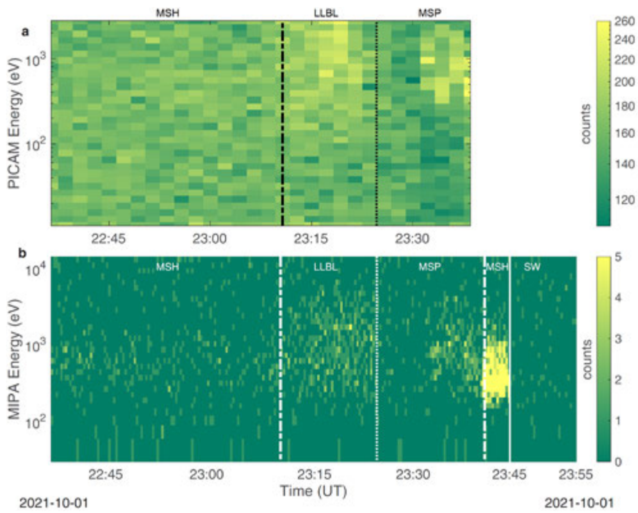

The ion spectrograms obtained by a) *PICAM* observations and b) *MIPA* measurements in the inner magnetosphere of Mercury. The dashed-dotted lines refer to the expected inbound and outbound magnetopause crossings, the dotted lines refer to the observed transition from low latitude boundary layer to the magnetospheric dusk lobe, while the solid line in b) marks the bow shock crossing. Labels refer to the different regions crossed by the spacecraft, specifically: magnetosheath (MSH), low latitude boundary layer (LLBL), inner magnetosphere (MSP), and solar wind (SW). Color bars report ion counts.

VENUS & MARS

Venus and Mars are Earth's neighbors at a distance of approximately 0.7 astronomical units (au) and 1.5 au from the Sun, respectively. They have orbital periods around the Sun of 224 and 687 days, respectively. While Venus is approximately the same size as the Earth, Mars only has about half the size of the Earth. Where Venus has a very dense and hot atmosphere, Mars's is tenuous and cold. Both planets do not have an internal magnetic field, however, their interaction with the solar wind creates a so-called induced magnetosphere.

TIANWEN-1

Tianwen-1 ("questions to heaven") is China's first Mars mission, consisting of an orbiter and a rover named *Zhurong*. Before *Zhurong* only NASA has successfully landed and operated spacecraft on Mars. The mission is designed to conduct a comprehensive remote sensing of the Red Planet, as well as surface investigations. The IWF contributed to a magnetometer aboard the orbiter.

Since the switch-on of the *Mars Orbiter MAGnetometer (MOMAG)* on 13 November 2021, it has been in continuous operation with two operational modes: 32 Hz for 120 min around periapsis and for 60 min around apoapsis, and 1 Hz for the rest of the 8-hour orbit. *MOMAG* demonstrated good performance, nevertheless all measurements indicated various spacecraft magnetic effects due to the lack of a magnetic cleanliness program and the rather short 3.2 m boom. The two-sensor gradiometer formation, where the outboard sensor is located at the end of the boom and the inboard sensor at 0.9 m from the outboard, is used to remove the spacecraft magnetic effects successfully in year 2022, and the cleaned scientific data are expected to be issued to public soon in the future.

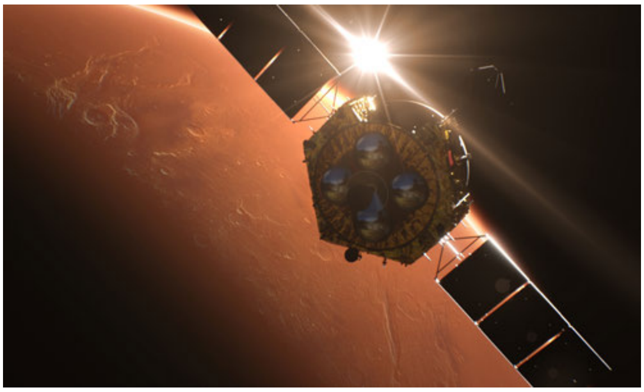

Illustration of *Tianwen-1* in orbit around Mars (© CASC)

ESCAPE OF THE MARS ATMOSPHERE OVER TIME

The loss of C^+ and O^+ ions and hence the Martian CO_2 atmosphere was modeled with a global hybrid model, which includes the upper atmosphere responses due to the evolving higher EUV flux of the Sun in the past 4.1 billion years of the planet's history. Pick up ions that are scattered towards the planet are used for the estimation of sputtered atmospheric particles, including ^{36}Ar and ^{38}Ar isotopes. Furthermore, the total ion escape, sputtering and also photochemical escapes rates are compared. The fractionation of atmospheric $^{36}Ar/^{38}Ar$ isotopes through volcanic outgassing and sputtering from its initial chondritic value of 5.3, as measured in the 4.1 billion years old Mars meteorite ALH 84001, until the present day is reproduced. Depending on the cessation time of the Martian magnetic dynamo at about 3.6-4.0 Gyr, one needs to assume the atmospheric CO_2 partial pressure was about 0.01-0.4 bar without and 0.4-1.8 mbar by including surface sinks (see figure below). In such evolution scenarios, Ar sputtering started after the ancient Mars magnetosphere vanished.

Lichtenegger et al., Icarus, 382, 115009, 2022.

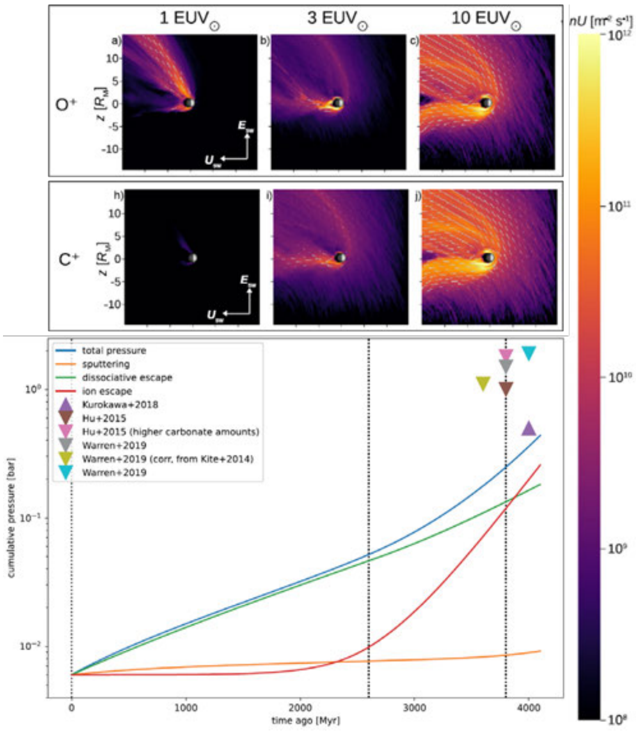

O^+ and C^+ ions in global hybrid simulation runs. The coloring on the xz (y=0) planes gives the bulk number flux. Below, modeled CO_2 surface pressure evolution from present to 4.1 Gyr caused by the various atmospheric escape processes. Maximum (down-pointing triangles) and minimum (up-pointing triangle) pressure estimates of the early Mars atmosphere are also shown from the literature.

MIRROR MODE STRUCTURES IN MARS' MAGNETOSHEATH

Mirror Mode Structures (MMS) are magnetic bottles trapping dense plasma and characterized by compressive magnetic field signatures in antiphase with the plasma density. Triggered by a temperature anisotropy, they partake in the energy exchanges in the turbulent magnetosheath between the upstream solar wind plasma and a planet's ionized environment. At Mars, NASA's *Mars Atmosphere and Volatile EvolutioN (MAVEN)* mission has been probing the magnetosheath plasma since October 2014. Statistical studies of MMS can now be performed.

In a first step, these datasets were used in combination to identify MMS for the first time unambiguously. It was found that these MMS, created behind a quasi-perpendicular bow shock where the plasma was unstable to the generation of mirror modes, were convected down to the magnetic pile-up boundary with scales of about 15-30 solar wind proton gyroradii, in agreement with previous detections at Venus and at comets. A set of magnetic-field only criteria was optimized for future statistical studies.

A second step was to evaluate the position of the bow shock with the development of a fast predictor-corrector algorithm to automatically detect it in spacecraft data, based on magnetic field measurements. From 2014 to 2021, 14929 shock crossings were identified with a precision of ±0.05 Mars radius, with the calculation of 2D and 3D fits to the shock surface depending on Martian year, atmospheric season and solar EUV flux. A database of these crossings, together with the shock nature (quasi-perpendicular or quasi-parallel crossings) is openly available.

Simon Wedlund et al., JGR Space Physics, 127, e2021JA029811, 2022.
Simon Wedlund et al., JGR Space Physics, 127, e2021JA029942, 2022.

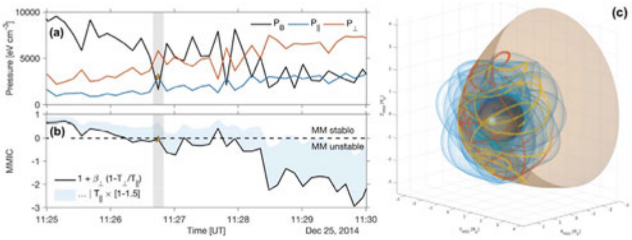

Unambiguous identification of MMS on 25 December 2014 and automatic detection of bow shock crossings. (a) Parallel and perpendicular ion pressures $P_{\parallel}$ and $P_{\perp}$ and magnetic pressure PB. (b) Mirror Mode Instability Criterion (MMIC). The gray-shaded zone highlights the times when the clearest MMS is detected throughout the interval. (c) Automatic detection of bow shock in Mars Solar Orbital coordinates normalized to the planet's radius. The average bow shock surface of Gruesbeck et al. is in brown, the 2014-2021 orbit of *MAVEN* is in blue. Crossings from inside-to-outside (outside-to-inside) of the shock surface are shown as orange (yellow) circles.

JUPITER AND SATURN

Jupiter and Saturn, the two largest planets in our solar system, together with their numerous moons remain fascinating targets for in-situ investigations: Saturn was orbited by the *Cassini* spacecraft from 2004 until 2017. Since 2016 the *Juno* spacecraft has been around Jupiter, and it is planned to stay there until 2025. ESA will launch the *JUICE* mission to Jupiter and its icy moons in 2023, and NASA will follow in 2024 with the *Europa Clipper* mission.

In 2022, *JUICE* and its ten scientific instruments were brought into flight configuration and the mission critical electromagnetic compatibility, vibration, acoustic, magnetic stray field and end-to-end operation test campaigns were accomplished successfully.

JUICE

JUpiter ICy moons Explorer (JUICE) was selected as ESA's first "Large-class" mission of the Cosmic Vision program. With its powerful instrument package, it will provide the most detailed analysis yet of Jupiter as an archetype for gas giants across the Universe.

The launch of *JUICE* is planned for April 2023. A several months long test phase of all instruments, which includes the deployment of e.g. the magnetometer boom, the Langmuir probe booms and the radio antennas, will start right after launch.

After three gravity assist maneuvers at Earth and one at Venus, *JUICE* is scheduled to arrive at Jupiter in mid-2031 to make detailed observations of the gas giant and three of its largest moons, which are thought to have water oceans below their icy surfaces. Towards the end of the mission *JUICE* will be the first spacecraft ever to orbit a moon other than our own - Jupiter's largest moon Ganymede.

The IWF participates on Co-Investigator basis in three of the ten scientific instruments aboard *JUICE*: *J-MAG*, *PEP* and *RPWI*.

The *Jupiter MAGnetometer (J-MAG)* is led by Imperial College London and will measure the magnetic field vector and magnitude in the spacecraft vicinity in the bandwidth DC to 64 Hz. It is a conventional dual sensor fluxgate configuration combined with an absolute scalar sensor based on quantum-interference technology. Science outcome from *J-MAG* will contribute to a much better understanding of the formation of the Galilean satellites, an improved characterization of their oceans and interiors, and will provide deep insight into the behaviour of rapidly rotating magnetic bodies. The IWF supplied the atomic scalar sensor *(MAGSCA)* for *J-MAG*, which was developed in close collaboration with TU Graz.

The highlights for the *MAGSCA* activities in 2022 were the completion of the spare model, the end-to-end performance test with the flight model mounted on the spacecraft and the preparation of the test phase of the instrument after launch, which will last for several days.

The *Particle Environment Package (PEP)* is a suite of different kind of sensors to characterize the plasma environment of the Jovian system and the composition of the exospheres of Callisto, Ganymede, and Europa. *PEP* is led by the Swedish Institute of Space Physics and the IWF participates in the *PEP* consortium with scientific studies related to the plasma interaction and exosphere formation of the Jovian satellites.

The IWF has also been responsible for the calibration of the radio antennas of the *Radio and Plasma Wave Investigation (RPWI).* Besides the three dipole radio antennas, *RPWI* also harbors a search-coil magnetometer and four Langmuir probes.

RPWI will cover the Jovian radio spectrum in the frequency range from DC to 45 MHz, and the magnetic field measurements will go from DC to 20 kHz. The Langmuir probes on the tips of four 3 m long booms will perform plasma and 3D electric field measurements.

Scientists and engineers put their heads together to equip *JUICE* with a unique set of solar panels, antennas, probes and booms that will help the spacecraft overcome challenges that no other European mission has faced before. To keep the high-tech equipment safe during the launch, everything will be tucked away, ready to be deployed only once *JUICE* has separated from its Ariane 5 host rocket in space. With all external equipment in position, *JUICE* is now ready to begin its long and difficult journey to Jupiter (© ESA, acknowledgment: ATG Medialab).

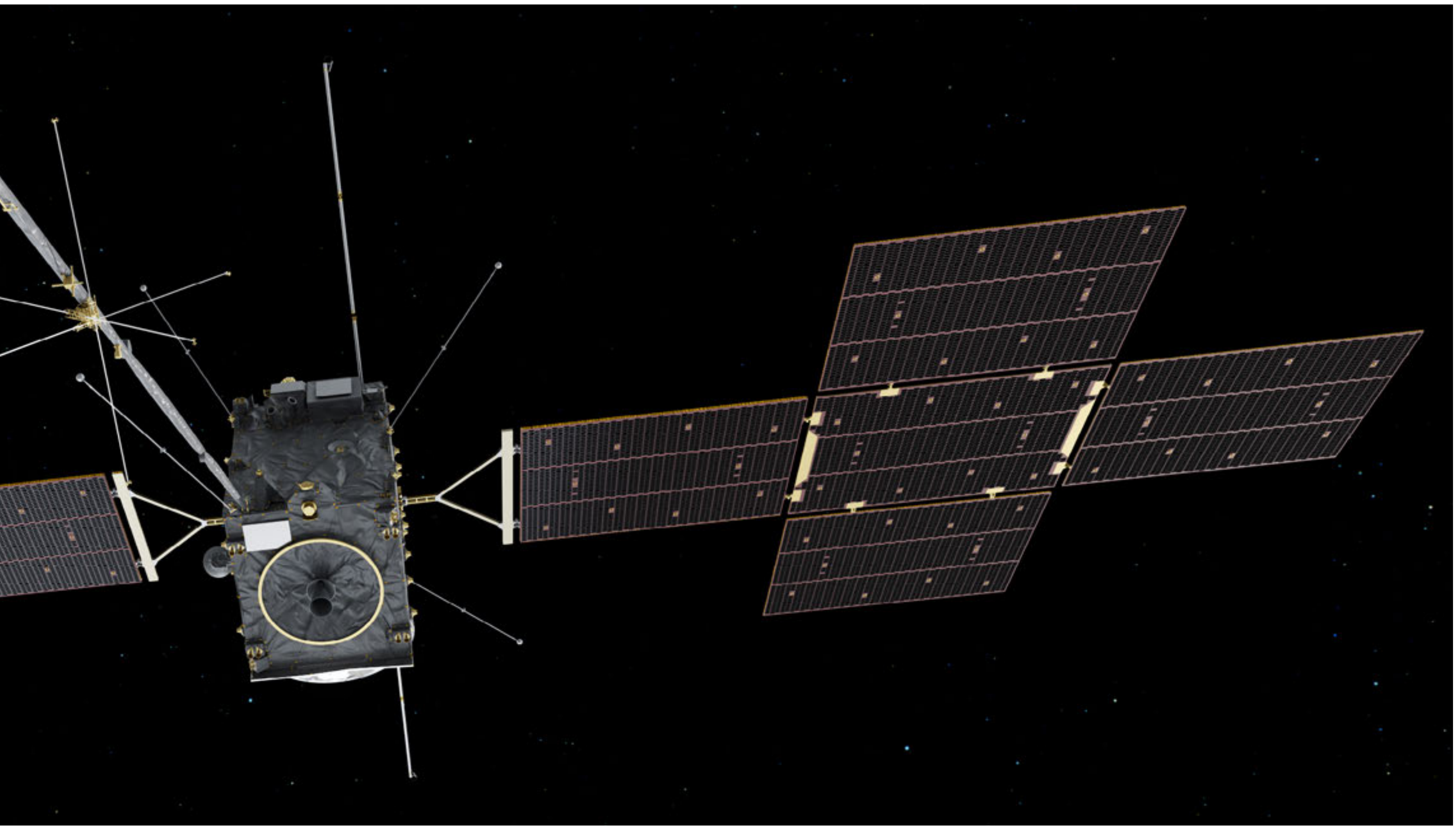

JUNO

NASA's *Juno* mission is dedicated to the investigation of Jupiter's gravitational and magnetic field, its polar magnetosphere, deep atmosphere and winds, as well as core composition and mass distribution. The spacecraft entered a polar orbit around Jupiter in July 2016 and its controlled de-orbit is scheduled for 2025. One of the instruments on board is the *Waves* instrument, which uses a dipole antenna to measure electromagnetic field components of incident waves. In 2022 it was used to determine the fine and coarse spectral structures of Jovian broad-banded and narrow-banded kilometric radiation.

SATURN STUDIES

The enormous wealth of *Cassini* data is still leading to new scientific results. A recent study used the Wideband Receiver of the *Cassini RPWS (Radio and Plasma Wave Science*) instrument for a study of the spectral fine structures of Saturn Kilometric Radiation (SKR). A newly defined classification scheme was introduced to identify spectral features and make statistical studies about their occurrence. E.g., in the figure one can see an areal region in the time-frequency spectrum, lines with negative or positive slope, and a feature nicknamed "caterpillar". The latter is a newly discovered spectral structure of SKR lasting for several hours mostly below 40 kHz, and its constant central frequency with a typical bandwidth of 10-15 kHz makes it look like a caterpillar in a time-frequency spectrogram.

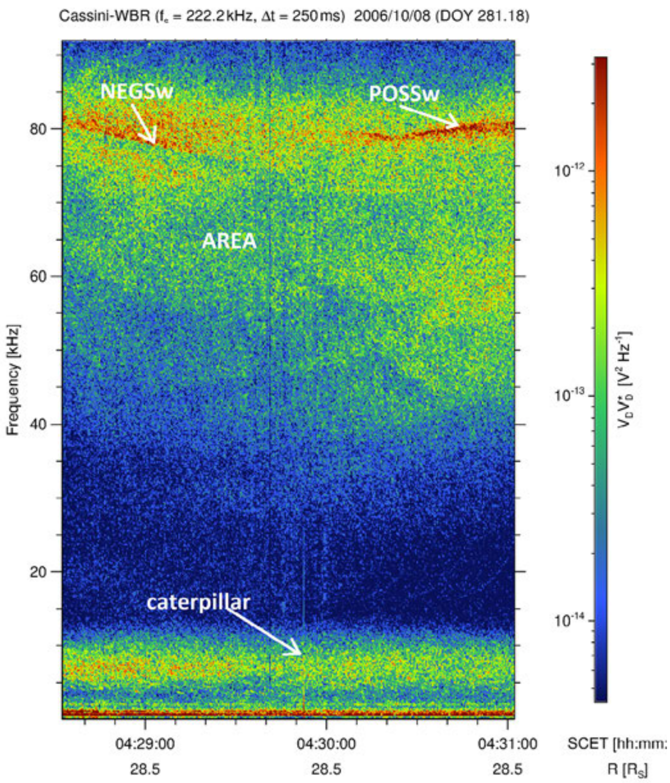

Another *Cassini* data study led to the detection of clear first harmonic emissions of SKR in which both ordinary and extraordinary mode fundamental emissions were found to be accompanied by weaker extraordinary harmonic emissions at twice the frequency of the fundamental.

Fischer et al., Ann. Geophys., 40, 485-501, 2022.
Wu et al., JGR Space Physics, 127, e2022JA030776, 2022.

The study of Saturn Narrowband (NB) radio emissions was continued after a previous work suggested the possible reflection of 5 kHz NB emissions at the magnetosheath. A new study showed that this is indeed the case, as some examples were found in which NB disappeared immediately after the crossing of Saturn's magnetopause. The mechanism can explain the occurrence of 5 kHz NB at large distances and equatorial latitudes since these emissions can bypass the Enceladus plasma torus by reflection at the magnetosheath. Furthermore, a new special type of Saturn narrowband emissions was detected and named Saturn Anomalous Myriametric (SAM) radiation. SAM events usually drift in frequency over time (with a rate of a few kHz per day), and they have a mean duration similar to Saturn's rotation period. They preferentially occur at high spacecraft latitudes, and they often have a first harmonic in the extraordinary mode. They are found in the same frequency range (below 40 kHz) as the newly detected "caterpillars", but they are distinctly different from them.

Wu et al., GRL, 49, e2021GL096990, 2022.
Wu et al., GRL, 49, e2022GL099237, 2022.

Cassini RPWS Wideband Receiver spectrogram up to 90 kHz going over 150 seconds and showing spectral fine structures of Saturn kilometric radiation.

COMETS

Comets are the remainders of the building blocks of the solar system after the planetary formation had finished. They are located in two distant regions around the solar system: between 30 and 50 astronomical units (au) from the Sun in the Kuiper belt, and further than 2000 au in the Oort cloud. Through close encounters (comet-comet, or possibly a nearby passing star) some of these can be pushed out of their orbit and will start to move towards the Sun. When such an object passes Jupiter's orbit, the solar irradiance is strong enough to start heating up the surface of the comet and to start the sublimation of (sub) surface volatiles. This leads to the escape of gas and dust, which create the characteristic coma and tails of a comet.

The *Comet Interceptor* mission was adopted by ESA on 8 June 2022 and the prime contractor to build the spacecraft was selected in November.

COMET INTERCEPTOR

Comet Interceptor is ESA's first F(ast)-class mission, now formally adopted on 8 June 2022. A prime contractor (OHB, Italy) has been selected to build the spacecraft. The goal of this mission is to investigate a dynamically new comet, i.e. a comet which has just been kicked-out of the Kuiper belt or the Oort cloud, and has not yet had a close encounter with the Sun. This will ensure a look at a pristine object, which will provide detailed information about the structure and composition of the early building blocks of the solar system.

Comet Interceptor is the first multi-spacecraft mission to visit a comet, consisting of three parts, which will fly by the target at different distances. The mother spacecraft (*A* - ESA), which will also serve as a relay station, will stay furthest from the comet, two smaller subcraft (*B1* - JAXA, *B2* - ESA) will approach the target closer. The mission is planned to be launched in 2029.

The IWF is building parts of two instruments on *Comet Interceptor*: for spacecraft *A* the Data Processing Unit (DPU) for the *Mass Analyser for Neutrals and ions at Comets (MANiaC)* and for *B2* the front-end electronics of the *FluxGate magnetometer (BFG)*, part of the *Dust Field and Plasma package (DFP)*, led by the Space Research Centre of the Polish Academy of Sciences (Centrum Badań Kosmicznych, CBK).

In 2022, the *MANiaC* DPU design was focused on the consolidation of all external interfaces. Due to changes within the instrument consortium, new partners joined the team and therefore new interface specifications had to be incorporated. With Q4 2022, the design was frozen, the electronical schematic completed and the PCB layout activity has been started. A major step forward was the finalization of the EEE components list and the initiation of the parts procurement process. The design of the boot software was finalized, the code generation completed and the test phase has been initiated. In terms of the application software, the requirement engineering is still ongoing.

In 2022 the focus for *BFG* was on consolidating the design of the magnetometer with its thermal, mechanical and electrical interfaces to the *DFP* common electronics units as well as the *B2* daughter spacecraft. There was a successful completion of the Preliminary Design Review in the middle of the year and the selection of the flight components, materials and processes was started. In November the first instrument model (i.e. Engineering Model) was delivered to CBK and successfully integrated into the electronics.

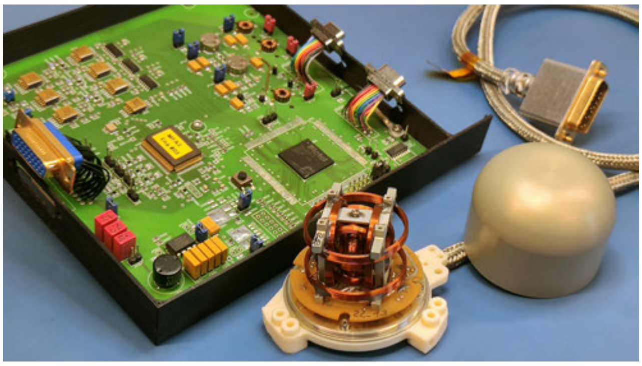

BFG Engineering Model (© OeAW/IWF/Valavanoglou).

COPHYLAB

CoPhyLab started as a joint German, Swiss, and Austrian research project between TU Braunschweig, the University of Bern, and the IWF to investigate cometary processes in space simulation laboratories. Later on, the following external partners joined: MPS Göttingen, DLR Berlin, University of Stirling, Luleå University of Technology, Qian Xuesen Laboratory of Space Technology in China, and Open University. The project aimed to increase the understanding of the *Rosetta* mission results by conducting selected experiments in a controlled environment.

In 2022, the project funding was concluded but the CoPhyLab laboratory and infrastructure is still used by the project partners. This includes extended laboratory visits at TU Braunschweig and joint experiments and data evaluation at all project partner sites. A special focus was given to the establishment of a defined cometary sample material both as a refractory analogue but also in the creation of a granular ice in the size range of a few µm with an almost perfect spherical shape. These new materials are to be used as a standard reproducible cometary analogue for further experiments.

Kreuzig et al., Rev. Sci. Instrum., 92, 115102, 2022.
Lethuillier et al., MNRAS, 515, 3420-3438, 2022.

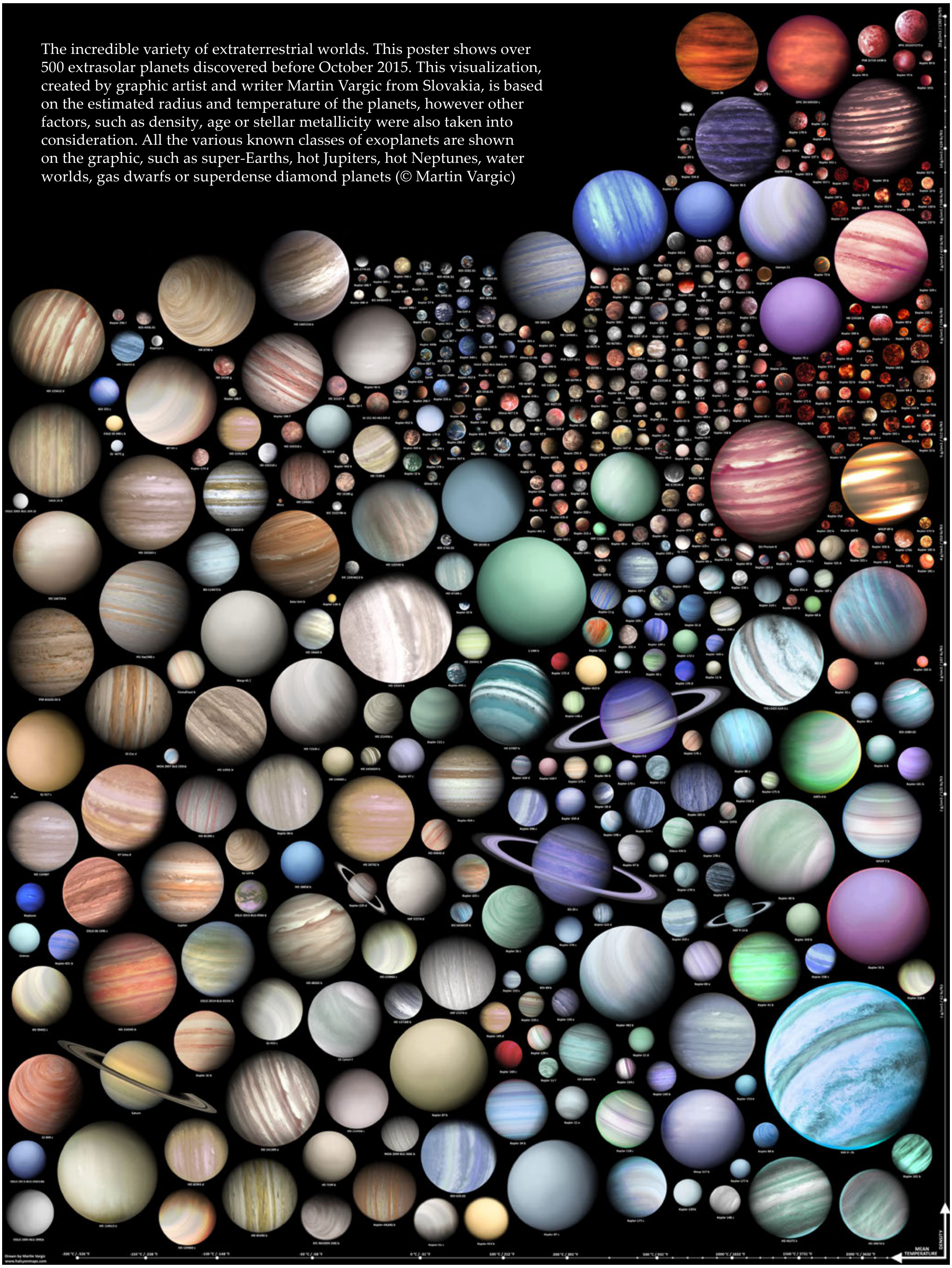

The incredible variety of extraterrestrial worlds. This poster shows over 500 extrasolar planets discovered before October 2015. This visualization, created by graphic artist and writer Martin Vargic from Slovakia, is based on the estimated radius and temperature of the planets, however other factors, such as density, age or stellar metallicity were also taken into consideration. All the various known classes of exoplanets are shown on the graphic, such as super-Earths, hot Jupiters, hot Neptunes, water worlds, gas dwarfs or superdense diamond planets (© Martin Vargic)

EXOPLANETARY SYSTEMS

The investigation of planets orbiting stars other than the Sun - also known as exoplanets - has developed strongly in the past decades. The first exoplanet was detected in 1995. More than 5300 exoplanets are now known. Improved instrumentation and analysis techniques have led to the detection of smaller and lighter planets, particularly orbiting bright, nearby stars, which therefore enable in-depth structure and atmospheric characterization. Although hot Neptunes and (ultra-) hot Jupiters are still prime targets for atmospheric characterization, smaller planets are entering the realm of the planets for which the atmosphere can be obvserved. This is particularly thanks to the advent of the *James Webb Space Telescope (JWST)* that was launched on Christmas day of 2021 and started science operations in July 2022. *JWST's* large collecting area and broad suite of instruments is driving a revolution in our view of exoplanetary atmospheres and of the cosmos at large. Members of the IWF are involved in a number of *JWST* observing programs aiming at characterizing exoplanetary atmospheres. For some of them, *JWST* has already collected data in 2022, but more will come in the upcoming years.

The main exoplanet missions in which the IWF is involved with hardware and/or science are *CHEOPS, CUTE, PLATO, ARIEL*, and *ATHENA*. The IWF concentrates on the study and characterization of planetary atmospheres and of the star-planet interaction phenomenon using both theory and observations, focusing particularly on the analysis of planet formation, exoplanet weather and climate, atmospheric clouds and chemistry as well as atmospheric mass loss. The research is based on the collection and analysis of ground- and space-based observations to constrain the models, as well as on the modeling of planet and cloud formation from first principles.

With the aim of detecting the metastable Helium infrared triplet probing planetary upper atmospheres, transits of the hot Jupiter WASP-80b have been observed with the *GIANO-B* high-resolution spectrograph attached to the Telescopio Nazionale Galileo (La Palma, Spain). Surprisingly, the observations led to no detection, providing the first demonstration that planetary atmospheres can have a significantly subsolar Helium content.

Planetary atmospheric evolution models have been employed to reproduce the width of the observed exoplanet mass-radius relation. This is one of the first attempts to constrain planetary atmospheric evolution through the observed mass-radius relation. The results led us to identify the planetary mass ranges within which atmospheric accretion or atmospheric escape control atmospheric evolution and the observed mass-radius relation.

The *CUTE* data reduction pipeline has been completed and published. The pipeline is now routinely employed to reduce data collected by the *CUTE* CubeSat mission.

Artist's impression of *JWST* (© ESA/ATG medialab).

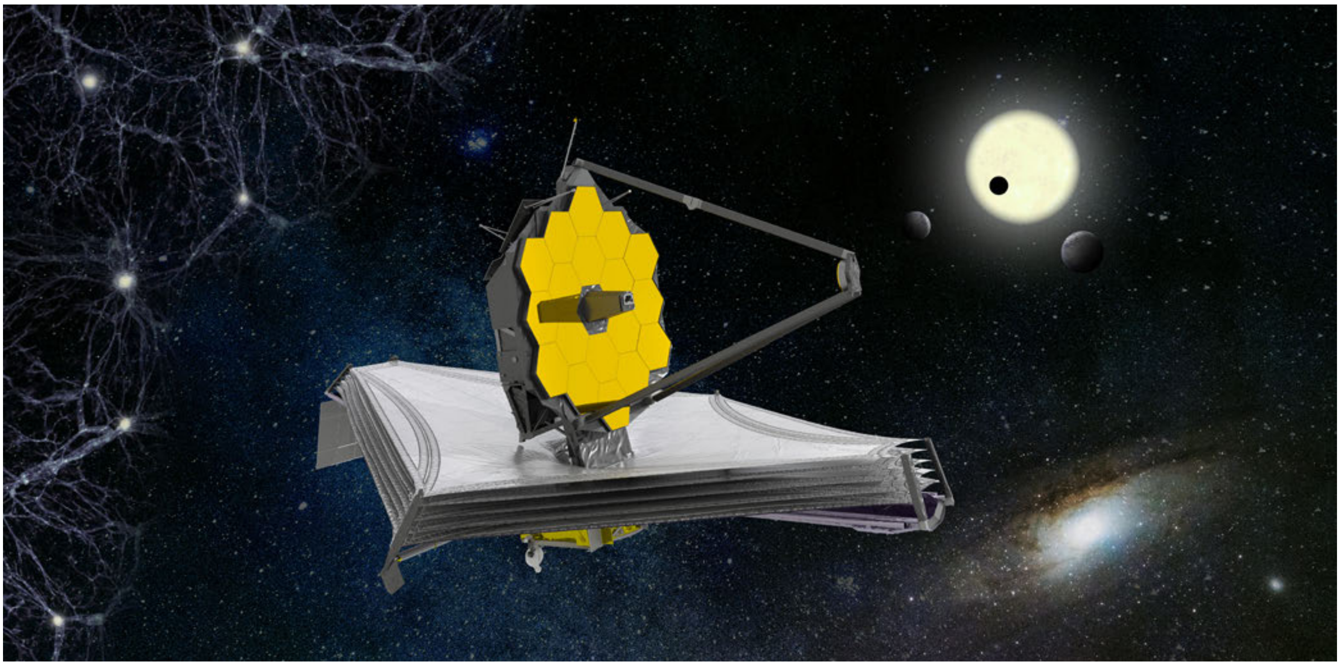

CHEOPS

CHEOPS (CHaracterising ExOPlanet Satellite), successfully launched in December 2019, started regular science operations in April 2020. The mission aims at studying extrasolar planets by means of ultra-high precision photometry. The main science goals are to precisely measure the radii of Neptune- to Earth-sized planets to constrain the internal composition and atmospheric evolution, study the atmospheric properties of transiting giant planets, and look for new planets particularly in already known systems. In 2022, the *CHEOPS* consortium started to work on the development of the science case for the first mission extension that is foreseen to begin in 2023.

The IWF is responsible for the *Back-End-Electronics* that is one of the two onboard computers and it is responsible controlling the data flow and the thermal stability of the telescope structure. The institute also developed and maintains the mission's signal-to-noise calculator. Within the Guaranteed Time Observations of the *CHEOPS* consortium, the IWF co-chairs the working group aiming at improving our understanding of the mass-radius relation of planets, of processes affecting planetary atmospheric evolution, and of system architecture.

In 2022, *CHEOPS* continued nominal science operations, demonstrating that the satellite performs and ages as expected. The European consortium in charge of the majority of observing time made use of *CHEOPS* data to publish more than a dozen refereed articles.

CHEOPS measurements enable one to draw with high accuracy the shape and extent of the mass-radius (MR) relation that can be used to constrain planetary atmospheric evolution. This is important because exoplanets in the mass range between Earth and Saturn show a large radius, and thus density, spread for a given mass. Planetary evolution modeling has been employed to reproduce the MR distribution of the 198 so far detected planets with mass and radius measured to the ≤45% and ≤15% level, respectively, and less massive than 108 Earth masses. The simulations simultaneously account for hydrodynamic atmospheric escape and thermal evolution, as well as for the entire range of possible stellar rotation evolution histories. The predicted radius spread reproduces well the observed MR distribution, except for two distinct groups of outliers comprising about 10% of the population.

The first group consists of very close-in Saturn-mass planets with Jupiter-like radii for which modeling underpredicts the radius likely because it lacks additional (internal) heating similar to that responsible for inflation in hot Jupiters. The second group consists of warm sub-Neptunes (400-800 K), which should host massive primordial hydrogen-dominated atmospheres, but instead present high densities indicating small gaseous envelopes (<1-2%). This suggests that their formation, internal structure, and evolution is different from that of atmospheric evolution through escape of hydrogen-dominated envelopes accreted onto rocky cores. On average the observed characteristics of low-mass planets (≤10-15 Earth masses) strongly depend on the impact of atmospheric escape, and thus of the evolution of the host star's activity level, while primordial parameters are less relevant. Instead, for more massive planets, the parameters at formation play the dominant role in shaping the final MR distribution. In general, the intrinsic spread in the evolution of the activity of the host stars can explain just about a quarter of the observed radius spread.

Kubyshkina & Fossati, A&A, 668, A178, 2022.

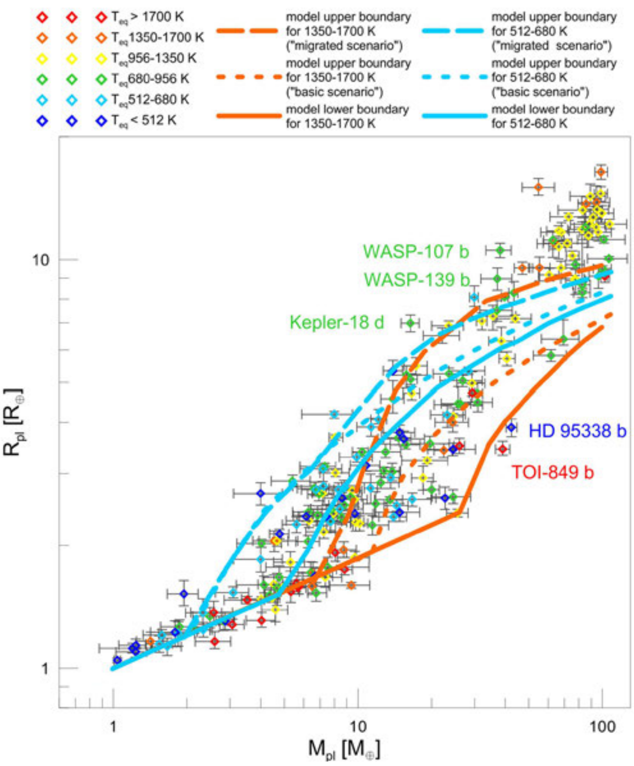

MR distribution of the selected observed planets in comparison to modeling results. The light blue and orange solid and long-dashed lines enclose the maximum predicted spread in planetary radius at the age of 5 Gyr obtained considering the entire set of atmospheric evolutionary tracks computed in the 512-680 K and 1350-1700 K temperature intervals, respectively.

CUTE

CUTE (Colorado Ultraviolet Transit Experiment) is a NASA-funded 6U-form CubeSat led by the University of Colorado that was launched in 2021. *CUTE* performs low-resolution transmission spectroscopy of transiting extrasolar planets at near-ultraviolet wavelengths. It studies the upper atmosphere of short-period extrasolar planets with the aim of observationally constraining atmospheric escape processes, which are key to understand planetary evolution, and detect heavy metals, which constrain the presence and composition of aerosols in the lower atmosphere. Furthermore, *CUTE*'s continuous temporal coverage of planetary transits allows one to detect transit asymmetries, which are possibly connected with the presence of planetary magnetic fields. Following a rather long commissioning phase, *CUTE* started to deliver scientific data in 2022.

The IWF is the only technological contributor to the mission outside of the University of Colorado (Boulder), where *CUTE* was built. The institute developed the data simulator, the data signal-to-noise calculator, the ground data reduction software, and the algorithms defining the onboard data reduction software.

With the arrival of the first science data in 2022, the IWF has finalized the development of the ground data reduction pipeline. It has been structured with a modular approach, which also considers scalability and adaptability to other missions carrying on-board a long-slit spectrograph. CONTROL provides end-to-end data reduction of *CUTE* data without human intervention and supervision. The pipeline can perform dark and bias subtraction, flat-field correction, corrections for bad/hot pixels, cosmic-ray correction, spectral extraction, background subtraction, wavelength calibration, and flux calibration as required by the user. The data reduction pipeline is therefore also able to combine dark, bias, and flat frames to produce master calibration frames. Cosmic-ray rejection is performed using contiguous science frames. The pipeline, which is freely available for download, is written in IDL 8.5.1 and is designed to work on both UNIX and WINDOWS systems. The pipeline has been tested for compatibility with previous IDL versions down to version 7.1. The intermediate and final output files generated by the pipeline are in FITS format, similar to all data products.

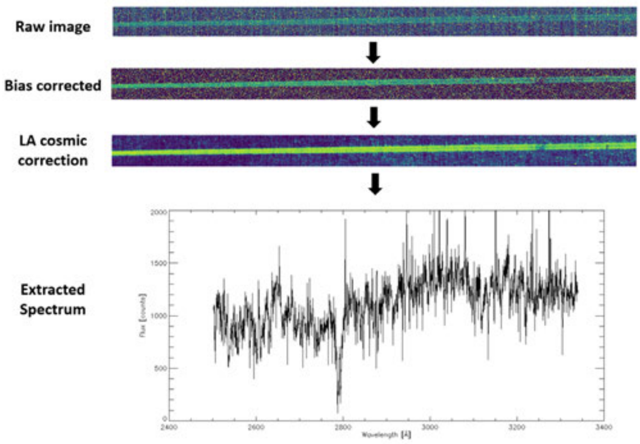

Example data reduction steps carried out by the *CUTE* pipeline on flight data.

Sreejith et al., PASP, 134, 114506, 2022.

PLATO

PLATO (PLAnetary Transits and Oscillations of stars) is ESA's third medium (M-class) mission, led by DLR. Its objective is to find and study a large number of exoplanetary systems, with emphasis on the properties of terrestrial planets in the habitable zone around solar-like stars. *PLATO* has also been designed to investigate seismic activity of stars, enabling the precise characterization of the host star, including its age.

The IWF co-leads the work package aiming at studying planetary habitability and takes part in two further work packages (one on stellar characterization and one on planetary evolution) aiming at gaining the knowledge and preparing the tools necessary to best exploit the data. The institute contributes to the development of the I*nstrument Controller Unit (ICU)* with the development of the *Router and Data Compression Unit (RDCU)*. Launch is expected in 2026.

PLATO consists of 24 telescopes for nominal and two telescopes for fast observations. Each telescope has its dedicated front-end-electronics, reading and digitizing the CCD content. Twelve nominal and two fast DPUs collect the data from the front-end-electronics and extract the areas of interest. The *RDCU* is a key element in the data processing chain, providing the communication between the DPUs and the *ICU*. The second task of the *RDCU* is the lossless compression of the science data. For performance reasons, the compression algorithm is implemented in an FPGA.

In 2022, the team concentrated on the assembly and test of the qualification model. In parallel, the solder qualification for the *PLATO RDCU* board, in particular the soldering of passive electronic components with the vapor phase equipment, has been successful completed. This achievement reduces the workload for the PCB assembly significantly. The logic design for the data compressor has been updated, to implement changes in accordance with the results from testing and post place and route simulations. The test of the qualification model is ongoing, the delivery has been shifted to 2023. As a first step towards the flight model production, the PCB layout was updated. In particular, the impedance control for all SpaceWire signals was optimized to improve the signal integrity of the links.

ARIEL

ARIEL (Atmospheric Remote-sensing Infrared Exoplanet Large-survey) is ESA's fourth medium (M-class) mission, led by University College London, to be launched in 2029. It will investigate the atmospheres of several hundred exoplanets to address fundamental questions on how planetary systems form and evolve. During its four-year mission, *ARIEL* will observe 1000 exoplanets ranging from Jupiter- and Neptune- down to super-Earth-size in the visible and infrared with its meter-class telescope. The analysis of *ARIEL* spectra and photometric data will enable extracting the chemical fingerprints of gases and condensates in planetary atmospheres, including the elemental composition for the most favorable targets, with a particular focus on carbon and oxygen. Thermal and scattering properties of the atmosphere will also be studied.

ARIEL consists of a one-meter telescope feeding two infrared low-resolution spectrographs and the fine guiding sensor (FGS), working in the optical. To improve the satellite's pointing stability, the FGS provides optical photometry of the target in three broad bands that are used to control instrumental systematics, measure intrinsic stellar variability, and constrain the presence of high-altitude aerosols in planetary atmospheres. The IWF co-leads the upper atmosphere working group and is involved in testing the mission's performances, advancing the atmospheric retrieval tools and improving the inference of fundamental parameters (e.g. mass, age) of the host stars.

ATHENA

ATHENA (Advanced Telescope for High-ENergy Astrophysics), is ESA's second large (L-class) mission in the Cosmic Vision 2015-2025 plan. Its objective is to study hot gas in clusters and groups of galaxies and the intergalactic medium, to determine how ordinary matter assembles into large-scale structures. The second topic is the growth of black holes and their impact on the universe. The observations in the X-ray range of the electromagnetic spectrum will help to understand the high energetic processes close to the event horizon of black holes and provide more details for the baryonic component, locked in ultra-hot gas.

The institute will contribute to the *Wide Field Imager (WFI)* with the development of the *Central Processing Module (CPM)*. The study concerning processor performance has been completed in 2022. The instrument design was continued and further optimizations envisaged to reduce mass and space, but also optimize costs. Due to the unclear situation with the *ATHENA* mission, the consortium decided to build a so-called demonstrator. The goal is to have prototypes for all instrument sub-units, to establish a working instrument, demonstrating its capabilities and performance. The team submitted a proposal within the ASAP#19 call to fund the necessary EEE components for the demonstrator.

NON-DETECTION OF METASTABLE HELIUM IN THE ATMOSPHERE OF THE HOT JUPITER WASP-80B

Because of its proximity to an active K-type star, the hot Jupiter WASP-80b is a possible excellent target for detecting and measuring HeI absorption in the upper atmosphere. Four transits of WASP-80b have been obtained to look for absorption from the near-infrared metastable HeI triplet. Furthermore, a three-dimensional hydrodynamic model has been employed to understand the observational results. No signature of planetary absorption at the position of the HeI triplet has been found, setting an upper limit of 0.7% (95% confidence level). Assuming a solar He to H abundance ratio, HeI absorption should have been detected. Considering a stellar wind 25 times weaker than solar, the non-detection could be reproduced only by assuming a He to H abundance ratio about 16 times smaller than solar. Instead, considering a stellar wind ten times stronger than solar, the non-detection could be reproduced only with a He to H abundance ratio about ten times smaller than solar. WASP-80b is not the only planet with an estimated subsolar He to H abundance ratio, which suggests the presence of efficient physical mechanisms (e.g. phase separation, magnetic fields) capable of significantly modifying the He to H content in the upper atmosphere of hot Jupiters. The planetary macroscopic properties and the shape of the stellar spectral energy distribution are not sufficient for predicting the presence or absence of detectable metastable He in a planetary atmosphere, since the He abundance also appears to play a major role.

Fossati et al., A&A, 658, A136, 2022.

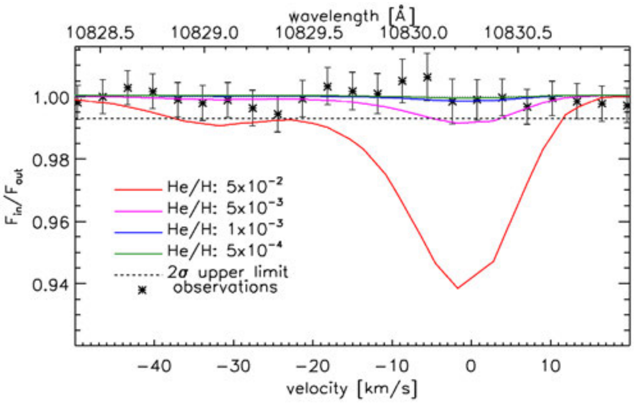

Comparison between observations and simulations computed for different values of the He to H abundance ratio.

THE RETRIEVAL OF HAT-P-11B'S ATMOSPHERE WITH THE BART CODE

The Bayesian Atmospheric Radiative Transfer (BART) code is an open-source, open-development package to characterize extrasolar planetary atmospheres. BART combines a thermochemical equilibrium abundance (TEA), a radiative transfer (TRANSIT), and a Bayesian statistical (MC3) module to constrain atmospheric temperatures and molecular abundances for given spectroscopic observations. The TRANSIT package is an efficient line-by-line radiative transfer code for one-dimensional atmospheres producing transmission and hemisphere-integrated emission spectra. TRANSIT handles line-by-line opacities and collision-induced absorption from several sources. BART has been applied to the *Spitzer* and *Hubble Space Telescope (HST)* transit observations of the Neptune-sized planet HAT-P-11b. The analysis of the combined *HST* and *Spitzer* data generally agrees with those from previous studies, finding atmospheric models with enhanced metallicity (≳100x solar) and high-altitude clouds (≲1 mbar level). When analyzing only the *HST* data, the models favor high-metallicity atmospheres, in contrast with analyses, which arises probably from different choices of chemistry modeling and the enhanced parameter correlations found when neglecting the *Spitzer* observations.

Cubillos et al., PSJ, 3, 81, 2022.

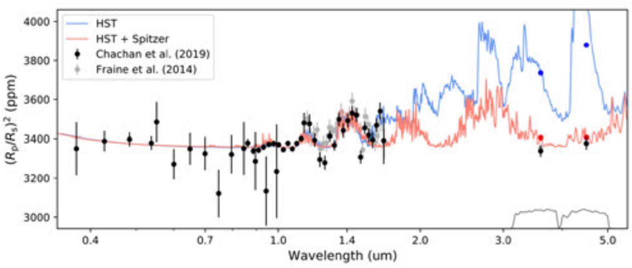

HAT-P-11b *HST* and *Spitzer* transmission spectra collected from the literature in comparison with BART best-fitting synthetic spectra computed with and without considering the *Spitzer* observations. The gray curves at the bottom show the Spitzer transmission filter.

ORIGIN AND EVOLUTION OF AIRLESS BODIES IN THE INNER SOLAR SYSTEM AND BEYOND

The origin and evolution of different airless bodies from large planetesimals, planetary embryos, the Moon, Mercury and recently discovered hot, rocky and most likely magmatic exoplanets such as CoRot-7b, HD 219134 b and 55 Cnc e were investigated. It is shown that one has to consider all the relevant radiation and plasma parameters of the host star that act together with the particular planetary body so that the formation of surface-related silicate atmospheres and exospheres will evolve. It is shown that magma ocean degassed silicate atmospheres or thin gaseous envelopes from planetary building blocks, or airless bodies in inner system will experience an extreme plasma interaction with its environment and the stellar wind (see figure). One can see that the silicates that are released in the exosphere of hot rocky exoplanets that orbit in close distances around their host stars should produce huge tails with distances of up to about 400 000 kilometers, as in the case of sodium at Corot-7b. The field of exoplanet mineralogy will be opened if one can observe particles that belong to the silicate exospheres of such planets. It is discussed, what can be learned from the study of the solar wind interaction of Mercury's exospheric environment by *BepiColombo* in comparison with the expected observations at hot rocky exoplanets with silicate atmospheres by (future) space telescopes such as *JWST* or *ARIEL* and ground-based telescopes and instruments like *SPHERE* and *ESPRESSO* on the *VLT*, and vice versa.

Lammer et al., Space Sci. Rev., 218, 15, 2022.

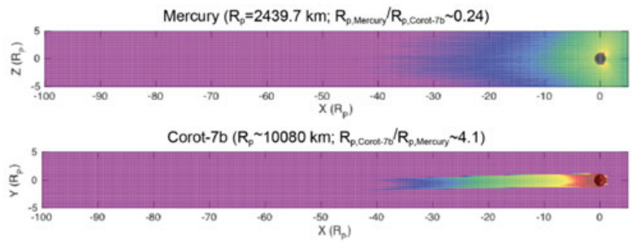

Top panel: Simulated solar wind interaction with Mercury's sputtered Na tail. Bottom panel: A similar scenario but with the expected stellar wind plasma interaction of the close-in hot exoplanet Corot-7b, which is about 4 times larger than Mercury. The x and z-axis are given in planetary radii. In the simulation a potential magma ocean on the planet's dayside is neglected. Such a magma ocean and a related outgassed silicate atmosphere will modify the exospheric configuration around the planet.

GLOBAL 3D MULTI-FLUID SIMULATION OF ESCAPING ATMOSPHERES OF CLOSE-IN EXOPLANETS

A 3D self-consistent multi-fluid hydrodynamic model was developed for the simulation of H-He expanding upper atmospheres of hot close-orbit exoplanets (hot Jupiters and warm Neptunes). The model enables calculation of the related transit absorption of exoplanets in various spectral lines, including Lyα, metastable HeI 10830 Å line, and the lines of different heavy trace elements (e.g., O, C, Si, Na, Ca, Mg, K, Fe). In the most general case, an upper atmosphere of the modeled exoplanet is taken to consist of H, H^+, H_2, H_2^+, H_3^+, He, He^+ and He_2^+ components, for which the equations of continuity, momentum, and energy are solved numerically, and the full set of related chemical reactions is calculated. For each host star, an appropriate XUV spectrum in the range of 10-912 Å is used, including the appropriately estimated near-IR and near-UV parts. The transmission and attenuation of the stellar radiation flux is calculated in each spectral interval in accordance with the wavelength-dependent absorption cross-sections. Along with the escaping exoplanetary atmosphere, the model simulates, with the same numeric algorithms, the stellar wind (SW), enabling therefore a self-consistent global view of the interacting planetary and stellar material flows at the scale of the entire stellar system.

For the hot Jupiter HD189733b, the influence of a high-energy stellar radiation flux, SW, and Lyα cooling were studied, aimed to reproduce the available observations. It was found that the measured width of the HeI absorption profile can be achieved in simulations only for the energy-limited escape regime of the upper atmosphere, realized with significantly reduced Lyα cooling. Based on the performed simulations versus observations, the helium abundance in the upper atmosphere of HD189733b was constrained to rather low values of He/H ~ 0.006.

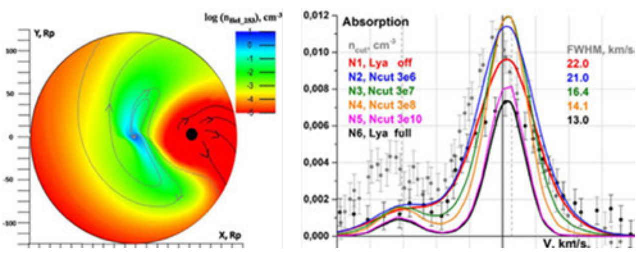

Left: Distribution of HeI density in the orbital plane of HD189733b, simulated for weak SW and reduced Lyα cooling; Right: HeI profiles simulated for He/H = 0.006 and different degrees of Lyα cooling, parametrized via cutoff hydrogen density n_{cut}.

It was also shown that under the SW conditions similar to those at the Sun, the Lyα absorption at the level of ~7% takes place mostly within the Roche lobe due to thermal line broadening, whereas for an order of magnitude stronger SW, a significant absorption of ~15% at high blue-shifted velocities of up to ~100 km/s happens in the bow shock region, due to Doppler broadening. The performed simulations enabled explaining of the difference between the observations performed in different campaigns by supposing the varying stellar activity and the related fluctuations of the ionizing radiation and the SW.

Rumenskikh et al., Astrophys. J., 927, 238, 2022.

For the system of warm Neptunes TOI-421b,c, a significant escape of upper atmospheres was shown for both planets. The double shock structures, generated around the planets in course of their interaction with the SW plasma flow were revealed. According to the performed simulations, the detectable level of stellar Lyα absorption during the transits of planets can be reached only for the moderate or strong SW with sufficiently high density. In this case, the energetic neutral atoms provide significant absorption at the high velocity blue wing of the Lyα line, whereas the corresponding transit light curves exhibit an early ingress and extended egress features. At the same time, the metastable HeI absorption at the position of the 10830 Å line was shown to reach the detectable levels only for the farthest planet (TOI-421c), if the helium abundance appears comparable to the solar value.

Berezutsky, MNRAS, 515, 706-715, 2022.

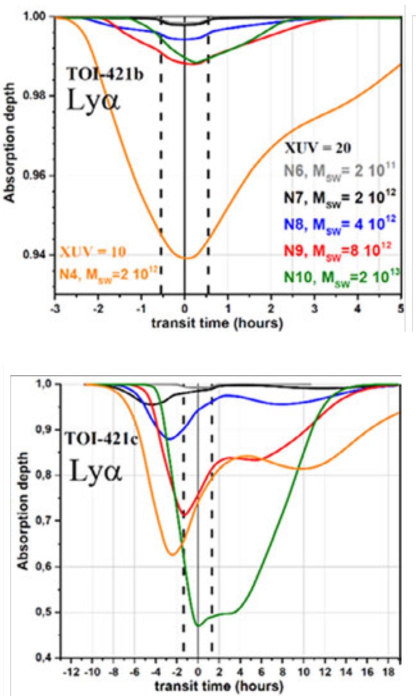

The TLCs of TOI-421b (top) and TOI-421c (bottom) in Lyα averaged over the blue wing of the line [-250; -100] km/s, obtained for different densities of SW and a typical for TOI-421 XUV flux. Dashed vertical lines mark the first and the forth contact points of the transits.

TiO_2 NANO-CLUSTERS AS CLOUD FORMATION SEEDS IN EXOPLANET ATMOSPHERES

Cloud particles form when a supersaturated gas condenses on the surface of a nucleus. On most terrestrial planets these nuclei originate from the planetary surface. On gaseous exoplanets such as hot Jupiters however, these nuclei need to be produced from the gas phase. This happens through a process called nucleation, where individual molecules of a species, in our case TiO_2, collide and stick together to form clusters. If these clusters are thermally stable, they grow until they are big enough to achieve solid state properties. At this point, they may serve as cloud condensation nuclei (CCN) and trigger the formation of large-scale clouds.

In order to calculate the formation rate of these CCN, accurate thermochemical data of all involved small clusters are needed, such as their geometry and binding energy. These cluster properties are calculated through computationally intensive quantum-chemical density functional theory (DFT). Because there are several parameterizations for DFT, 129 different versions were tested. The one that best reproduced laboratory measurements was then used. A total of 90,000 candidate isomers for cluster sizes up to size 15 ($Ti_{15}O_{30}$) was created. They were optimized using a self-developed hierarchical approach to find the most energetically favorable isomers for each cluster.

When compared to older cluster data, it was found that using the new results, nucleation stops at a lower temperature and becomes inefficient at a higher altitude in the exoplanet atmosphere and raises the theoretical lower boundary of cloud particles.

Sindel et al., A&A, 668, A35, 2022.

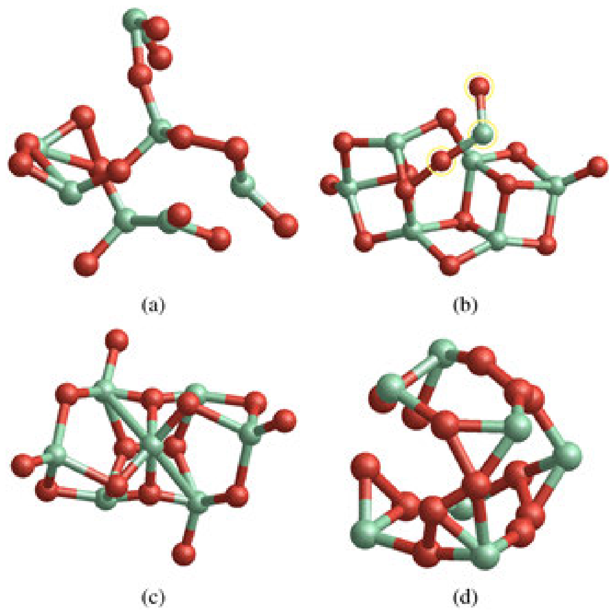

Four example candidate isomers for a cluster of seven TiO_2 molecules (Ti_7O_{14}). These candidates were generated and then optimized with the hierarchical approach to find their respective binding energies.

MODELING CLOUD PARTICLE COLLISIONS IN EXOPLANET ATMOSPHERES

Clouds remain a key challenge for exoplanet observations, altering the local atmospheric composition through condensation as well as obscuring deeper atmospheric layers. Cloud particle-particle collisions can significantly alter the cloud particle porosity, size and number density distributions within an atmosphere. Fully consistent modeling of cloud particle collisions alongside nucleation, condensation, evaporation, and settling is computationally intensive. HyLandS is a hybrid moment-two bin, kinetic cloud formation model including a parameterization for particle-particle collisions that was inspired by modeling approaches applied in planet-forming disks.

Cloud particle-particle collisions are found to be important at the deep cloud deck. Turbulence induced relative velocities between cloud particles is the dominant driver of collisions. Furthermore, collision velocities are large enough for exoplanet atmospheres to induce fragmentation of cloud particles. For the higher gravity atmospheres of brown dwarfs, there is either no significant change when including collisions, or only a small amount of coagulation.

The optical depth of clouds is computed for mixed composition cloud particles using Mie theory. Fragmentation of cloud particles in exoplanet atmospheres enhances the cloud optical depth at optical wavelengths and in the mid-infrared where the silicate features are located. These results challenge assumptions about cloud particle material composition or size derived from observations, and show that complex models involving all microphysical processes are necessary to fully interpret the next generation of observations.

Samra et al., A&A, 663, A47, 2022.

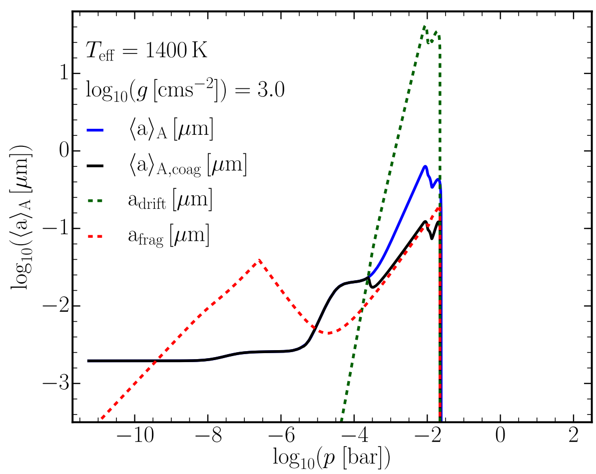

Average cloud particle sizes, $\langle a \rangle_A$ [μm], for a cool exoplanet atmosphere. Collisions (black line) reduce the average particle size when compared to a no collisions (blue line). This results in more, smaller cloud particles, which may have implications for upcoming observations of exoplanets.

A 3D GENERAL CIRCULATION MODEL TO FOLLOW ENERGY TRANSPORT OVER CENTENNIAL TIME SCALES

The state of the interior of hot Jupiters, that orbit their host star very closely, is an open question: Their interiors appear to be much hotter than those of solar system gas giants of similar age. Consequently, hot Jupiters have anomalously large planetary radii and therefore have bulk densities that are at least 0.25 times smaller than Jupiter and Saturn in our own solar system.

To explain the "hot Jupiter radius anomaly" or "inflation" three mechanisms are proposed: a) delayed cooling from their hot birth state, b) magnetic interactions and c) downward transport of energy from the strongly irradiated atmosphere into the interior.

A novel 3D General Circulation Model (GCM) has been developed that is numerically highly efficient and at the same time accurate enough to follow the atmospheric energy transport. The model is in excellent agreement with other 3D GCMs for the two hot Jupiters test cases, WASP-43b and HD 209458b. This new 3D GCM was applied to the inflated ultra-hot Jupiter WASP-76b that will be observed with the *James Webb Space Telescope (JWST)*. The hypothesis that energy from the irradiated atmosphere can be transported downwards via large scale circulation was tested. WASP-76b was initialized with a very hot inner boundary at 10 bar (adiabat layer) and allowed to cool down over a simulation time of 235 years.

The 3D GCM predicted for the atmosphere of WASP-76b that the innermost atmosphere layers in such an inflated hot Jupiter would eventually stabilize on a "hot adiabat". This corresponds to an interior temperature $T_{int} > 500$ K due to downward transport of stellar energy from the very top of the atmosphere.

These simulations represent the longest 3D GCM study to date that tackles thermal evolution of hot Jupiters. The consistently solved full radiative transfer allows to follow the thermal evolution of such a planet over centennial time scales, hence, to model the climate of an extrasolar planet. These 3D simulations demonstrated that stellar energy alone can not maintain a "hot adiabat" scenario which was proposed in the literature in order to explain the radius inflation of Jupiters. Instead, it was found that our WASP-76b model cools beyond the hot adiabat and stabilizes on a "cool adiabat".

Thus, it can be concluded that hypothesis c) (downward transport of stellar energy) is not responsible for the inflation of hot Jupiters. If it is not possible to transport enough energy downward to heat the interior even in the ultra-hot exoplanet WASP-76b with its very high atmosphere temperature of 2200 K, then such a transport is not able to heat up the interior of most other hot Jupiters that receive less stellar energy than WASP-76b. Thus, an additional source of energy likely induced by magnetic mechanisms is required to explain the hot Jupiter radius anomaly.

Schneider et al., A&A, 664, 56, 2022.
Schneider et al., A&A, 666, L11, 2022.

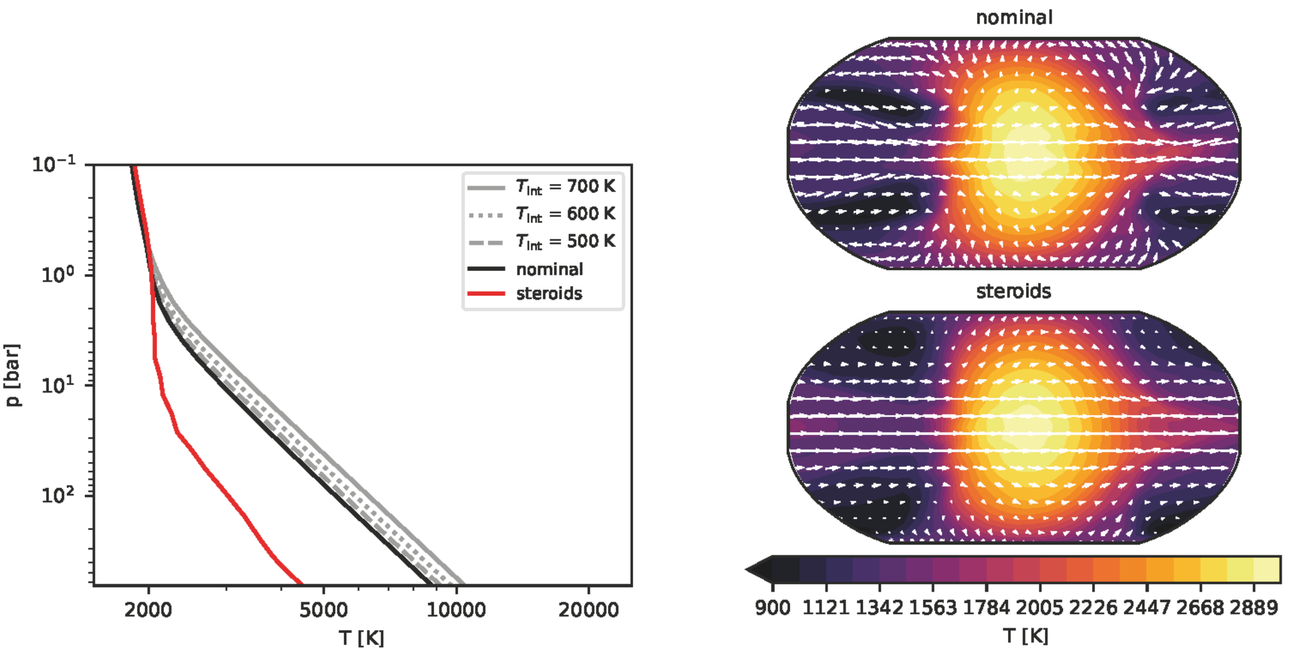

Left: Atmospheric temperature profiles for different interior temperatures (T_{int}, gray) for the ultra-hot Jupiter WASP-76b. The final temperature profile of the nominal model (black) after 86,000 days is shown which corresponds to $T_{int} \approx 434$ K. This is too cold to explain the inflation of this planet, ruling out downward energy transport as the source of inflation in this planet. Another model which settles on a cool adiabat (red) confirms this. Right: Overview of the two climate models (top: nominal, bottom: steroid), showing temperature profiles (color) and winds (white arrows) for the simulated WASP-76b at p = 1.2 bar. Depending on the adiabat in the interior, changes in the wind jet width and speed can appear.

INFLUENCE OF SURFACE COMPOSITION ON THE DIVERSITY OF CLOUD CONDENSATES

Our ability to observe the chemical composition of exoplanets is limited to the transparent upper layers of their atmospheres. In particular, the condensation of clouds can lead to an optically thick cover, which renders any direct spectral observations of the lower atmospheres quite difficult, including the surface properties of rocky exoplanets connected to our search for habitable exoplanets. How can we then still find out the existence of liquid water on the surface and the habitability of rocky exoplanets? Based on thermochemical equilibrium models, the cloud formation over various common crust compositions at surface temperatures between 300 K and 1000 K was simulated. A large variety of cloud condensates was found, from liquid and crystalline water (H_2O), graphite (C), ammonium chloride (NH_4Cl) and ammonium hydrosulfide (NH_4SH), as well as halides (KCl, NaCl) and sulphur compounds like troilite (FeS) and disulphur (S_2). The stability and chemical composition of these cloud layers is found to depend critically on surface pressure and temperature, as well as on the element composition of the surface. Thus, an observational determination of cloud properties would allow to characterize some surface properties, for example it is found that the occurrence of certain sulphur compounds as clouds requires high surface pressures as we know is true for the case of Venus.

Herbort et al., A&A, 658, A180, 2022.

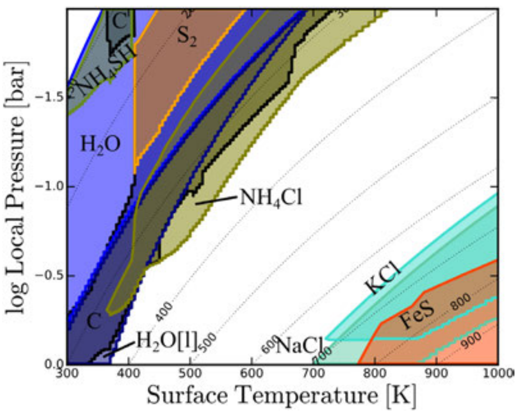

The expected cloud materials as function of pressure in the atmosphere (vertical axis) and surface temperature of the rocky planet (horizontal axis) when the rock is assumed to be composed of the CI chondrite element mixture. There is a remarkable lack of cloud condensations close to the surface between 400 K and 700 K.

MIXING AND DIFFUSION IN PROTOPLANETARY DISC CHEMISTRY

Mixing and diffusion are important processes in chemical models for planetary atmospheres, but have only rarely been included in protoplanetary disk models so far. An iterative scheme was developed to solve the respective coupled second-order reaction-diffusion equations in the ProDiMo thermo-chemical models. A series of five TTauri disk models were presented with the mixing parameter α_{mix} between 0 and 10^{-2}, taking into account: (a) the radiative transfer feedback of the opacities of icy grains that are mixed upwards; (b) the feedback of the changing molecular abundances on the gas temperature structure caused by exothermic reactions and increased line heating and cooling; and (c) the impact on observables like Spectral Energy Distributions (SEDs), infrared line emission spectra, and CO channel maps as observable with ALMA.

Only for the most abundant species, such as H_2, CO, CH_4, the neutral atoms in higher layers, and the ices in the midplane, the transport rates can locally dominate over the chemical production and loss rates. These species are hence transported away from their regions of maximum concentration. At the locations where these chemicals are finally destroyed, for example by photo-reactions, their reaction products fuel the local chemistry, creating an active ion-molecule chemistry, with a rich mixture of ices, molecules and ions and new, unusual chemical formation pathways. As a result, more molecules like OH and H_2O in the upper disc layers are produced, important for molecular observations in the infrared, for example with *JWST*. Already for weak mixing ($\alpha_{mix}=10^{-4}$), ices are mixed up sufficiently high to allow for direct photon-ice interactions, which produces observable spectral emission features.

Woitke et al, A&A, 668, A164, 2022.

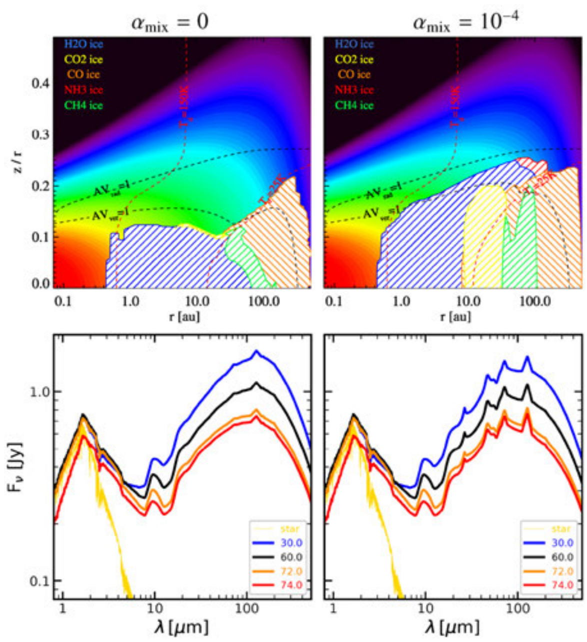

Influence of vertical turbulent mixing on the ice abundances and spectral ice emission features as observable with *JWST*. Top: Location of the ices in radius r and height z over the midplane of the disk. The background colors show the nuclei density n⟨H⟩ from 10^2 cm^{-3} (black) to 10^{16} cm^{-3} (red). Bottom: Calculated SEDs for different inclination angles at a distance of 140 pc.

Exterior view of the ESA SLR Station during night time satellite laser ranging operation at Teide Observatory (© ESA).

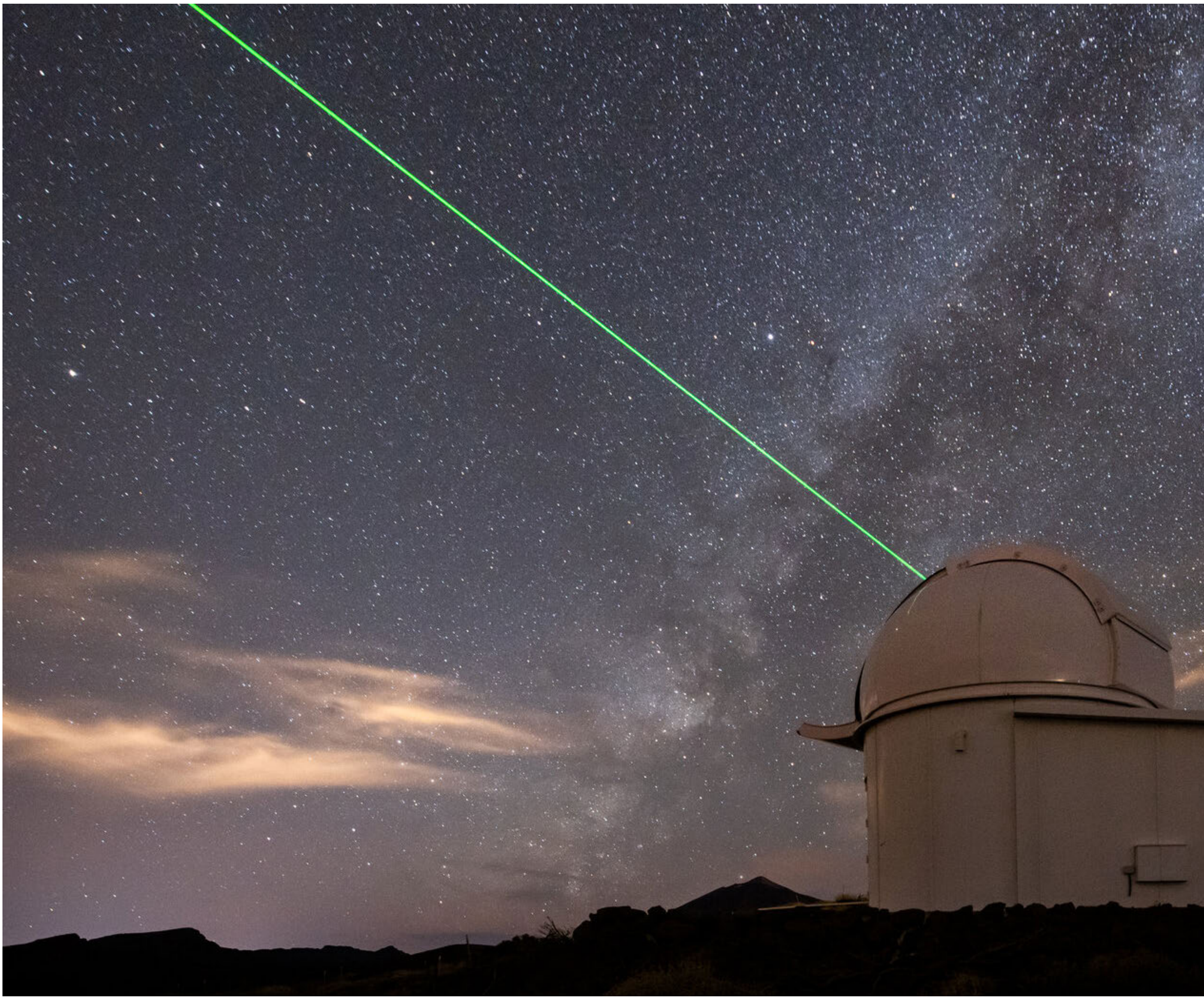

SATELLITE LASER RANGING

The IWF's Satellite Laser Ranging (SLR) station at the Lustbühel Observatory in Graz works in the areas space ecology and safety by tracking more than 150 targets which are equipped with laser retro-reflectors. In 2022, the new Izaña-1 SLR station was handed over to ESA with the main laser ranging and detection components fabricated in Graz. Within the RADS project, a tool was developed to simulate SLR residuals of satellites in arbitrary rotation conditions to efficiently design backup retroreflectors on future satellite missions. The spin period and attitude of the defunct *Jason-2* satellite was studied throughout ESA's tumbling motion project.

TENERIFE SLR STATION ACCEPTANCE

An increasing demand of facilities capable of doing satellite laser ranging, space debris laser ranging or optical communication pushes the demand to create accurate, cost-efficient, reliable and yet simple components to be integrated into SLR stations.

In 2022, the new Izaña-1 SLR station on Teide passed the final acceptance test and was handed over to ESA. The SLR group of the IWF was developing the core components of the SLR station - the laser and detection package. For these packages a modular approach is used primarily based on Commercial-Off-The-Shelf components. The whole fabrication process ranging from optical raytracing simulation, computer aided design, integration of the components to the testing and validation of the equipment tracking and ranging to satellites is performed at the IWF.

Laser packages consist of the laser with two separate beam expansion telescopes with a collimated part in between, which can be used for imaging of e.g. the backscattered laser beam or the visualization of stars for alignment purposes. A combination of wave plates and polarizing beam splitters allow for power adjustment and measurement. One of the lenses is mounted on an electronically movable lens holder which gives the possibility of flexible variation of the beam divergence and a tip-tilt mirror enables remote direction control of the laser beam. Furthermore, start pulse detection is integrated.

Detection packages are mounted in one of the Nasmyth foci of an astronomical telescope. In the beam path direction, the field of view iris is followed by optics to collimate the entering photons to approx. 1 cm with some flexibility to tune the telescope's field of view. Dichroic mirrors separate the incoming light w.r.t. wavelength and distribute it to various sensor modules (e.g. single photon avalanche detectors for green and infrared, single photon light curve detection, optical guiding cameras and beam adjustment cameras). Both sensor and detection package operate a temperature control system and the necessary interfaces to connect to e.g. event timers, power supply or control pc.

The IWF is also involved in the future upgrade of the Izaña station allowing it to perform space debris laser ranging. Within the activity which started 2022, the IWF is currently developing a new type of large aperture beam expansion telescope facilitating a compact design with reduced beam divergence to be embedded in a split configuration transmit and receive system.

RETROREFLECTOR-BASED ATTITUDE DETECTION

Defunct satellites or space debris can begin to rotate due to numerous forces acting on the body. A prerequisite for future removal missions is a profound knowledge of the orbit and attitude of such objects. Rotational parameters can be measured utilizing different techniques such as satellite laser ranging (SLR), space debris laser ranging, radar or light curves. Within the ESA study Retroreflector-based Attitude Detection System (RADS) the design and placement of additional corner cube retroreflectors (CCRs) on side faces of satellites was studied. Within the International Laser Ranging Service (ILRS) approximately 40 SLR stations are cooperating generating precise ranging data of a large number of satellites. The placement of CCRs on future satellite missions would allow accurate monitoring of the tumbling behavior.

A modular simulation tool is introduced allowing to simulate SLR residuals (the difference between the predicted and measured ranges to the CCRs). Rotating satellites produce a distinct periodical residual pattern connected to the movement of the CCRs with respect to the center of mass of the satellite. Different parameters (satellite, orbit, CCRs, rotation period, rotation axis, reference coordinate frame) can be arbitrarily adjusted, allowing to design CCRs according to specific needs of the satellite operator. In the figure below a box-type satellite body is rotated with a rotation period of 150 seconds with CCRs arranged approx. 1 meter from each other. The CCRs are color-coded with respect to the surface they are belonging to. Due to the rotation a repeated transition from reflections of surfaces with 2 CCRs (green), 4 CCRs (black) and 1 CCR (purple) is visible. Based on the placement of the CCRs, from the residual pattern it is possible to identify visible surfaces, determine the rotation direction or period and to draw conclusions on the laser beam incident angle.

Steindorfer et al., In Proc. 73rd IAC, 2022.

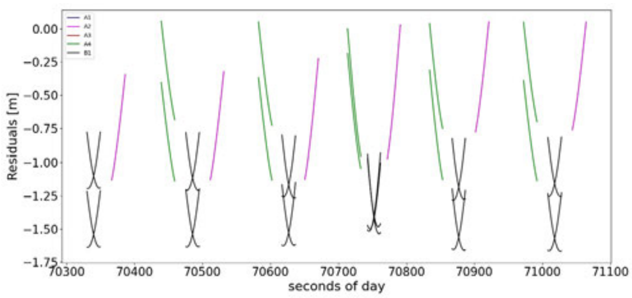

Simulated SLR residuals of a box-type satellite. The individually colored tracks belong to signals from CCRs of the individual surfaces of the satellite.

JASON 2 TUMBLING ANALYSIS

Within the ESA project "Tumbling Motion Assessment for Space Debris Objects" attitude dynamic characterization is studied with state-of-the-art high-rate Satellite Laser Ranging (SLR) and photon counting systems operating at the single photon sensitivity level. Space debris observations support physical research in Space Situational Awareness to better understand the behavioral characteristics for the development and validation of accurate environmental interaction models. Especially long-term orbit determination, conjunction analysis, reentry and impact predictions are of interest. Emerging technologies that can benefit from space debris observation and characterization are: 1) Rendezvous and Proximity Operations for satellite servicing, refueling and mission extension, 2) Active Debris Removal services for safety and sustainability of space operations, including human flight.

Graz performs observations in the visible and near-IR bands at high temporal resolution that reveals short duration signal features not detectable by other systems including millisecond glints of sunlight reflected off tumbling satellites. High-rate data is analyzed applying a set of post-processing methods that determine frequency and periodicity spectra to characterize in-orbit behavior of the observed space debris population. The methods include Savitzky-Golay filters, fast Fourier transformation, phase dispersion minimization or autocorrelation. Tiny shifts in the observed signal lines throughout the pass are known as an apparent rotation effect and can be used to determine the inertial orientation of the satellite's spin axis. The case of the tumbling and decommissioned satellite Jason-2 (orbital altitude of 1,300 km) demonstrates fusion of SLR and photometric data. The combination of different observational techniques improves accuracy of the fitted trend (see figure), documenting a spin-up from 75 s to 40 s within 1.5 years. Such spin energy increase over time can e.g. result from solar radiation pressure continuously exerting force and torque on the solar panels.

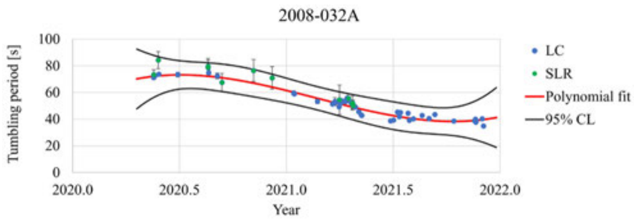

Tumbling period trend of decommissioned *Jason-2* satellite studied based on Graz satellite laser ranging and light curve data.

TECHNOLOGIES

NEW DEVELOPMENTS

One possible aspect to reduce costs of space exploration and hence allowing for more frequent missions is to reduce the spacecraft size and consequently the launch masses. Scientific instruments also have to decrease their resource requirements such as volume, mass, and power, but at the same time achieve at least the same performance as heritage instruments. Therefore, the development of new instrument technologies is essential for competitive and excellent space research.

NEXT GENERATION ASPOC

For future science missions, active spacecraft potential control down to <10 V is crucial to be able to operate sensitive scientific payloads. This does not only apply to large and medium-sized spacecraft, but also to micro- and nano-spacecraft, such as CubeSats. The IWF, together with FOTEC, started a two-year technology study with the goal to develop a miniaturized version (50% power, 40% mass) of the *ASPOC* instruments built for NASA's *MMS* mission, which, eight years after launch, are still operating flawlessly.

In a final review held by ESA, the presented roadmap to reach TRL-7 (Technical Readiness Level 7) emphasized that all goals of the study have been met:

- Modular design allows an optional operation with an ion or electron emission module
- Tungsten multi-needle emitters replace capillary emitters (increased mass efficiency)
- The used Indium-Gallium alloy reduces the heater power consumption by 68 % compared to *MMS*
- Improved wetting properties, enabling the feeding system to achieve increased reliability
- Revised electronics design results in reduced mass and less power consumption

These values qualify the *next-generation ASPOC (ASPOC-NG)* as a candidate for the *DEBYE* mission to study.

The *ASPOC-NG* mounted on in the FOTEC test chamber (© OeAW/IWF/Jeszenszky).

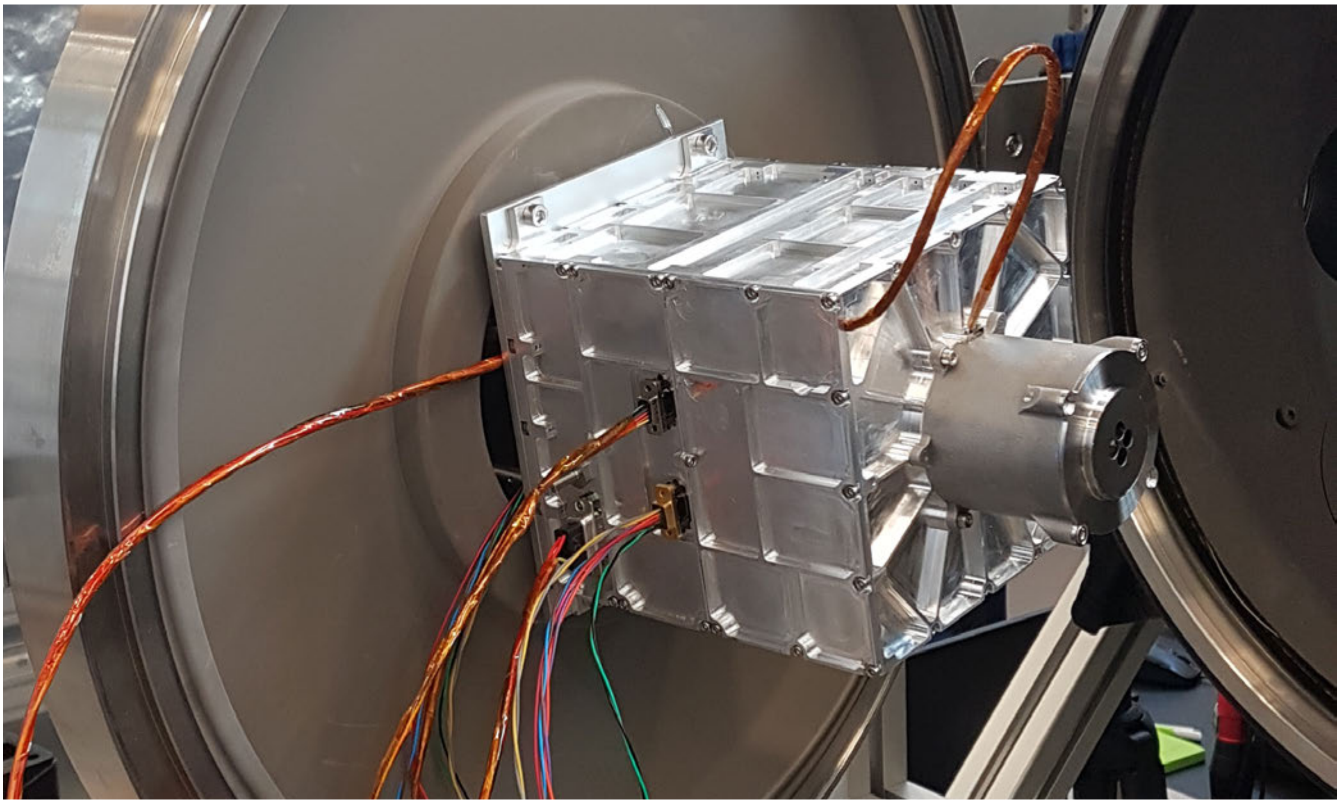

MAGNETOMETER FRONT-END ASIC

The IWF and the Institute of Electronics of the Graz University of Technology (TUG) are collaborating on the next generation of the space proven Magnetometer Front-end ASIC (MFA). It includes the readout electronics for magnetic field sensors which is optimized in terms of size and power consumption. The next generation Application Specific Integrated Circuit (ASIC) will feature an improved dynamic range and increased radiation hardness. It will be space qualified in the frame of the *FORSESAIL* mission.

In 2022, a triple-axis feedback chip (MFA-4.3), with each feedback channel containing a high performance digital-to-analog converter (DAC) and a fully differential current source, was manufactured and extensively tested. XFAB Silicon Foundries was selected as chip manufacturer because of the excellent noise performance of the transistor elements which come with a well-defined radiation characterization. The measured signal-to-noise ratio (98.3 dB) and total harmonic distortion (80 dB) of the MFA-4.3 are unfortunately lower than expected from the simulation results (104.2 dB and 100.2 dB, respectively). The cause of the performance limitations was evaluated and design modifications were implemented in the next prototype microchip (MFA-4.4). It was released for production in November 2022. Simulation results indicate a signal-to-noise ratio of 116 dB and a total harmonic distortion of nearly 100 dB which would fulfill the initially defined requirements. Only one feedback channel is implemented on the MFA-4.4 in order to avoid inter-channel interference and to reduce the complexity of the digital interface. Instead, it includes a single-channel forward path with a low noise input amplifier, an N-path filter stage for the extraction of the amplitude modulated signal from the fluxgate sensor and a low-bit analog-to-digital converter.

The MFA-4.4 front-end chip occupies a total area of about 4.6 mm^2.

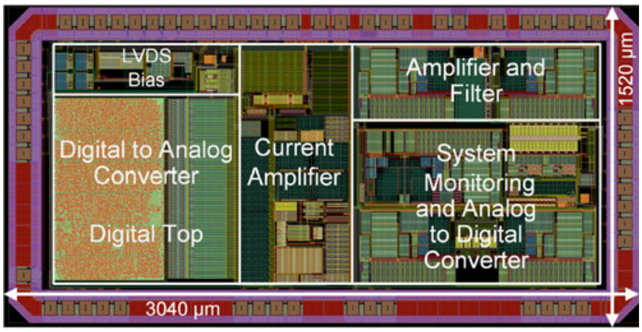

Layout of the MFA 4.4 microchip. It contains one feedback (digital-to-analog converter and current source) and one forward path (low noise input amplifier, filter with synchronous demodulator and a low-bit analog-to-digital converter).

MACHINE LEARNING ACTIVITIES

Funded through the European Commission's Horizon 2020 program, Europlanet 2024 Research Infrastructure (RI) provides free access to planetary simulation and analysis facilities, data services and tools, a ground-based observational network and program of community support activities. The work package "Machine Learning (ML) Solutions for Data Analysis and Exploitation in Planetary Science", led by the IWF, develops ML powered data analysis and exploitation tools optimized for planetary science and integrates expert knowledge on ML into the planetary community. The goal is to build a multi-purpose toolset for ML-based data analysis that will be applicable to a range of scientific research questions in planetary science with minor or easily achievable customization efforts. The scientific research questions range from the automatic detection of various features (e.g., bow shock and magnetopause crossings around Mercury and Earth, interplanetary mass ejections in in-situ solar wind observations or surface features on Mars - see figure) to different classification problems (e.g., surface composition on Mercury, plasma wave emissions, or mineral identification).

Left: *Mars Reconnaissance Orbiter/HiRISE* image of mounds on Mars. Middle: Ground truth mask. Right: Predicted mask.

Machine learning software technology was also explored within the Marie Curie Innovative Training Network for European Joint Doctorates (MC ITN EJD) CHAMELEON. A tool for fitting spectral energy distributions for planet-forming disks is developed in order to utilize large sets of ProDiMo (PROtoplanetary DIsk MOdel) thermo-chemical disk models.

INFRASTRUCTURE

Space-born instruments are exposed to harsh environments, e.g., vacuum, large temperature ranges, radiation, and high mechanical loads during launch. They are expected to be highly reliable, providing full functionality over the entire mission duration, which could last for more than a decade.

The IWF operates several test facilities and special infrastructure for the production of flight hardware. A high-performance computer helps the scientists to cope with the enormous data, which have to be analyzed for space missions.

For manufacturing and assembly of the electronics, in particular the flight units, very often specific mechanical tools and jigs are necessary. In 2022, the IWF decided to purchase and install a 3D printer, to produce these jigs and support tools in house. Typical applications are building prototypes of the electronics housings, for a first fit test and support structures used during assembly. Another application is the protection of components, in particular those from 3D-Plus during, the pre-tinning process. These components are surfaces very sensitive against tin splatter, because of their electrical interconnection traces at the outer surface. All surfaces are protected by thin walled caps, made by 3D printing.

For further information on the IWF infrastructure refer to www.oeaw.ac.at/en/iwf/institute/infrastructure.

In the IWF vacuum lab (© OeAW/Klaus Pichler).

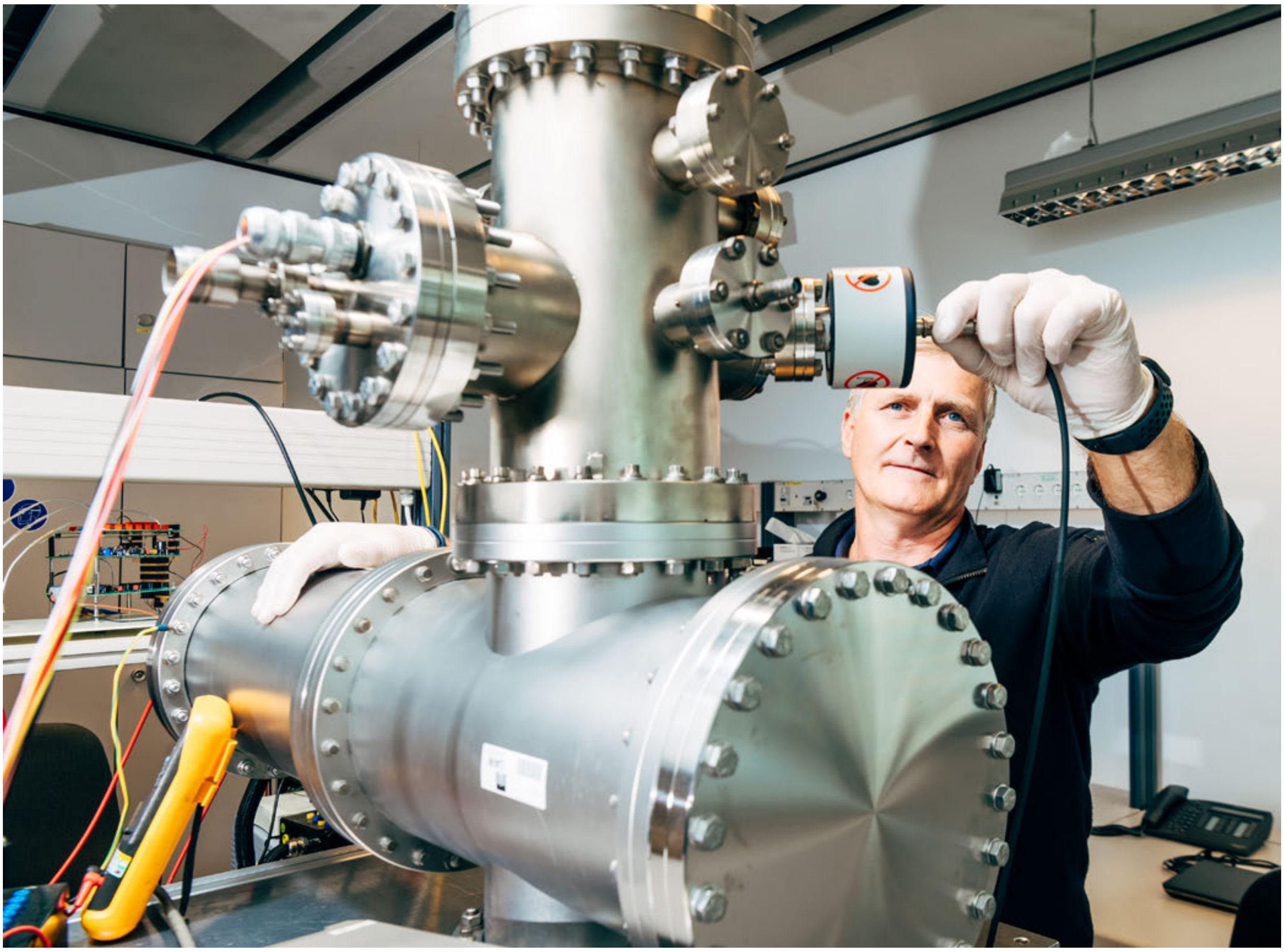

Impressions from the IWF birthday party © IWF/Harry Schiffer).

IMPACT BEYOND SCIENCE

IWF GRAZ. LEADING AUSTRIA INTO SPACE. SINCE 1971.

As a dependable partner for international space agencies, the IWF has been successfully leading Austria into space for more than 50 years. With scientific know-how and high-precision instruments, the IWF is on board of numerous spacecraft exploring our solar system and our home galaxy, the Milky Way.

The achievements of the institute have contributed significantly to Austria's development over the past five decades into an internationally recognized and important space center. This success was celebrated on 28 June 2022. Around 150 people gathered at the IWF in Graz. Congratulations were extended by OeAW President Anton Zeilinger, BMK Section Head Henriette Spyra, BMBWF Minister Martin Polaschek, Mayor Elke Kahr, Head of Science and Research of the Styrian Government Wolfgang Stangl, and ESA Science Director Günther Hasinger.

Among the guests were numerous representatives from science and industry, including TU Graz Rector Harald Kainz and University of Graz Rector Peter Riedler. Students of the Graz Model School were invited to the opening of the exhibition "Young Art Meets Space Research @ IWF". This special kind of ancestral gallery, composed by the young artists, showed portraits of all IWF directors and their fields of research.

Former Director Wolfgang Baumjohann gave a review of 50 years of the IWF. Director Christiane Helling took the guests on a journey into the future, from the solar system to the galaxy, to distant, alien worlds and presented the young talent program for interdisciplinary space and planetary sciences YRP@Graz. She thanked Children's Museum Director Jörg Ehtreiber and his team for their successful collaboration on the anniversary exhibition MISSION POSSIBLE!, which was shown in the CoSA - Center of Science Activities between 18 December 2021 and 11 September 2022 and attracted 15,514 visitors, of which over 4,000 were schoolchildren.

Christiane Helling cuts the birthday cake in the presence of Anton Zeilinger, Henriette Spyra, Harald Kainz, Peter Riedler, and Wolfgang Baumjohann (© IWF/Harry Schiffer).

YRP@GRAZ: IWF'S NEW YOUNG RESEARCHER PROGRAM

In 2022, the Young Researcher Program in interdisciplinary space science and planetary research YRP@Graz was inaugurated during IWF's 50th anniversary ceremony. The close collaboration between the IWF and the two local universities, Graz University of Technology (TU Graz) and University of Graz, helps future researchers to gain first experiences in science.

The program has two main pillars: "Pupils and Undergraduates" and "PhD Students". For the first pillar the IWF offers, e.g., lectures at schools or internships at the institute. The second pillar was designed to offer students a full PhD study in Graz. In the first year of YRP@Graz three PhD positions were opened which were funded by each of the three participating institutions. 23 interviewees of 14 nationalities were selected from 118 candidates who submitted their application through an anonymized application form.

The first cohort of YRP@Graz funded PhD students span a wide range of research topics:

- Substructures of Coronal Mass Ejections and their Solar Source Region
  PhD Student: Greta Cappello
  Supervisors: Manuela Temmer, Astrid Veronig (University of Graz)
- Quantum Vector Magnetometer based on the Nonlinear Hanle Effect
  PhD Student: Sunny Laddha
  Supervisors: Roland Lammegger (TU Graz), Werner Magnes (OeAW)
- The Gas and Dust in edge-on TTauri Disks
  PhD Student: Elena Suslina
  Supervisors: Peter Woitke, Christiane Helling (OeAW)

PUBLIC OUTREACH

The IWF is engaging actively in science education and public outreach.

Highlight of 2022 was the Austrian "Lange Nacht der Forschung" (LNF) on 20 May, which attracted almost 1000 people, visiting 13 stations in Schmiedlstraße and at the Lustbühel Observatory. Paper rockets were built and launched (see figure), labs and the planetary garden could be visited, "Martian faces" were soldered, and lectures on various themes were held non-stop. Through the telescopes of the Styrian Astronomers' Association (StAV), the visitors could observe solar activity by day and take a fascinating look at the starry sky by night. A huge THANK YOU goes to Johannes Kügerl and his students from BG/BRG Kirchengasse, students from the Graz University of Technology and last but not least the tireless students from Akademisches Gymnasium, Gymnasium Sacré Coeur Graz and BG/BRG Seebacher, who supported the IWF team so tirelessly.

During the LNF, hundreds of paper rockets were launched into "near-Earth space" (© OeAW/IWF/Scherr).

In summer, Martin Polaschek, Federal Minister for Education, Science and Research, and OeAW President Heinz Faßmann visited the IWF.

Werner Magnes, Christiane Helling, Martin Polaschek und Gunter Laky in the IWF cleanroom (© OeAW/Harry Schiffer).

On 30 September, Martin Volwerk and Daniel Schmid presented the mystery of Northern lights to the visitors of the European Researchers' Night in Vienna.

In the new IWF colloquium and seminar series, international guest speakers (colloquium) and local speakers (seminar) inform about current research topics and scientific results every Thursday at 2 pm. In 2022, 16 colloquia and 17 seminars were given, most of them are available on IWF's YouTube channel. The topics ranged from "The path to habitable worlds" to "In situ mass spectrometry with ESA's comet missions".

Throughout the year, several public lectures were given. Christiane Helling talked about the uniqueness of the Earth and the great variety of exoplanets at the Halle für Kunst, the Forum Joanneum Research, as part of the lecture series "Facetten der Physik" at the University of Graz and "alumniTalks" at TU Graz.

In the frame of the TUG/KFU Physics Colloquium Summer 2022 Peter Woitke talked about the physico-chemical processes in planet-forming disks. At URANIA Steiermark in Graz Wolfgang Voller talked about the autumn and winter sky. Bruno Besser opened the 23rd Annual Meeting of the Wiener Arbeitsgemeinschaft für Astronomie (WAA), presenting 50 years of IWF. Ruth-Sophie Taubner held a lecture on icy moons for the Burgenländische Arbeitskreis Astronomie (BAA) and gave an insight into the amazing world of being an astrobiologist in the European Astrobiology Institute (EAI) seminar series.

Following the OeAW young science initiative "Akademie im Klassenzimmer" Martin Volwerk visited the BG/BRG Leibnitz and introduced the phenomenon of the Northern light to the scholars. For the Science Academy Niederösterreich he held a workshop on planet Venus.

Topics discussed in the space blog of the Austrian newspaper "Der Standard" were life on Mars, *JWST's* "teething troubles", and Giuseppe *(Bepi)Colombo*.

In the Servus TV show "P.M. Wissen" Michael Steindorfer explained how space debris can be better localized.

OeAW President Faßmann during his visit of the IWF (© OeAW/IWF/Steller).

RECOGNITION

Christiane Helling was appointed as member of the Scientific Advisory Committee of the Leibniz-Institut für Sonnenphysik in Freiburg, Germany.

The long-time IWF Director Wolfgang Baumjohann was elected to the new OeAW Presidium Committee as President of the Division of Mathematics and Natural Sciences.

Christian Möstl received a Consolidator Grant from the European Research Council (ERC) to further expand his research on the practicable prediction of solar storms. The ERC Grant enabled him to form the new Austrian Space Weather Office of GeoSphere Austria in Graz.

Patricio Cubillos was awarded an associate position in the *CHEOPS* science team.

Kevin-Alexander Blasl received the Outstanding Student Presentation Award (OSPA) of the American Geophysical Union and Patrick Barth the Outstanding Student and PhD Candidate Presentation (OSPP) Award of the European Geosciences Union.

The newspaper Kleine Zeitung nominated Martin Reiß as "Head of the Year from Southern and Western Styria" in the category "Economy and Research". He is now working as a staff scientist at NASA's Goddard Space Flight Center.

MEETINGS

Wolfgang Baumjohann served as Vice Director and chair of the Program Committee of the Summer School Alpbach, which took place from 12 to 21 July and was dedicated to "Comparative Plasma Physics in the Universe". Every year, 60 students and about 25 lecturers and tutors from ESA's member states are invited to this meeting.

T. Amerstorfer, U. Amerstorfer, T. Balduin, M. Boudjada, G. Fischer, L. Fossati, Ch. Helling, G. Kargl, H. Lammer, H. Lecoq Molinos, R. Nakamura, M. Steindorfer, R.-S. Taubner, K. Torkar, and M. Volwerk were members of 25 scientific program and/or organizing committees at 15 international meetings.

LECTURING

In summer 2022 and in winter term 2022/2023 IWF members gave (online) lectures at the University of Graz, Graz University of Technology, University of Vienna, TU Braunschweig, and FH Wiener Neustadt.

Since 1 July 2023, the OeAW has got a new Presiding Committee: Christiane Wendehorst, Heinz Faßmann, Ulrike Diebold, Wolfgang Baumjohann (f.l.t.r., © OeAW/Peter Rigaud).

THESES

Besides lecturing, IWF members are supervising Bachelor, Diploma, Master and Doctoral Theses. In 2022, the following supervised theses have been completed:

Cappello, G.: Non-local thermodynamic equilibrium modelling of hot and ultra-hot Jupiter atmospheres, Master Thesis, Università degli Studi di Torino, 120 p., 2022.

Herbort, O.: Atmospheres of Rocky Exoplanets, Doctoral Thesis, University of St. Andrews, 171 p., 2022.

Kutnohorsky, V.: CCD Datenreduktion - Entwicklung der Datenreduktionspipeline für differentielle Photometrie am Lustbühel Observatorium, Bachelor Thesis, Universität Graz, 72 p., 2022.

Samra, D.: Mineral Snowflakes on Exoplanets and Brown Dwarfs, Doctoral Thesis, University of St. Andrews, 167 p., 2022.

INTERNSHIPS

During summer time, five high-school students performed an internship at the IWF. They worked on the exploration of the Earth's magnetosphere using satellite data, calibrated magnetic field sensors for current missions and tested new magnetometer developments, studied small cometary dust particles with *Rosetta/MIDAS* data, conducted functional and performance tests of the *PLATO/RDCU* electronics board, and analyzed and simulated light curves of satellites at Lustbühel Observatory. One university student worked on expanding 3D General Circulation Model results into the low-pressure regime of exoplanet atmospheres.

NEW PROJECTS

In 2022, the following third party projects with a budget greater than 100,000 EUR were acquired:

Project	Lead
FWF - Tracking magnetic helicity transport in the heliosphere	Y. Narita
FWF - The rise and fall of space plasma instabilities	C. Simon Wedlund
FWF - Improving Ambient Solar Wind Modeling and Prediction	M. Reiß
FFG - *MANiaC* Engineering (Functional) Models	H. Jeszenszky
FFG - Development of Fluxgate Magnetometer	A. Valavanoglou
DiGOS - GNNS SLR Testbed	M. Steindorfer
DiGOS - ELRS Upgrade	M. Steindorfer
EU - ExoHost	L. Fossati

IN MEMORIAM

CHRISTIAN HAGEN (8.10.1977 - 11.5.2022)

Dipl.-Ing. Christian Hagen passed away suddenly and unexpectedly on 11 May 2022. Christian was 44 years old.

Christian Hagen started his professional career at the Space Research Institute as a student on 1 April 2006. With a diploma thesis written at the IWF, he completed his electrical engineering studies at the Graz University of Technology in 2009. Christian developed into an inventive circuit designer, an excellent software developer, and a patient and precise integration and test engineer.

During his more than 16 years in the IWF magnetometer group, he has applied his extensive technical skills to the design, construction, and testing of numerous spaceborne instruments. They are, for example, on the way to Mercury aboard *BepiColombo*, orbiting Earth in different orbits with *CSES* and *Magnetospheric MultiScale*, and flying to Jupiter with the *JUICE* satellite.

In the course of his work, Christian Hagen was in regular exchange with colleagues from numerous national and international partner institutions (TU Graz, Geosphere Austria, TU Braunschweig, Imperial College London, National Space Science Center Beijing). His professionalism was appreciated as much as his personal commitment. Christian did not need many words to share his excellent ideas with the team and often stayed in the background with his modest manner.

With Christian Hagen, we lose a highly intelligent, conscientious and extremely empathic employee who was also close to many colleagues at the IWF as a friend. We mourn the loss of a valuable person and colleague who leaves a great gap as a member of our Institute. Christian will forever hold a special place in our memories.

PETER PESEC (23.2.1942 - 26.11.2022)

Dr. Peter Pesec, a technological enabler of satellite geodesy from its very beginning, passed away peacefully at the age of 80 years on 26 November 2022.

After he had completed his studies of Theoretical Physics and Mathematics at the University of Graz in 1969, and following a two years post-doc position there, Peter Pesec joined the satellite geodesy group of the IWF in 1971. In its early years of satellite geodesy large satellite cameras were used in order to establish a global network as a reference frame for large-scale geodetic applications. In Graz it was a BMK-75 camera, which was very successfully controlled by Peter Pesec as project scientist.

Satellite triangulation was followed by Doppler positioning from 1976 on, and it was again Peter Pesec who was responsible for the implementation and operation of the institute's Doppler equipment. In parallel, Peter Pesec was also instrumental in the planning of the observatory Graz-Lustbühel. From 1982 on, satellite laser ranging (SLR) became operational, with the Graz SLR station among the best worldwide. And in 1985 the GPS era started in Graz, again with Peter Pesec as the technological key enabler.

It was Peter Pesec who developed the Austrian GPS Geodynamics Network and he was also very instrumental in establishing a satellite transponder station at the Greek island of Gavdos for the calibration of satellite altimeter systems.

The whole range of his R&D activities required a close cooperation with numerous international partners with Peter Pesec as an experienced and strongly influential scientist in the establishment of global satellite technology from its very beginning. With him we lose a very devoted and still modest pathfinder, and above all, a wonderful friend.

PUBLICATIONS

REFEREED ARTICLES

Alho, M., R. Jarvinen, C. Simon Wedlund, H. Nilsson, E. Kallio, T.I. Pulkkinen: Remote sensing of cometary bow shocks: Modelled asymmetric outgassing and pickup ion observations, *MNRAS*, **506**, 4735-4749, doi, 2021.

Aizawa, S., M. Persson, T. Menez, N. Andre, R. Modolo, V. Genot, B. Sanchez-Cano, M. Volwerk, J.-Y. Chaufray, C. Baskevitch, D. Heyner, Y. Saito, Y. Harada, F. Leblanc, A. Barthe, E. Penou, A. Fedorov, J.-A. Sauvaud, S. Yokota, U. Auster, I. Richter, J. Mieth, T.S. Horbury, P. Louarn, C.J. Owen, G. Murakami: LatHyS global hybrid simulation of the BepiColombo second Venus flyby, *Planet. Space Sci.*, **218**, 105499, doi, 2022.

Alberti, T., A. Milillo, D. Heyner, L.Z. Hadid, H.-U. Auster, I. Richter, Y. Narita: The "singular" behavior of the solar wind scaling features during Parker Solar Probe-BepiColombo radial alignment, *Astrophys. J.*, **926**, 174, doi, 2022.

Alberti, T., Y. Narita, L.Z. Hadid, D. Heyner, A. Milillo, C. Plainaki, H.-U. Auster, I. Richter: Tracking of magnetic helicity evolution in the inner heliosphere. A radial alignment study, *Astron. Astrophys.*, **664**, L8, doi, 2022.

Alho, M., M. Battarbee, Y. Pfau-Kempf, Yu.V. Khotyaintsev, R. Nakamura, G. Cozzani, U. Ganse, L. Turc, A. Johlander, K. Horaites, V. Tarvus, H. Zhou, M. Grandin, M. Dubart, K. Papadakis, J. Suni, H. George, M. Bussov, M. Palmroth: Electron signatures of reconnection in a global eVlasiator simulation, *Geophys. Res. Lett.*, **49**, e2022GL098329, doi, 2022.

Alqeeq, S.W., O. Le Contel, P. Canu, A. Retino, T. Chust, L. Mirioni, L. Richard, Y. Ait-Si-Ahmed, A. Alexandrova, A. Chuvatin, N. Ahmadi, S.M. Baraka, R. Nakamura, F.D. Wilder, D.J. Gershman, P.A. Lindqvist, Yu.V. Khotyaintsev, R.E. Ergun, J.L. Burch, R.B. Torbert, C.T. Russell, W. Magnes, R.J. Strangeway, K.R. Bromund, H. Wei, F. Plaschke, B.J. Anderson, B.L. Giles, S.A. Fuselier, Y. Saito, B. Lavraud: Investigation of the homogeneity of energy conversion processes at dipolarization fronts from MMS measurements, *Phys. Plasmas*, **29**, 012906, doi, 2022.

Ambily, S., M. Sarpotdar, J. Mathew, B.G. Nair, A.G. Sreejith, K. Nirmal, J. Murthy, M. Safonova, R. Mohan, V.K. Aggarval, S. Nagabhushanam, S. Jeeragal: The near ultraviolet transient surveyor (NUTS): An ultraviolet telescope to observe variable sources, *Exp. Astron.*, **54**, 119–135, doi, 2022.

Artemyev, A.V., V. Angelopoulos, X.-J. Zhang, A. Runov, A. Petrukovich, R. Nakamura, E. Tsai, C. Wilkins: Thinning of the magnetotail current sheet inferred from low-altitude observations of energetic electrons, *J. Geophys. Res.*, **127**, e2022JA030705, doi, 2022.

Bailey, R.L., R. Leonhardt, C. Möstl, C. Beggan, M.A. Reiss, A. Bhaskar, A.J. Weiss: Forecasting GICs and geoelectric fields from solar wind data using LSTMs: Application in Austria, *Space Weather*, **20**, e2021SW002907, doi, 2022.

Barabash, S., A. Fedorov, J.J. Sauvaud, R. Lundin, C.T. Russell, Y. Futaana, T.L. Zhang, H. Andersson, K. Brinkfeldt, A. Grigoriev, M. Holmström, M. Yamauchi, K. Asamura, W. Baumjohann, H. Lammer, A.J. Coates, D.O. Kataria, D.R. Linder, C.C. Curtis, K.C. Hsieh, B.R. Sandel, M. Grande, H. Gunell, H.E.J. Koskinen, E. Kallio, P. Riihelä, T. Säles, W. Schmidt, J. Kozyra, N. Krupp, M. Fränz, J. Woch, J. Luhmann, S. McKenna-Lawlor, C. Mazelle, J.-J. Thocaven, S. Orsini, R. Cerulli-Irelli, A. Mura, A. Milillo, M. Maggi, E. Roelof, P. Brandt, K. Szego, J.D. Winningham, R.A. Frahm, J. Scherrer, J.R. Sharber, P. Wurz, P. Bochsler: Author Correction: The loss of ions from Venus through the plasma wake (Nature, 450, 650-653, 2007), *Nature*, **605**, E10, doi, 2022.

Barnard, L., M.J. Owens, C.J. Scott, M. Lockwood, C.A. de Koning, T. Amerstorfer, J. Hinterreiter, C. Möstl, J.A. Davies, P. Riley: Quantifying the uncertainty in CME kinematics derived from geometric modelling of Heliospheric Imager data, *Space Weather*, **20**, e2021SW002841, doi, 2022.

Barros, S.C.C., B. Akinsanmi, G. Boué, A.M.S. Smith, J. Laskar, S. Ulmer-Moll, J. Lillo-Box, D. Queloz, A. Collier Cameron, S.G. Sousa, D. Ehrenreich, M.J. Hooton, G. Bruno, B.-O. Demory, A.C.M. Correia, O.D.S. Demangeon, T.G. Wilson, A. Bonfanti, S. Hoyer, Y. Alibert, R. Alonso, G. Anglada Escudé, D. Barbato, T. Bárczy, D. Barrado, W. Baumjohann, M. Beck, T. Beck, W. Benz, M. Bergomi, N. Billot, X. Bonfils, F. Bouchy, A. Brandeker, C. Broeg, J. Cabrera, V. Cessa, S. Charnoz, C.C.V. Damme, M.B. Davies, M. Deleuil, A. Deline, L. Delrez, A. Erikson, A. Fortier, L. Fossati, M. Fridlund, D. Gandolfi, A. García Muñoz, M. Gillon, M. Güdel, K.G. Isaak, K. Heng, L. Kiss, A. Lecavelier des Etangs, M. Lendl, C. Lovis, D. Magrin, V. Nascimbeni, P.F.L. Maxted, G. Olofsson, R. Ottensamer, I. Pagano, E. Pallé, H. Parviainen, G. Peter, G. Piotto, D. Pollacco, R. Ragazzoni, N. Rando, H. Rauer, I. Ribas, S. Salmon, N.C. Santos, G. Scandariato, D. Ségransan, A.E. Simon, M. Steller, Gy.M. Szabó, N. Thomas, S. Udry, B. Ulmer, V. Van Grootel, N.A. Walton: Detection of the tidal deformation of WASP-103b at 3 σ with CHEOPS, *Astron. Astrophys.*, **657**, A52, doi, 2022.

Barros, S.C.C., B. Akinsanmi, G. Boué, A.M.S. Smith, J. Laskar, S. Ulmer-Moll, J. Lillo-Box, D. Queloz, A. Collier Cameron, S.G. Sousa, D. Ehrenreich, M.J. Hooton, G. Bruno, B.-O. Demory, A.C.M. Correia, O.D.S. Demangeon, T.G. Wilson, A. Bonfanti, S. Hoyer, Y. Alibert, R. Alonso, G. Anglada Escudé, D. Barbato, T. Bárczy, D. Barrado, W. Baumjohann, M. Beck, T. Beck, W. Benz, M. Bergomi, N. Billot, X. Bonfils, F. Bouchy, A. Brandeker, C. Broeg, J. Cabrera, V. Cessa, S. Charnoz, C.C.V. Damme, M.B. Davies,

M. Deleuil, A. Deline, L. Delrez, A. Erikson, A. Fortier, L. Fossati, M. Fridlund, D. Gandolfi, A. García. Muñoz, M. Gillon, M. Güdel, K.G. Isaak, K. Heng, L. Kiss, A. Lecavelier des Etangs, M. Lendl, C. Lovis, D. Magrin, V. Nascimbeni, P.F.L. Maxted, G. Olofsson, R. Ottensamer, I. Pagano, E. Pallé, H. Parviainen, G. Peter, G. Piotto, D. Pollacco, R. Ragazzoni, N. Rando, H. Rauer, I. Ribas, S. Salmon, N.C. Santos, G. Scandariato, D. Ségransan, A.E. Simon, M. Steller, Gy.M. Szabó, N. Thomas, S. Udry, B. Ulmer, V. Van Grootel, N.A. Walton: Detection of the tidal deformation of WASP-103b at 3 σ with CHEOPS (Corrigendum), *Astron. Astrophys.*, **658**, C1, doi, 2022.

Barstow, J.K., Q. Changeat, K.L. Chubb, P.E. Cubillos, B. Edwards, R.J. MacDonald, M. Min, I.P. Waldmann: A retrieval challenge exercise for the Ariel mission, *Exp. Astron.*, **53**, 447–471, doi, 2022.

Baumjohann, W., R. Treumann: Auroral kilometric radiation - The electron cyclotron maser paradigm, *Front. Astron. Space Sci.*, **9**, 1053303, doi, 2022.

Berezutsky, A.G., I.F. Shaikhislamov, M.S. Rumenskikh, M.L. Khodachenko, H. Lammer, I.B. Miroshnichenko: On the transit spectroscopy features of warm Neptunes in the TOI-421 system, revealed with their 3D aeronomy simulations, *MNRAS*, **515**, 706-715, doi, 2022.

Beth, A., H. Gunell, C. Simon Wedlund, C. Goetz, H. Nilsson, M. Hamrin: First investigation of the diamagnetic cavity boundary layer with a 1D3V PIC simulation, *Astron. Astrophys.*, **667**, A143, doi, 2022.

Blasl, K.A., T.K.M. Nakamura, F. Plaschke, R. Nakamura, H. Hasegawa, J.E. Stawarz, Y.-H. Liu, S. Peery, J.C. Holmes, M. Hosner, D. Schmid, O.W. Roberts, M. Volwerk: Multi-scale observations of the magnetopause Kelvin-Helmholtz waves during southward IMF, *Phys. Plasmas*, **29**, 012105, doi, 2022.

Blecic, J., J. Harrington, P.E. Cubillos, M.O. Bowman, P.M. Rojo, M. Stemm, R.C. Challener, M.D. Himes, A.J. Foster, I. Dobbs-Dixon: An open-source Bayesian Atmospheric Radiative Transfer (BART) code. III. Initialization, atmospheric profile generator, post-processing routines, *Planet. Sci. J.*, **3**, 82, doi, 2022.

Borsa, F., L. Fossati, T. Koskinen, M.E. Young, D. Shulyak: High-resolution detection of neutral oxygen and non-LTE effects in the atmosphere of KELT-9b, *Nat. Astron.*, **6**, 226–231, doi, 2022.

Borsa, F., P. Giacobbe, A.S. Bonomo, M. Brogi, L. Pino, L. Fossati, A.F. Lanza, V. Nascimbeni, A. Sozzetti, F. Amadori, S. Benatti, K. Biazzo, A. Bignamini, W. Boschin, R. Claudi, R. Cosentino, E. Covino, S. Desidera, A.F.M. Fiorenzano, G. Guilluy, A. Harutyunyan, A. Maggio, J. Maldonado, L. Mancini, G. Micela, E. Molinari, M. Molinaro, I. Pagano, M. Pedani, G. Piotto, E. Poretti, M. Rainer, G. Scandariato, H. Stoev: The GAPS programme at TNG. XXXIII. HARPS-N detects multiple atomic species in emission from the dayside of KELT-20b, *Astron. Astrophys.*, **663**, A141, doi, 2022.

Bourrier, V., A. Deline, A. Krenn, J.A. Egger, A.C. Petit, L. Malavolta, M. Cretignier, N. Billot, C. Broeg, H.-G. Florén, D. Queloz, Y. Alibert, A. Bonfanti, A.S. Bonomo, J.-B. Delisle, O.D.S. Demangeon, B.-O. Demory, X. Dumusque, D. Ehrenreich, R.D. Haywood, S.B. Howell, M. Lend, A. Mortier, G. Nigro, S. Salmon, S.G. Sousa, T.G. Wilson, V. Adibekyan, R. Alonso, G. Anglada, T. Bárczy, D. Barrado y. Navascues, S.C.C. Barros, W. Baumjohann, M. Beck, W. Benz, F. Biondi, X. Bonfils, A. Brandeker, J. Cabrera, S. Charnoz, Sz. Csizmadia, A. Collier Cameron, M. Damasso, M.B. Davies, M. Deleuil, L. Delrez, L. Di Fabrizio, A. Erikson, A. Fortier, L. Fossati, M. Fridlund, D. Gandolfi, M. Gillon, M. Güdel, K. Heng1, S. Hoyer, K.G. Isaak, L.L. Kiss, J. Laskar, A. Lecavelier des Etangs, V. Lorenzi, C. Lovis, D. Magrin, A. Massa, P.F.L. Maxted, V. Nascimbeni, G. Olofsson, R. Ottensamer, I. Pagano, E. Pallé, G. Peter, G. Piotto, D. Pollacco, R. Ragazzoni, N. Rando, H. Rauer, I. Ribas, N.C. Santos, G. Scandariato, D. Ségransan, A.E. Simon, A.M.S. Smith, M. Steller, Gy.M. Szabó, N. Thomas, S. Udry, V. Van Grootel, F. Verrecchia, N. Walton, T. Beck, M. Buder, F. Ratti, B. Ulmer, V. Viotto: A CHEOPS-enhanced view of the HD 3167 system, *Astron. Astrophys.*, **668**, A31, doi, 2022.

Brandeker, A., K. Heng, M. Lendl, J.A. Patel, B.M. Morris, C. Broeg, P. Guterman, M. Beck, P.F.L. Maxted, O. Demangeon, L. Delrez, B.-O. Demory, D. Kitzmann, N.C. Santos, V. Singh, Y. Alibert, R. Alonso, G. Anglada, T. Bárczy, D. Barrado y Navascues, S.C.C. Barros, W. Baumjohann, T. Beck, W. Benz, N. Billot, X. Bonfils, G. Bruno, J. Cabrera, S. Charnoz, A. Collier Cameron, C. Corral van Damme, Sz. Csizmadia, M.B. Davies, M. Deleuil, A. Deline, D. Ehrenreich, A. Erikson, J. Farinato, A. Fortier, L. Fossati, M. Fridlund, D. Gandolfi, M. Gillon, M. Güdel, S. Hoyer, K.G. Isaak, L. Kiss, J. Laskar, A. Lecavelier des Etangs, C. Lovis, A. Luntzer, D. Magrin, V. Nascimbeni, G. Olofsson, R. Ottensamer, I. Pagano, E. Pallé, G. Peter, G. Piotto, D. Pollacco, D. Queloz, R. Ragazzoni, N. Rando, H. Rauer, I. Ribas, G. Scandariato, D. Ségransan, A.E. Simon, A.M.S. Smith, S.G. Sousa, M. Steller, Gy.M. Szabó, N. Thomas, S. Udry, V. Van Grootel, N. Walton, D. Wolter: CHEOPS geometric albedo of the hot Jupiter HD 209458 b, *Astron. Astrophys.*, **659**, L4, doi, 2022.

Branduardi-Raymont, G., M. Berthomier, Y.V. Bogdanova, J.A. Carter, M. Collier, A. Dimmock, M. Dunlop, R.C. Fear, C. Forsyth, B. Hubert, E.A. Kronberg, K.M. Laundal, M. Lester, S. Milan, K. Oksavik, N. Østgaard, M. Palmroth, F. Plaschke, F.S. Porter, I.J. Rae, A. Read, A.A. Samsonov, S. Sembay, Y. Shprits, D.G. Sibeck, B. Walsh, M. Yamauchi: Exploring solar-terrestrial interactions via multiple imaging observers, *Exp. Astron.*, **54**, 361–390, doi, 2022.

Carleo, I., P. Giacobbe, G. Guilluy, P.E. Cubillos, A.S. Bonomo, A. Sozzetti, M. Brogi, S. Gandhi, L. Fossati, D. Turrini, K. Biazzo, F. Borsa, A.F. Lanza, L. Malavolta, A. Maggio, L. Mancini, G. Micela, L. Pino, E. Poretti, M. Rainer, G. Scandariato, E. Schisano, G. Andreuzzi, A. Bignamini, R. Cosentino, A. Fiorenzano, A. Harutyunyan, E. Molinari, M. Pedani, S. Redfield, H. Stoev: The GAPS programme at TNG XXXIX. Multiple molecular species in the atmosphere of the warm giant planet WASP-80 b unveiled at high resolution with GIANO-B, *Astron. J.*, **164**, 101, doi, 2022.

Cavalazzi, B., F. Westall, L. Noack, R.-S. Taubner, T. Milojevic, K. Finster: Special issue: Open questions and next steps in astrobiology in Europe – celebrating 20 years of EANA, *Int. J. Astrobiol.*, **21**, 261-267, doi, 2022.

Challener, R.C., J. Harrington, P.E. Cubillos, J. Blecic, B. Smalley: Spitzer dayside emission of WASP-34b, *Planet. Sci. J.*, **3**, 86, doi, 2022.

Chen, M., Z. Pan, T.-L. Zhang, X. Hao, Y. Li, K. Liu, X. Li, Y. Wang, C. Shen, H. Chen, Z. Wang, X. Qiang: Deployable boom for Mars Orbiter magnetometer onboard "Tianwen-1", *JUSTC*, **52**, 7, doi, 2022.

Chen, Y., M. Wu, S. Xiao, A. Du, G. Wang, Y Chen, Z. Pan, T.-L. Zhang: Magnetic fluctuations associated with small-scale magnetic holes in the Martian magnetosheath, *Front. Astron. Space Sci.*, **9**, 858300, doi, 2022.

Chen, Y.Q., G.Q. Wang, M.Y. Wu, S.D. Xiao, T.-L. Zhang: Electron-scale magnetic peaks upstream of Mercury's bow shock: MESSENGER observations, *Astrophys. J.*, **935**, 82, doi, 2022.

Chen, Y.Q., G.Q. Wang, M.Y. Wu, S.D. Xiao, T.-L. Zhang: Study of the electron-scale magnetic peaks in the magnetotail current sheet observed by the Magnetospheric Multiscale mission, *J. Geophys. Res.*, **127**, e2021JA030135, doi, 2022.

Chen, Y.Q., M. Wu, A.M. Du, S.D. Xiao, G.Q. Wang, T.-L. Zhang: A case study of the induced magnetosphere boundary at the Martian subsolar region, *Astrophys. J.*, **927**, 171, doi, 2022.

Cubillos, P.E., J. Harrington, J. Blecic, M.D. Himes, P.M. Rojo, T.J. Loredo, N.B. Lust, R.C. Challener, A.J. Foster, M.M. Stemm, A.S.D. Foster, S.D. Blumenthal: An open-source Bayesian Atmospheric Radiative Transfer (BART) code. II. The transit radiative transfer module and retrieval of HAT-P-11b, *Planet. Sci. J.*, **3**, 81, doi, 2022.

Dang, T., J. Lei, B. Zhang, T.-L. Zhang, Z. Yao, J. Lyon, X. Ma, S. Xiao, M. Yan, O. Brambles, K. Sorathia, V. Merkin: Oxygen ion escape at Venus associated with three-dimensional Kelvin-Helmholtz instability, *Geophys. Res. Lett.*, **49**, e2021GL096961, doi, 2022.

Davies, E.E., R.M. Winslow, C. Scolini, R.J. Forsyth, C. Möstl, N. Lugaz, A.B. Galvin: Multi-spacecraft observations of the evolution of Interplanetary Coronal Mass Ejections between 0.3 and 2.2 au: Conjunctions with the Juno spacecraft, *Astrophys. J.*, **933**, 127, doi, 2022.

Debrecht, A., J. Carroll-Nellenback, A. Frank, E.G. Blackman, L. Fossati, R. Murray-Clay, J. McCann: Effects of charge exchange on the evaporative wind of HD 209458b, *MNRAS*, **517**, 1724-1736, doi, 2022.

Deline, A., M.J. Hooton, M. Lendl, B. Morris, S. Salmon, G. Olofsson, C. Broeg, D. Ehrenreich, M. Beck, A. Brandeker, S. Hoyer, S. Sulis, V. Van Grootel, V. Bourrier, O. Demangeon, B.-O. Demory, K. Heng, H. Parviainen, L.M. Serrano, V. Singh, A. Bonfanti, L. Fossati, D. Kitzmann, S.G. Sousa, T.G. Wilson, Y. Alibert, R. Alonso, G. Anglada, T. Bárczy, D. Barrado Navascues, S.C.C. Barros, W. Baumjohann, T. Beck, A. Bekkelien, W. Benz, N. Billot, X. Bonfils, J. Cabrera, S. Charnoz, A. Collier Cameron, C. Corral van Damme, Sz. Csizmadia, M.B. Davies, M. Deleuil, L. Delrez, T. de Roche, A. Erikson, A. Fortier, M. Fridlund, D. Futyan, D. Gandolfi1, M. Gillon, M. Güdel, P. Gutermann, J. Hasiba, K.G. Isaak, L. Kiss, J. Laskar, A. Lecavelier des Etangs, C. Lovis, D. Magrin, P.F.L. Maxted, M. Munari, V. Nascimbeni, R. Ottensamer, I. Pagano, E. Pallé, G. Peter, G. Piotto, D. Pollacco, D. Queloz, R. Ragazzoni, N. Rando, H. Rauer, I. Ribas, N.C. Santos, G. Scandariato, D. Ségransan, A.E. Simon, A.M.S. Smith, M. Steller, Gy.M. Szabó, N. Thomas, S. Udry, I. Walter, N. Walton: The atmosphere and architecture of WASP-189 b probed by its CHEOPS phase curve, *Astron. Astrophys.*, **659**, A74, doi, 2022.

Dimmock, A.P., Yu.V. Khotyaintsev, A. Lalti, E. Yordanova, N.J.T. Edberg, K. Steinvall, D.B. Graham, L.Z. Hadid, R.C. Allen, A. Vaivads, M. Maksimovic, S.D. Bale, T. Chust, V. Krasnoselskikh, M. Kretzschmar, E. Lorfèvre, D. Plettemeier, J. Souček, M. Steller, S. Štverák, P. Trávníček, A. Vecchio, T.S. Horbury, H. O'Brien, V. Evans, V. Angelini: Analysis of multiscale structures at the quasi-perpendicular Venus bow shock. Results from Solar Orbiter's first Venus flyby, *Astron. Astrophys.*, **660**, A64, doi, 2022.

Erkaev, N.V., C. Weber, J.-M. Grießmeier, H. Lammer, V.A. Ivanov, P. Odert: Can radio emission escape from the magnetosphere of υ Andromedae b - a new method to constrain the minimum mass of Hot Jupiters, *MNRAS*, **512**, 4869-4876, doi, 2022.

Ferus, M., V. Adam, G. Cassone, S. Civiš, V. Čuba, E. Chatzitheodoridis, B. Drtinová, B. LeFloch, A. Heays, S. Jheeta, Á. Kereszturi, A. Knížek, M. Krůs, P. Kubelík, H. Lammer, L. Lenža, L. Nejdl, A. Pastorek, L. Petera, P. Rimmer, R. Saladino, F. Saija, L. Sproß, J. Šponer, J. Šponer, Z. Todd, M. Vaculovičová, K. Zemánková, V. Chernov: Ariel - a window to the origin of life on early earth?, *Exp. Astron.*, **53**, 679-728, doi, 2022.

Fischer, G., U. Taubenschuss, D. Píša: Classification of spectral fine structures of Saturn kilometric radiation, *Ann. Geophys.*, **40**, 485-501, doi, 2022.

Fossati, L., G. Guilluy, I.F. Shaikhislamov, I. Carleo, F. Borsa, A.S. Bonomo, P. Giacobbe, M. Rainer, C. Cecchi-Pestellini, M.L. Khodachenko, M.A. Efimov, M.S. Rumenskikh, I.B. Miroshnichenko, A.G. Berezutsky, V. Nascimbeni, M. Brogi, A.F. Lanza, L. Mancini, L. Affer, S. Benatti, K. Biazzo, A. Bignamini, D. Carosati, R. Claudi, R. Cosentino, E. Covino, S. Desidera, A. Fiorenzano, A. Harutyunyan, A. Maggio, L. Malavolta, J. Maldonado, G. Micela, E. Molinari, I. Pagano, M. Pedani, G. Piotto, E. Poretti, G. Scandariato, A. Sozzetti, H. Stoev: The GAPS programme at TNG. XXXII. The revealing non-detection of metastable HeI in the atmosphere of the hot Jupiter WASP-80b, *Astron. Astrophys.*, **658**, A136, doi, 2022.

France, K., B. Fleming, A. Youngblood, J. Mason, J.J. Drake, U.V. Amerstorfer, M. Barstow, V. Bourrier, P. Champey, L. Fossati, C.S. Froning, J.C. Green, F. Grisé, G. Gronoff, T. Hellickson, M. Jin, T.T. Koskinen, A.F. Kowalski, N. Kruczek, J.L. Linsky, S.J. Lipscy, R.L. McEntaffer, D.E. McKenzie, D.M. Miles, T. Patton, S. Savage, O. Siegmund, C. Spittler, B.W. Unruh, M. Volz: Extreme-ultraviolet stellar characterization for atmospheric physics and evolution mission: Motivation and overview, *J. Astron. Telesc. Instrum. Syst.*, **8**, 014006, doi, 2022.

Genestreti, K., X. Li, Y.-H. Liu, J.L. Burch, R.B. Torbert, S.A. Fuselier, T.K.M. Nakamura, B.L. Giles, D.J. Gershman, R.E. Ergun, C.T. Russell, R.J. Strangeway: On the origin of "patchy" energy conversion in electron diffusion regions, *Phys. Plasmas*, **29**, 082107, doi, 2022.

Gillmann, C., M.J. Way, G. Avice, D. Breuer, G.J. Golabek, D. Höning, J. Krissansen-Totton, H. Lammer, J.G. O'Rourke, M. Persson, A.-C. Plesa, A. Salvador, M. Scherf, M.Y. Zolotov: The long-term evolution of the atmosphere of Venus: Processes and feedback mechanisms. Interior-exterior exchanges, *Space Sci. Rev.*, **218**, 56, doi, 2022.

Goetz, C., E. Behar, A. Beth, D. Bodewits, S. Bromley, J. Burch, J. Deca, A. Divin, A.I. Eriksson, P.D. Feldman, M. Galand, H. Gunel, P. Henri, K. Heritier, G.H. Jones, K.E. Mandt, H. Nilsson, J.W. Noonan, E. Odelstad, J.W. Parker, M. Rubin, C. Simon Wedlund, P. Stephenson, M.G.G.T. Taylor, E. Vigren, S.K. Vines, M. Volwerk: The Plasma Environment of Comet 67P/Churyumov-Gerasimenko, *Space Sci. Rev.*, **218**, 65, doi, 2022.

Goetz, C., H. Gunell, M. Volwerk, A. Beth, A. Eriksson, M. Galand, P. Henri, H. Nilsson, C. Simon Wedlund, M. Alho, L. Andersson, N. Andre, J. De Keyser, J. Deca, Y. Ge, K.-H. Glassmeier, R. Hajra, T. Karlsson, S. Kasahara, I. Kolmasova, K. LLera, H. Madanian, I. Mann, C. Mazelle, E. Odelstad, F. Plaschke, M. Rubin, B. Sanchez-Cano, C. Snodgrass, E. Vigren: Cometary plasma science. Open science questions for future space missions, *Exp. Astron.*, **54**, 1129–1167, doi, 2022.

Grach, V.S., A.V. Artemyev, A.G. Demekhov, X.-J. Zhang, J. Bortnik, V. Angelopoulos, R. Nakamura, E. Tsai, C. Wilkins, O.W. Roberts: Relativistic electron precipitation by EMIC waves: Importance of nonlinear resonant effects, *Geophys. Res. Lett.*, **49**, e2022GL099994, doi, 2022.

Guilluy, G., P. Giacobbe, I. Carleo, P.E. Cubillos, A. Sozzetti, A.S. Bonomo, M. Brogi, S. Gandhi, L. Fossati, V. Nascimbeni, D. Turrini, E. Schisano, F. Borsa, A.F. Lanza, L. Mancini, A. Maggio, L. Malavolta, G. Micela, L. Pino, M. Rainer, A. Bignamini, R. Claudi, R. Cosentino, E. Covino, S. Desidera, A. Fiorenzano, A. Harutyunyan, V. Lorenzi, C. Knapic, E. Molinari, E. Pacetti, I. Pagano, M. Pedani, G. Piotto, E. Poretti: The GAPS programme at TNG XXXVIII. Five molecules in the atmosphere of the warm giant planet WASP-69b detected at high spectral resolution, *Astron. Astrophys.*, **665**, A104, doi, 2022.

Harrington, J., M.D. Himes, P.E. Cubillos, J. Blecic, P.M. Rojo, R.C. Challener, N.B. Lust, M.O. Bowman, S.D. Blumenthal, I. Dobbs-Dixon, A.S.D. Foster, A.J. Foster, M.R. Green, T.J. Loredo, K.J. McIntyre, M.M. Stemm, D.C. Wright: An open-source Bayesian Atmospheric Radiative Transfer (BART) code. I. Design, tests, and application to exoplanet HD 189733b, *Planet. Sci. J.*, **3**, 80, doi, 2022.

Hart, R.A., C.T. Russell, T.-L. Zhang: Statistical study of lightning-generated whistler-mode waves observed by Venus Express, *Icarus*, **380**, 114993, doi, 2022.

Hasegawa, H., R.E. Denton, T.K.M. Nakamura, K.J. Genestreti, T.D. Phan, R. Nakamura, K.-J. Hwang, N. Ahmadi, Q.Q. Shi, M. Hesse, J.L. Burch, J.M. Webster, R.B. Torbert, B.L. Giles, D.J. Gershman, C.T. Russell, R.J. Strangeway, H.Y. Wei, P.-A. Lindqvist, Y.V. Khotyaintsev, R.E. Ergun, Y. Saito: Magnetic field annihilation in a magnetotail electron diffusion region with electron-scale magnetic island, *J. Geophys. Res.*, **127**, e2022JA030408, doi, 2022.

Hayakawa, H., K. Hattori, M. Sôma, T. Iju, B.P. Besser, S. Kosaka: An overview of sunspot observations in 1727-1748, *Astrophys. J.*, **941**, 151, doi, 2022.

Heays, A.N., T. Kaiserová, P.B. Rimmer, A. Knížek, L. Petera, S. Civiš, L. Juha, R. Dudžák, M. Krus, M. Scherf, H. Lammer, R. Pascal, M. Ferus: Nitrogen oxide production in laser-induced breakdown simulating impacts on the Hadean atmosphere, *J. Geophys. Res. Planets*, **127**, e2021JE006842, doi, 2022.

Herbort, O., P. Woitke, Ch. Helling, A.L. Zerkle: The atmospheres of rocky exoplanets. II. Influence of surface composition on the diversity of cloud condensates, *Astron. Astrophys.*, **658**, A180, doi, 2022.

Herzig, T., N.I. Kömle, W. Macher, G. Bihari, P. Gläser: Site selection, thermodynamics, environment and life support analysis for the PneumoPlanet inflatable lunar habitat concept, *Planet. Space Sci.*, **224**, 105595, doi, 2022.

Heuer, S.V., K.J. Genestreti, T.K.M. Nakamura, R.B. Torbert, J.L. Burch, R. Nakamura: Calculating the electron diffusion region aspect ratio with magnetic field gradients, *Geophys. Res. Lett.*, **49**, e2022GL100652, doi, 2022.

Hooton, M.J., S. Hoyer, D. Kitzmann, B.M. Morris, A.M.S. Smith, A. Collier Cameron, D. Futyan, P.F.L. Maxted, D. Queloz, B.-O. Demory, K. Heng, M. Lendl, J. Cabrera, Sz. Csizmadia, A. Deline, H. Parviainen, S. Salmon, S. Sulis, T.G. Wilson, A. Bonfanti, A. Brandeker, O.D.S. Demangeon, M. Oshagh, C.M. Persson, G. Scandariato, Y. Alibert, R. Alonso, G. Anglada Escudé, T. Bárczy, D. Barrado, S.C.C. Barros, W. Baumjohann, M. Beck, T. Beck, W. Benz, N. Billot, X. Bonfils, V. Bourrier, C. Broeg, M.-D. Busch, S. Charnoz, M.B. Davies, M. Deleuil, L. Delrez, D. Ehrenreich, A. Erikson, J. Farinato, A. Fortier, L. Fossati, M. Fridlund, D. Gandolfi, M. Gillon, M. Güdel, K.G. Isaak, K. Jones, L. Kiss, J. Laskar, A. Lecavelier des Etangs, C. Lovis, A. Luntzer, D. Magrin, V. Nascimbeni, G. Olofsson, R. Ottensamer, I. Pagano, E. Pallé, G. Peter, G. Piotto, D. Pollacco, R. Ragazzoni, N. Rando, F. Ratti, H. Rauer, I. Ribas, N.C. Santos, D. Ségransan, A.E. Simon, S.G. Sousa, M. Steller, Gy.M. Szabó, N. Thomas, S. Udry, B. Ulmer, V. Van Grootel, N.A. Walton: Spi-OPS: Spitzer and CHEOPS confirm the near-polar orbit of MASCARA-1 b and reveal a hint of dayside reflection, *Astron. Astrophys.*, **658**, A75, doi, 2022.

Hosner, M., R. Nakamura, T.K.M. Nakamura, D. Schmid, E.V. Panov, F. Plaschke: Statistical investigation of electric field fluctuations around the lower-hybrid frequency range at dipolarization fronts in the near-earth magnetotail, *Phys. Plasmas*, **29**, 012111, doi, 2022.

Hoyer, S., A. Bonfanti, A. Leleu, L. Acuña, L.M. Serrano, M. Deleuil, A. Bekkelien, C. Broeg, H.-G. Florén, D. Queloz, T.G. Wilson, S.G. Sousa, M.J. Hooton, V. Adibekyan, Y. Alibert, R. Alonso, G. Anglada, J. Asquier, T. Bárczy, D. Barrado, S.C.C. Barros, W. Baumjohann, M. Beck, T. Beck, W. Benz, N. Billot, F. Biondi, X. Bonfils, A. Brandeker, J. Cabrera, S. Charnoz, A. Collier Cameron, Sz. Csizmadia, M.B. Davies, L. Delrez, O.D.S. Demangeon, B.-O. Demory, D. Ehrenreich, A. Erikson, A. Fortier, L. Fossati, M. Fridlund, D. Gandolfi, M. Gillon, M. Güdel, N. Hara, K. Heng, K.G. Isaak, J.M. Jenkins, L.L. Kiss, J. Laskar, D.W. Latham, A. Lecavelier des Etangs, M. Lendl, C. Lovis, A. Luntzer, D. Magrin, P.F.L. Maxted, V. Nascimbeni, G. Olofsson, R. Ottensamer, I. Pagano, E. Pallé, C.M. Persson, G. Peter, D. Piazza, G. Piotto, D. Pollacco, R. Ragazzoni, N. Rando, H. Rauer, I. Ribas, G.R. Ricker, S. Salmon, N.C. Santos, G. Scandariato, S. Seager, D. Ségransan, A.E. Simon, A.M.S. Smith, M. Steller, Gy.M. Szabó, N. Thomas, J.D. Twicken, S. Udry, V. Van Grootel, R.K. Vanderspek, N.A. Walton, K. Westerdorff, J.N. Winn: Characterization of the HD108236 system with CHEOPS and TESS. Confirmation of a fifth transiting planet, *Astron. Astrophys.*, **668**, A117, doi, 2022.

Hu, X.W., G.Q. Wang, Z.H. Pan, T.-L. Zhang: Application of the Wang-Pan method based on mirror mode structures on the in-flight calibration of magnetometers (in Chinese), *Chin. J. Geophys.*, **65**, 1940-1950, doi, 2022.

Hwang, K.-J., H. Hasegawa, K. Nykyri, T.K.M. Nakamura, S. Wing: Editorial: Micro- to macro-scale dynamics of Earth's flank magnetopause, *Front. Astron. Space Sci.*, **9**, 911633, doi, 2022.

Jianing, Z., B. Cheng, Y. Tong, Y. Miao, B. Zhou, A. Pollinger, X. Zhu, Y. Yang, X. Gou, Y. Zhang, J. Wang, L. Li, W. Magnes, R. Lammegger, Z. Zeren, X. Shen: Comparison of scalar magnetic field data of China Seismo-Electromagnetic Satellite and Swarm Bravo satellite, *Front. Earth Sci.*, **10**, 866438, doi, 2022.

Jones, K., B.M. Morris, B.-O. Demory, K. Heng, M.J. Hooton, N. Billot, D. Ehrenreich, S. Hoyer, A.E. Simon, M. Lendl, O.D.S. Demangeon, S.G. Sousa, A. Bonfanti, T.G. Wilson, S. Salmon, Sz. Csizmadia, H. Parviainen, G. Bruno, Y. Alibert, R. Alonso, G. Anglada, T. Bárczy, D. Barrado, S.C.C. Barros, W. Baumjohann, M. Beck, T. Beck, W. Benz, X. Bonfils, A. Brandeker, C. Broeg, J. Cabrera, S. Charnoz, A. Collier Cameron, M.B. Davies, M. Deleuil, A. Deline, L. Delrez, A. Erikson, A. Fortier, L. Fossati, M. Fridlund, D. Gandolfi, M. Gillon, M. Güdel, K.G. Isaak, L.L. Kiss, J. Laskar, A. Lecavelier des Etangs, C. Lovis, D. Magrin, P.F.L. Maxted, V. Nascimbeni, G. Olofsson, R. Ottensamer, I. Pagano, E. Pallé, G. Peter, G. Piotto, D. Pollacco, D. Queloz, R. Ragazzoni, N. Rando, F. Ratti, H. Rauer, C. Reimers, I. Ribas, N.C. Santos, G. Scandariato, D. Ségransan, A.M.S. Smith, M. Steller, Gy.M. Szabó, N. Thomas, S. Udry, V. Van Grootel, I. Walter, N.A. Walton, W. Wang Jungo: The stable climate of KELT-9b, *Astron. Astrophys.*, **666**, A118, doi, 2022.

Jorge, D.M., I.E.E. Kamp, L.B.F.M. Waters, P. Woitke, R.J. Spaargaren: Forming planets around stars with non-solar elemental composition, *Astron. Astrophys.*, **660**, A85, doi, 2022.

Kallio, E., R. Jarvinen, S. Massetti, T. Alberti, A. Milillo, S. Orsini, E. De Angelis, G. Laky, J. Slavin, J.M. Raines, T.I. Pulkkinen: Ultra-low frequency waves in the Hermean magnetosphere: On the role of the morphology of the magnetic field and the foreshock, *Geophys. Res. Lett.*, **49**, e2022GL101850, doi, 2022.

Khorshid, N., M. Min, J.M. Désert, P. Woitke, C. Dominik: SimAb: A simple, fast, and flexible model to assess the effects of planet formation on the atmospheric composition of gas giants, *Astron. Astrophys.*, **667**, A147, doi, 2022.

Koller, F., M. Temmer, L. Preisser, F. Plaschke, P. Geyer, L.K. Jian, O.W. Roberts, H. Hietala, A.T. LaMoury: Magnetosheath jet occurrence rate in relation to CMEs and SIRs, *J. Geophys. Res.*, **127**, e2021JA030124, doi, 2022.

Kömle, N.I.: Commentary: Xiao et al.: First in-situ temperature measurements at the far side of the lunar surface, *Nat. Sci. Rev.*, **9**, nwac185, doi, 2022.

Krasnoselskikh, V., B.T. Tsurutani, T. Dudok deWit, S. Walker, M. Balikhin, M. Balat-Pichelin, M. Velli, S.D. Bale, M. Maksimovic, O. Agapitov, W. Baumjohann, M. Berthomier, R. Bruno, S.R. Cranmer, B. de Pontieu, D. de Sousa Meneses, J. Eastwood, R. Erdelyi, R. Ergun, V. Fedun, N. Ganushkina, A. Greco, L. Harra, P. Henri, T. Horbury, H. Hudson, J. Kasper, Y. Khotyaintsev, M. Kretzschmar, S. Krucker, H. Kucharek, Y. Langevin, B. Lavraud, J.-P. Lebreton, S. Lepri, M. Liemohn, P. Louarn, E. Moebius, F. Mozer, Z. Nemecek, O. Panasenco, A. Retino, J. Safrankova, J. Scudder, S. Servidio, L. Sorriso-Valvo, J. Soucek, A. Szabo, A. Vaivads, G. Vekstein, Z. Vörös, T. Zaqarashvili, G. Zimbardo, A. Fedorov: ICARUS: in-situ studies of the solar corona beyond Parker Solar Probe and Solar Orbiter, *Exp. Astron.*, **54**, 277–315, doi, 2022.

Kreuzig, C., G. Kargl, A. Pommerol, J. Knollenberg, A. Lethuillier, N.S. Molinski, T. Gilke, D. Bischoff, C. Feller, E. Kührt, H. Sierks, N. Hänni, H. Capelo, C. Güttler, D. Haack, K. Otto, E. Kaufmann, M. Schweighart, W. Macher, P. Tiefenbacher, B. Gundlach, J. Blum: The CoPhyLab comet-simulation chamber, *Rev. Sci. Instr.*, **92**, 115102, doi, 2022.

Kubyshkina, D.: Stellar rotation and its connection to the evolution of hydrogen-dominated atmospheres of exoplanets, *Astron. Nachr.*, **343**, e10077, doi, 2022.

Kubyshkina, D., A.A. Vidotto, C.V. D'Angelo, S. Carolan, G. Hazra, I. Carleo: Atmospheric mass-loss and stellar wind effects in young and old systems - I. Comparative 3D study of TOI-942 and TOI-421 systems, *MNRAS*, **510**, 2111-2126, doi, 2022.

Kubyshkina, D., A.A. Vidotto, C.V. D'Angelo, S. Carolan, G. Hazra, I. Carleo: Atmospheric mass loss and stellar wind effects in young and old systems - II. Is TOI-942 the past of TOI-421 system?, *MNRAS*, **510**, 3039-3045, doi, 2022.

Kubyshkina, D., L. Fossati: The mass-radius relation of intermediate-mass planets outlined by hydrodynamic escape and thermal evolution, *Astron. Astrophys.*, **668**, A178, doi, 2022.

Kwon, H.-J., K.-H. Kim, G. Jee, J. Seon, C. Lee, Y.-B. Ham, J. Hong, E. Kim, T. Bullett, H.-U. Auster, W. Magnes, S. Kraft: Disappearance of the polar cap ionosphere curing geomagnetic storm on 11 May 2019, *Space Weather*, **20**, e2022SW003054, doi, 2022.

Lacedelli, G., T.G. Wilson, L. Malavolta, M.J. Hooton, A. Collier Cameron, Y. Alibert, A. Mortier, A. Bonfanti, R.D. Haywood, S. Hoyer, G. Piotto, A. Bekkelien, A.M. Vanderburg, W. Benz, X. Dumusque, A. Deline, M. López-Morales, L. Borsato, K. Rice, L. Fossati, D.W. Latham, A. Brandeker, E. Poretti, S.G. Sousa, A. Sozzetti, S. Salmon, C.J. Burke, V. Van Grootel, M.M. Fausnaugh, V. Adibekyan, C.X. Huang, H.P. Osborn, A.J. Mustill, E. Pallé, V. Bourrier, V. Nascimbeni, R. Alonso, G. Anglada, T. Bárczy, D. Barrado y Navascues, S.C.C. Barros, W. Baumjohann, M. Beck, T. Beck, N. Billot, X. Bonfils, C. Broeg, L.A. Buchhave, J. Cabrera, S. Charnoz, R. Cosentino, Sz. Csizmadia, M.B. Davies, M. Deleuil, L. Delrez, O. Demangeon, B.-O. Demory, D. Ehrenreich, A. Erikson, E. Esparza-Borges, H.-G. Florén, A. Fortier, M. Fridlund, D. Futyan, D. Gandolfi, A. Ghedina, M. Gillon, M. Güdel, P. Gutermann, A. Harutyunyan, K. Heng, K.G. Isaak, J.M. Jenkins, L. Kiss, J. Laskar, A. Lecavelier des Etangs, M. Lendl, C. Lovis, D. Magrin, L. Marafatto, A.F. Martinez Fiorenzano, P.F.L Maxted, M. Mayor, G. Micela, E. Molinari, F. Murgas, N. Narita, G. Olofsson, R. Ottensamer, I. Pagano, A. Pasetti, M. Pedani, F.A. Pepe, G. Peter, D.F. Phillips, D. Pollacco, D. Queloz, R. Ragazzoni, N. Rando, F. Ratti, H. Rauer, I. Ribas, N.C. Santos, D. Sasselov, G. Scandariato, S. Seager, D. Ségransan, L.M. Serrano, A.E. Simon, A.M.S. Smith, M. Steinberger, M. Steller, Gy. Szabó, N. Thomas, J.D. Twicken, S. Udry, N. Walton, J.N. Winn: Investigating the architecture and internal structure of the TOI-561 system planets with CHEOPS, HARPS-N, and TESS, *MNRAS*, **511**, 4551–4571, doi, 2022.

Lammer, H., M. Scherf, Y. Ito, A. Mura, A. Vorburger, E. Guenther, P. Wurz, N.V. Erkaev, P. Odert: The exosphere as a boundary: Origin and evolution of airless bodies in the inner solar system and beyond including planets with silicate atmospheres, *Space Sci. Rev.*, **218**, 15, doi, 2022.

Lethuillier, A., C. Feller, E. Kaufmann, P. Becerra, N. Hänni, R. Diethelm, C. Kreuzig, B. Gundlach, J. Blum, A. Pommerol, G. Kargl, S. Laddha, K. Denisova, E. Kührt, H.L. Capelo, D. Haack, X. Zhang, J. Knollenberg, N.S. Molinski, T. Gilke, H. Sierks, P. Tiefenbacher, C. Güttler, K.A. Otto, D. Bischoff, M. Schweighart, A. Hagermann, N. Jäggi: Cometary dust analogues for physics experiments, *MNRAS*, **515**, 3420–3438, doi, 2022.

Leto, P., L.M. Oskinova, C.S. Buemi, M.E. Shultz, F. Cavallaro, C. Trigilio, G. Umana, L. Fossati, I. Pillitteri, J. Krtička, R. Ignace, C. Bordiu, F. Bufano, G. Catanzaro, L. Cerrigone, M. Giarrusso, A. Ingallinera, S. Loru, S.P. Owocki, K.A. Postnov, S. Riggi, J. Robrade, F. Leone: Discovery and origin of the radio emission from the multiple stellar system KQ Vel, *MNRAS*, **515**, 5523-5538, doi, 2022.

Lichtenegger, H.I.M., S. Dyadechkin, M. Scherf, H. Lammer, R. Adam, E. Kallio, U.V. Amerstorfer, R. Jarvinen: Non-thermal escape of the Martian CO2 atmosphere over time: Constrained by Ar isotopes, *Icarus*, **382**, 115009, doi, 2022.

Longobardo, A., T. Mannel, M. Kim, M. Fulle, A. Rotundi, V. Della Corte, G. Rinaldi, J. Lasue, S. Merouane, H. Cottin, M. Ciarniello, F. Dirri, E. Palomba: Combining Rosetta's GIADA and MIDAS data: Morphological vs dynamical properties of dust at 67P/Churyumov-Gerasimenko, *MNRAS*, **516**, 5611–5617, doi, 2022.

Lou, Y., X. Cao, M. Wu, B. Ni, T.-L. Zhang: Parametric sensitivity of electron scattering effects by electrostatic electron cyclotron harmonic waves, *J. Geophys. Res.*, **127**, e2022JA030322, doi, 2022.

Lugaz, N., T.M. Salman, B. Zhuang, N. Al-Haddad, C. Scolini, C.J. Farrugia, W. Yu, R.M. Winslow, C. Möstl, E.E. Davies, A.B. Galvin: A Coronal Mass Ejection and magnetic ejecta observed in situ by STEREO-A and Wind at 55° angular separation, *Astrophys. J.*, **929**, 149, doi, 2022.

Lui, A.T.Y., S.-I. Akasofu, Q. Zong, P.H. Yoon, R. Nakamura, G. Parks: Editorial: Towards a full understanding of magnetic storms and substorms, *Front. Astron. Space Sci.*, **9**, 944040, doi, 2022.

Malara, F., A. Settino, D. Perrone, O. Pezzi, G. Guzzi, F. Valentini: Exact shearing flow magnetized hybrid kinetic equilibria with inhomogeneous temperature, *Astrophys. J.*, **941**, 201, doi, 2022.

Marsch, E., Y. Narita: Lorentz invariance and the spinor-helicity formalism yield the U(1) and SU(3) fermion symmetry, *Eur. Phys. J. Plus*, **137**, 818, doi, 2022.

Marsch, E., Y. Narita: On isospin and flavour of leptons and quarks, *Eur. Phys. J. Plus*, **137**, 1353, doi, 2022.

Maxted, P.F.L., D. Ehrenreich, T.G. Wilson, Y. Alibert, A. Collier Cameron, S. Hoyer, S.G. Sousa, G. Olofsson, A. Bekkelien, A. Deline, L. Delrez, A. Bonfanti, L. Borsato, R. Alonso, G. Anglada Escudé, D. Barrado, S.C.C. Barros, W. Baumjohann, M. Beck, T. Beck, W. Benz, N. Billot, F. Biondi, X. Bonfils, A. Brandeker, C. Broeg, T. Bárczy, J. Cabrera, S. Charnoz, C. Corral Van Damme, Sz. Csizmadia, M.B. Davies, M. Deleuil, O.D.S. Demangeon, B.-O. Demory, A. Erikson, H.G. Florén, A. Fortier, L. Fossati, M. Fridlund, D. Futyan, D. Gandolfi, M. Gillon, M. Guedel, P. Guterman, K. Heng, K.G. Isaak, L. Kiss, J. Laskar, A. Lecavelier des Etangs, M. Lendl, C. Lovis, D. Magrin, V. Nascimbeni, R. Ottensamer, I. Pagano, E. Pallé, G. Peter, G. Piotto, D. Pollacco, F.J. Pozuelos, D. Queloz, R. Ragazzoni, N. Rando, H. Rauer, C. Reimers, I. Ribas, S. Salmon, N.C. Santos, G. Scandariato, A.E. Simon, A.M.S. Smith, M. Steller, M.I. Swayne, Gy.M. Szabó, D. Ségransan, N. Thomas, S. Udry, V. Van Grootel, N.A. Walton: Analysis of early science observations with the CHaracterising ExOPlanets Satellite (CHEOPS) using PYCHEOPS, *MNRAS*, **514**, 77-104, doi, 2022.

Maxted, P.F.L., N.J. Miller, S. Hoyer, V. Adibekyan, S.G. Sousa, N. Billot, A. Fortier, A.E. Simon, A. Collier Cameron, M.I. Swayne, P. Gutermann, A.H.M.J. Triaud, J. Southworth, Y. Alibert, R. Alonso, G. Anglada, T. Barczy, D. Barrado Navascues, S.C.C. Barros, W. Baumjohann, M. Beck, T. Beck, W. Benz, X. Bonfils, A. Brandeker, C. Broeg, M. Buder, J. Cabrera, S. Charnoz, C. Corral van Damme, Sz. Csizmadia, M.B. Davies, M. Deleuil, L. Delrez, O.

Demangeon, B.-O. Demory, D. Ehrenreich, A. Erikson, L. Fossati, M. Fridlund, D. Gandolfi, M. Gillon, M. Güdel, K. Heng, J.E. Hernandez Leon, K.G. Isaak, L.L. Kiss, J. Laskar, A. Lecavelier des Etangs, M. Lendl, C. Lovis, D. Magrin, M. Munari, V. Nascimbeni, G. Olofsson, R. Ottensamer, I. Pagano, E. Palle, G. Peter, G. Piotto, D. Pollacco, D. Queloz, R. Ragazzoni, N. Rando, H. Rauer, I. Ribas, N.C. Santos, G. Scandariato, D. Segransan, A.M.S. Smith, M. Steinberger, M. Steller, Gy.M. Szabo, N. Thomas, S. Udry, V. Van Grootel, N. Walton: Fundamental effective temperature measurements for eclipsing binary stars -III. SPIRou near-infrared spectroscopy and CHEOPS photometry of the benchmark G0V star EBLM J0113 + 31, *MNRAS*, **513**, 6042-6057, doi, 2022.

Morgado, B.E., G. Bruno, A.R. Gomes-Júnior, I. Pagano, B. Sicardy, A. Fortier, J. Desmars, P.F.L. Maxted, F. Braga-Ribas, D. Queloz, S.G. Sousa, J.L. Ortiz, A. Brandeker, A. Collier Cameron, C.L. Pereira, H.G. Florén, N. Hara, D. Souami, K.G. Isaak, G. Olofsson, P. Santos-Sanz, T.G. Wilson, J. Broughton, Y. Alibert, R. Alonso, G. Anglada, T. Bárczy, D. Barrado, S.C.C. Barros, W. Baumjohann, M. Beck, T. Beck, W. Benz, N. Billot, X. Bonfils, C. Broeg, J. Cabrera, S. Charnoz, S. Csizmadia, M.B. Davies, M. Deleuil, L. Delrez, O.D.S. Demangeon, B.O. Demory, D. Ehrenreich, A. Erikson, L. Fossati, M. Fridlund, D. Gandolfi, M. Gillon, M. Güdel, K. Heng, S. Hoyer, L.L. Kiss, J. Laskar, A. Lecavelier des Etangs, M. Lendl, C. Lovis, D. Magrin, L. Marafatto, V. Nascimbeni, R. Ottensamer, E. Pallé, G. Peter, D. Piazza, G. Piotto, D. Pollacco, R. Ragazzoni, N. Rando, F. Ratti, H. Rauer, C. Reimers, I. Ribas, N.C. Santos, G. Scandariato, D. Ségransan, A.E. Simon, A.M.S. Smith, M. Steller, G.M. Szabó, N. Thomas, S. Udry, V. Van Grootel, N.A. Walton, K. Westerdorff: A stellar occultation by the transneptunian object (50000) Quaoar observed by CHEOPS, *Astron. Astrophys.*, **664**, L15, doi, 2022.

Möstl, C., A.J. Weiss, M.A. Reiss, T. Amerstorfer, R.L. Bailey, J. Hinterreiter, M. Bauer, D. Barnes, J.A. Davies, R.A. Harrison, J.L. Freiherr von Forstner, E.E. Davies, D. Heyner, T. Horbury, S.D. Bale: Multipoint Interplanetary Coronal Mass Ejections observed with Solar Orbiter, BepiColombo, Parker Solar Probe, Wind, and STEREO-A, *Astrophys. J. Lett.*, **924**, L6, doi, 2022.

Nakamura, T.K.M., K.A. Blasl, H. Hasegawa, T. Umeda, Y.-H. Liu, S.A. Perry, F. Plaschke, R. Nakamura, J.C. Holmes, J.E. Stawarz, W.D. Nystrom: Multi-scale evolution of Kelvin-Helmholtz waves at the Earth's magnetopause during southward IMF periods, *Phys. Plasmas*, **29**, 012901, doi, 2022.

Nakamura, T.K.M., K.A. Blasl, Y.-H. Liu, S.A. Peery: Diffusive plasma transport by the magnetopause Kelvin-Helmholtz instability during southward IMF, *Front. Astron. Space Sci.*, **8**, 809045, doi, 2022.

Narita, Y., K.-H. Glassmeier, U. Motschmann: The wave telescope technique, *J. Geophys. Res.*, **127**, e2021JA030165, doi, 2022.

Narita, Y., T.N. Parashar, J. Wang: The Gary picture of short-wavelength plasma turbulence - the legacy of Peter Gary, *Front. Physics*, **10**, 942167, doi, 2022.

Norgren, C., D.B. Graham, M.R. Argall, K. Steinvall, M. Hesse, Yu.V. Khotyaintsev, A. Vaivads, P. Tenfjord, D.J. Gershman, P.-A. Lindqvist, J.L. Burch, F. Plaschke: Millisecond observations of nonlinear wave-electron interaction in electron phase space holes, *Phys. Plasmas*, **29**, 012309, doi, 2022.

Oberg, N., I. Kamp, S. Cazaux, P. Woitke, W.F. Thi: Circumplanetary disk ices. I. Ice formation vs. viscous evolution and grain drift, *Astron. Astrophys.*, **667**, A95, doi, 2022.

Orsini, S., A. Milillo, H. Lichtenegger, A. Varsani, S. Barabash, S. Livi, E. De Angelis, T. Alberti, G. Laky, H. Nilsson, M. Phillips, A. Aronica, E. Kallio, P. Wurz, A. Olivieri, C. Plainaki, J.A. Slavin, I. Dandouras, J.M. Raines, J. Benkhoff, J. Zender, J.-J. Berthelier, M. Dosa, G.C. Ho, R.M. Killen, S. McKenna-Lawlor, K. Torkar, O. Vaisberg, F. Allegrini, I.A. Daglis, C. Dong, C.P. Escoubet, S. Fatemi, M. Fränz, S. Ivanovski, N. Krupp, H. Lammer, F. Leblanc, V. Mangano, A. Mura, R. Rispoli, M. Sarantos, H.T. Smith, M. Wieser, F. Camozzi, A.M. Di Lellis, G. Fremuth, F. Giner, R. Gurnee, J. Hayes, H. Jeszenszky, B. Trantham, J. Balaz, W. Baumjohann, M. Cantatore, D. Delcourt, M. Delva, M. Desai, H. Fischer, A. Galli, M. Grande, M. Holmström, I. Horvath, K.C. Hsieh, R. Jarvinen, R.E. Johnson, A. Kazakov, K. Kecskemety, H. Krüger, C. Kürbisch, F. Leblanc, M. Leichtfried, E. Mangraviti, S. Massetti, D. Moissenko, M. Moroni, R. Noschese, F. Nuccilli, N. Paschalidis, J. Ryno, K. Seki, A. Shestakov, S. Shuvalov, R. Sordini, F. Stenbeck, J. Svensson, S. Szalai, K. Szego, D. Toublanc, N. Vertolli, R. Wallner, A. Vorburger: Inner southern magnetosphere observation of Mercury via SERENA ion sensors in BepiColombo mission, *Nat. Comm.*, **13**, 7390, doi, 2022.

Osborn, H.P., A. Bonfanti, D. Gandolfi, C. Hedges, A. Leleu, A. Fortier, D. Futyan, P. Gutermann, P.F.L. Maxted, L. Borsato, K.A. Collins, J. Gomes da Silva, Y. Gómez Maqueo Chew, M.J. Hooton, M. Lendl, H. Parviainen, S. Salmon, N. Schanche, L.M. Serrano, S.G. Sousa, A. Tuson, S. Ulmer-Moll, V. Van Grootel, R.D. Wells, T.G. Wilson, Y. Alibert, R. Alonso, G. Anglada, J. Asquier, D. Barrado y. Navascues, W. Baumjohann, T. Beck, W. Benz, F. Biondi, X. Bonfils, F. Bouchy, A. Brandeker, C. Broeg, T. Bárczy, S.C.C. Barros, J. Cabrera, S. Charnoz, A. Collier Cameron, S. Csizmadia, M.B. Davies, M. Deleuil, L. Delrez, B.-O. Demory, D. Ehrenreich, A. Erikson, L. Fossati, M. Fridlund, M. Gillon, M.A. Gómez-Muñoz, M. Güdel, K. Heng, S. Hoyer, K.G. Isaak, L. Kiss, J. Laskar, A. Lecavelier des Etangs, C. Lovis, D. Magrin, L. Malavolta, J. McCormac, V. Nascimbeni, G. Olofsson, R. Ottensamer, I. Pagano, E. Pallé, G. Peter, D. Piazza, G. Piotto, D. Pollacco, D. Queloz, R. Ragazzoni, N. Rando, H. Rauer, C. Reimers, I. Ribas, O.D.S. Demangeon, A.M.S. Smith, L. Sabin, N. Santos, G. Scandariato, U. Schroffenegger, R.P. Schwarz, A. Shporer, A.E. Simon, M. Steller, G.M. Szabó, D. Ségransan, N. Thomas, S. Udry, I. Walter, N. Walton: Uncovering the true periods of the young sub-Neptunes orbiting TOI-2076, *Astron. Astrophys.*, **664**, A156, doi, 2022.

Palmerio, E., C.O. Lee, M. Leila Mays, J.G. Luhmann, D. Lario, B. Sánchez-Cano, I.G. Richardson, R. Vainio, M.L. Stevens, C.M.S. Cohen, K. Steinvall, C. Möstl, A.J. Weiss, T. Nieves-Chinchilla, Y. Li, D.E. Larson, D. Heyner, S.D.

Bale, A.B. Galvin, M. Holmström, Y.V. Khotyaintsev, M. Maksimovic, I.G. Mitrofanov: CMEs and SEPs during November-December 2020: A challenge for real-time space weather forecasting, *Space Weather*, **20**, e2021SW002993, doi, 2022.

Panov, E.V., S. Lu, P.L. Pritchett: Magnetotail ion structuring by kinetic Ballooning-Interchange instability, *Geophys. Res. Lett.*, **49**, e2021GL096796, doi, 2022.

Parviainen, H., T.G. Wilson, M. Lendl, D. Kitzmann, E. Pallé, L.M. Serrano, E. Meier Valdes, W. Benz, A. Deline, D. Ehrenreich, P. Guterman, K. Heng, O.D.S. Demangeon, A. Bonfanti, S. Salmon, V. Singh, N.C. Santos, S.G. Sousa, Y. Alibert, R. Alonso, G. Anglada, T. Bárczy, D. Barrado y. Navascues, S.C.C. Barros, W. Baumjohann, M. Beck, T. Beck, N. Billot, X. Bonfils, A. Brandeker, C. Broeg, J. Cabrera, S. Charnoz, A. Collier Cameron, C. Corral Van Damme, Sz. Csizmadia, M.B. Davies, M. Deleuil, L. Delrez, B.-O. Demory, A. Erikson, J. Farinato, A. Fortier, L. Fossati, M. Fridlund, D. Gandolfi, M. Gillon, M. Güdel, S. Hoyer, K.G. Isaak, L.L. Kiss, E. Kopp, J. Laskar, A. Lecavelier des Etangs, C. Lovis, D. Magrin, P.F.L. Maxted, M. Mecina, V. Nascimbeni, G. Olofsson, R. Ottensamer, I. Pagano, G. Peter, D. Piazza, G. Piotto, D. Pollacco, D. Queloz, R. Ragazzoni, N. Rando, H. Rauer, I. Ribas, G. Scandariato, D. Ségransan, A.E. Simon, A.M.S. Smith, M. Steller, Gy.M. Szabó, N. Thomas, S. Udry, V. Van Grootel, N.A. Walton: CHEOPS finds KELT-1b darker than expected in visible light. Discrepancy between the CHEOPS and TESS eclipse depths, *Astron. Astrophys.*, **668**, A93, doi, 2022.

Pathak, N., R.E. Ergun, Y. Qi, S.J. Schwartz, T. Vo, M.E. Usanova, M. Hesse, T.D. Phan, J.F. Drake, S. Eriksson, N. Ahmadi, A. Chasapis, F.D. Wilder, J.E. Stawarz, J.L. Burch, K.J. Genestreti, R.B. Torbert, R. Nakamura: Evidence of a nonorthogonal X-line in guide-field magnetic reconnection, *Astrophys. J. Lett.*, **941**, L34, doi, 2022.

Perrone, D., S. Perri, R. Bruno, D. Stansby, R. D'Amicis, V.K. Jagarlamudi, R. Laker, S. Toledo-Redondo, J.E. Stawarz, D. Telloni, R. De Marco, C.J. Owen, J.M. Raines, A. Settino, B. Lavraud, M. Maksimovic, A. Vaivads, T.D. Phan, N. Fargette, P. Louarn, I. Zouganelis: Evolution of coronal hole solar wind in the inner heliosphere: Combined observations by Solar Orbiter and Parker Solar Probe, *Astron. Astrophys.*, **668**, A189, doi, 2022.

Persson, M., S. Aizawa, N. André, S. Barabash, Y. Saito, Y. Harada, D. Heyner, S. Orsini, A. Fedorov, C. Mazelle, Y. Futaana, L.Z. Hadid, M. Volwerk, G. Collinson, B. Sanchez-Cano, A. Barthe, E. Penou, S. Yokota, V. Génot, J.A. Sauvaud, D. Delcourt, M. Fraenz, R. Modolo, A. Milillo, H.-U. Auster, I. Richter, J.Z.D. Mieth, P. Louarn, C.J. Owen, T.S. Horbury, K. Asamura, S. Matsuda, H. Nilsson, M. Wieser, T. Alberti, A. Varsani, V. Mangano, A. Mura, H. Lichtenegger, G. Laky, H. Jeszenszky, K. Masunaga, C. Signoles, M. Rojo, G. Murakami: BepiColombo mission confirms stagnation region of Venus and reveals its large extent, *Nat. Comm.*, **13**, 7743, doi, 2022.

Rab, Ch., M. Weber, T. Grassi, B. Ercolano, G. Picogna, P. Caselli, W.-F. Thi, I. Kamp, P. Woitke: Interpreting molecular hydrogen and atomic oxygen line emission of T Tauri disks with photoevaporative disk-wind models, *Astron. Astrophys.*, **668**, A154, doi, 2022.

Rae, J., C. Forsyth, M. Dunlop, M. Palmroth, M. Lester, R. Friedel, G. Reeves, L. Kepko, L. Turc, C. Watt, W. Hajdas, T. Sarris, Y. Saito, O. Santolik, Y. Shprits, C. Wang, A. Marchaudon, M. Berthomier, O. Marghitu, B. Hubert, M. Volwerk, E.A. Kronberg, I. Mann, K. Murphy, D. Miles, Z. Yao, A. Fazakerley, J. Sandhu, H. Allison, Q. Shi: What are the fundamental modes of energy transfer and partitioning in the coupled Magnetosphere-Ionosphere system?, *Exp. Astron.*, **54**, 391–426, doi, 2022.

Raptis, S., T. Karlsson, A. Vaivads, C. Pollock, F. Plaschke, A. Johlander, H. Trollvik, P.-A. Lindqvist: Downstream high-speed plasma jet generation as a direct consequence of shock reformation, *Nat. Comm.*, **13**, 598, doi, 2022.

Raptis, S., T. Karlsson, A. Vaivads, C. Pollock, F. Plaschke, A. Johlander, H. Trollvik, P.-A. Lindqvist: Author Correction: Downstream high-speed plasma jet generation as a direct consequence of shock reformation (Nat. Comm, 13, 598, 2022), *Nat. Comm.*, **13**, 986, doi, 2022.

Retinò, A., Y. Khotyaintsev, O. Le Contel, M.F. Marcucci, F. Plaschke, A. Vaivads, V. Angelopoulos, P. Blasi, J. Burch, J. De Keyser, M. Dunlop, L. Dai, J. Eastwood, H. Fu, S. Haaland, M. Hoshino, A. Johlander, L. Kepko, H. Kucharek, G. Lapenta, B. Lavraud, O. Malandraki, W. Matthaeus, K. McWilliams, A. Petrukovich, J.-L. Pinçon, Y. Saito, L. Sorriso-Valvo, R. Vainio, R. Wimmer-Schweingruber: Particle energization in space plasmas: Towards a multi-point, multi-scale plasma observatory, *Exp. Astron.*, **54**, 427–471, doi, 2022.

Roberts, O.W., O. Alexandrova, L. Sorriso-Valvo, Z. Vörös, R. Nakamura, D. Fischer, A. Varsani, C.P. Escoubet, M. Volwerk, P. Canu, S. Lion, K. Yearby: Scale-dependent kurtosis of magnetic field fluctuations in the solar wind: A multi-scale study with Cluster 2003-2015, *J. Geophys. Res.*, **127**, e2021JA029483, doi, 2022.

Roberts, O.W., Y. Narita, R. Nakamura, Z. Vörös, D. Verscharen: The kinetic Alfven-like nature of turbulent fluctuations in the Earth's magnetosheath: MMS measurement of the electron Alfven ratio, *Phys. Plasmas*, **29**, 012308, doi, 2022.

Rodriguez, L., D. Barnes, S. Hosteaux, J.A. Davies, S. Willems, V. Pant, R.A. Harrison, D. Berghmans, V. Bothmer, J.P. Eastwood, P.T. Gallagher, E.K.J. Kilpua, J. Magdalenic, M. Mierla, C. Möstl, A.P. Rouillard, D. Odstrčil, S. Poedts: Comparing the Heliospheric Cataloging, Analysis, and Techniques Service (HELCATS) manual and automatic catalogues of Coronal Mass Ejections using Solar Terrestrial relations Observatory/Heliospheric Imager (STEREO/HI) data, *Solar Phys.*, **297**, 23, doi, 2022.

Rojas Mata, S., G. Stenberg Wieser, Y. Futaana, A. Bader, M. Persson, A. Fedorov, T.-L. Zhang: Proton temperature anisotropies in the Venus plasma environment during solar minimum and maximum, *J. Geophys. Res.*, **127**, e2021JA029611, doi, 2022.

Rüdisser, H.T., A. Windisch, U.V. Amerstorfer, C. Möstl, T. Amerstorfer, R.L. Bailey, M.A. Reiss: Automatic detection of interplanetary coronal mass ejections in solar wind in situ data, *Space Weather*, **20**, e2022SW003149, doi, 2022.

Rumenskikh, M.S., I.F. Shaikhislamov, M.L. Khodachenko, H. Lammer, I.B. Miroshnichenko, A.G. Berezutsky, L. Fossati: Global 3D simulation of the upper atmosphere of HD189733b and absorption in metastable HeI and Lyα lines, *Astrophys. J.*, **927**, 238, doi, 2022.

Samra, D., Ch. Helling, T. Birnstiel: Mineral snowflakes on exoplanets and brown dwarfs. Coagulation and fragmentation of cloud particles with HyLandS, *Astron. Astrophys.*, **663**, A47, doi, 2022.

Scandariato, G., V. Singh, D. Kitzmann, M. Lendl, A. Brandeker, G. Bruno, A. Bekkelien, W. Benz, P. Gutermann, P.F.L. Maxted, A. Bonfanti, S. Charnoz, M. Fridlund, K. Heng, S. Hoyer, I. Pagano, C.M. Persson, S. Salmon, V. Van Grootel, T.G. Wilson, J. Asquier, M. Bergomi, L. Gambicorti, J. Hasiba, Y. Alibert, R. Alonso, G. Anglada, T. Bárczy, D. Barrado y. Navascues, S.C.C. Barros, W. Baumjohann, M. Beck, T. Beck, N. Billot, X. Bonfils, C. Broeg, J. Cabrera, A. Collier Cameron, Sz. Csizmadia, M.B. Davies, M. Deleui, A. Deline, L. Delrez, O. Demangeon, B.-O. Demory, A. Erikson, A. Fortier, L. Fossati, D. Gandolfi, M. Gillon, M. Güdel, K.G. Isaak, L.L. Kiss, J. Laskar, A. Lecavelier des Etangs, C. Lovis, D. Magrin, V. Nascimbeni, G. Olofsson, R. Ottensamer, E. Pallé, H. Parviainen, G. Peter, G. Piotto, D. Pollacco, D. Queloz, R. Ragazzoni, N. Rando, H. Rauer, I. Ribas, N.C. Santos, D. Ségransan, L.M. Serrano, A.E. Simon, A.M.S. Smith, S.G. Sousa, M. Steller, Gy.M. Szabó, N. Thomas, S. Udry, B. Ulmer, N. Walton: Phase curve and geometric albedo of WASP-43b measured with CHEOPS, TESS, and HST WFC3/UVIS, *Astron. Astrophys.*, **668**, A17, doi, 2022.

Schmid, D., H. Lammer, F. Plaschke, A. Vorburger, N.V. Erkaev, P. Wurz, Y. Narita, M. Volwerk, W. Baumjohann, B.J. Anderson: Magnetic evidence for an extended hydrogen exosphere at Mercury, *J. Geophys. Res. Planets*, **127**, e2022JE007462, doi, 2022.

Schmid, D., Y. Narita, F. Plaschke, M. Volwerk, R. Nakamura, W. Baumjohann, D. Heyner, K. Pump, S. Aizawa: Solar-wind-dependent streamline model for Mercury's magnetosheath. A hydrodynamic magnetosheath model for Mercury, *Astron. Astrophys.*, **668**, A113, doi, 2022.

Schneider, A.D., L. Carone, L. Decin, U.G. Jørgensen, Ch. Helling: No evidence for radius inflation in hot Jupiters from vertical advection of heat, *Astron. Astrophys.*, **666**, L11, doi, 2022.

Schneider, A.S., L. Carone, L. Decin, U.G. Jørgensen, P. Mollière, R. Baeyens, S. Kiefer, Ch. Helling: Exploring the deep atmospheres of HD 209458b and WASP-43b using a non-gray general circulation model, *Astron. Astrophys.*, **664**, A56, doi, 2022.

Schöfer, P., S.V. Jeffers, A. Reiners, M. Zechmeister, B. Fuhrmeister, M. Lafarga, I. Ribas, A. Quirrenbach, P.J. Amado, J.A. Caballero, G. Anglada-Escudé, F.F. Bauer, V.J.S. Béjar, M. Cortés.-Contreras, E. Díez Alonso, S. Dreizler, E.W. Guenther, O. Herbort, E.N. Johnson, A. Kaminski, M. Kürster, D. Montes, J.C. Morales, S. Pedraz, L. Tal-Or: The CARMENES search for exoplanets around M dwarfs. Rotational variation in activity indicators of Ross 318, YZ CMi, TYC 3529-1437-1, and EV Lac, *Astron. Astrophys.*, **663**, A68, doi, 2022.

Serrano, L.M., D. Gandolfi, S. Hoyer, A. Brandeker, M.J. Hooton, S. Sousa, F. Murgas, D.R. Ciardi, S.B. Howell, W. Benz, N. Billot, H.-G. Florén, A. Bekkelien, A. Bonfanti, A. Krenn, A.J. Mustill, T.G. Wilson, H. Osborn, H. Parviainen, N. Heidari, E. Pallé, M. Fridlund, V. Adibekyan, L. Fossati, M. Deleuil, E. Knudstrup, K.A. Collins, K.W.F. Lam, S. Grziwa, S. Salmon, S.H. Albrecht, Y. Alibert, R. Alonso, G. Anglada-Escudé, T. Bárczy, D. Barrado y. Navascues, S.C.C. Barros, W. Baumjohann, M. Beck, T. Beck, A. Bieryla, X. Bonfils, P.T. Boyd, C. Broeg, J. Cabrera, S. Charnoz, B. Chazelas, J.L. Christiansen, A. Collier Cameron, P. Cortés.-Zuleta, Sz. Csizmadia, M.B. Davies, A. Deline, L. Delrez, O.D.S. Demangeon, B.-O. Demory, A. Dunlavey, D. Ehrenreich, A. Erikson, A. Fortier, A. Fukui, Z. Garai, M. Gillon, M. Güdel, G. Hébrard, K. Heng, C.X. Huang, K.G. Isaak, J.M. Jenkins, L.L. Kiss, J. Laskar, D.W. Latham, A. Lecavelier des Etangs, M. Lendl, A.M. Levine, C. Lovis, M.B. Lund, D. Magrin, P.F.L. Maxted, N. Narita, V. Nascimbeni, G. Olofsson, R. Ottensamer, I. Pagano, A.C.S.V. Pessanha, G. Peter, G. Piotto, D. Pollacco, D. Queloz, R. Ragazzoni, N. Rando, F. Ratti, H. Rauer, I. Ribas, G. Ricker, P. Rowden, N.C. Santos, G. Scandariato, S. Seager, D. Ségransan, A.E. Simon, A.M.S. Smith, M. Steller, Gy.M. Szabó, N. Thomas, J.D. Twicken, S. Udry, B. Ulmer, V. Van Grootel, R. Vanderspek, V. Viotto, N. Walton: The HD93963A transiting system: A 1.04 d super-Earth and a 3.65 d sub-Neptune discovered by TESS and CHEOPS, *Astron. Astrophys.*, **667**, A1, doi, 2022.

Shergelashvili, B.M., E. Philishvili, S. Buitendag, S. Poedts, M.L. Khodachenko: Categorization model of moving small-scale intensity enhancements in solar active regions, *Astron. Astrophys.*, **662**, A30, doi, 2022.

Simola, U., A. Bonfanti, X. Dumusque, J. Cisewski-Kehe, S. Kaski, J. Corander: Accounting for stellar activity signals in radial-velocity data by using change point detection techniques, *Astron. Astrophys.*, **664**, A127, doi, 2022.

Simon Wedlund, C., M. Volwerk, A. Beth, C. Mazelle, C. Möstl, J. Halekas, J.R. Gruesbeck, D. Rojas-Castillo: A fast bow shock location predictor-estimator from 2D and 3D analytical models: Application to Mars and the MAVEN mission, *J. Geophys. Res.*, **127**, e2021JA029942, doi, 2022.

Simon Wedlund, C., M. Volwerk, C. Mazelle, J. Halekas, D. Rojas-Castillo, J. Espley, C. Möstl: Making waves: Mirror mode structures around Mars observed by the MAVEN spacecraft, *J. Geophys. Res.*, **127**, e2021JA029811, doi, 2022.

Sindel, J.P., D. Gobrecht, Ch. Helling, L. Decin: Revisiting fundamental properties of TiO2 nanoclusters as condensation seeds in astrophysical environments, *Astron. Astrophys.*, **668**, A35, doi, 2022.

Singh, V., A.S. Bonomo, G. Scandariato, N. Cibrario, D. Barbato, L. Fossati, I. Pagano, A. Sozzetti: Probing Kepler's hottest small planets via homogeneous search and analysis of optical secondary eclipses and phase variations, *Astron. Astrophys.*, **658**, A132, doi, 2022.

Southworth, J., A.J. Barker, T.C. Hinse, Y. Jongen, M. Dominik, U.G. Jørgensen, P. Longa-Peña, S. Sajadian, C. Snodgrass, J. Tregloan-Reed, N. Bach-Moeller, M. Bonavita, V. Bozza, M.J. Burgdorf, R. Figuera Jaimes, Ch. Helling, J.A. Hitchcock, M. Hundertmark, E. Khalouei, H. Korhonen, L. Mancini, N. Peixinho, S. Rahvar, M. Rabus, J. Skottfelt, P. Spyratos: A search for transit timing variations in the HATS-18 planetary system, *MNRAS*, **515**, 3212-3223, doi, 2022.

Sreejith, A.G., L. Fossati, S. Ambily, A. Egan, N. Nell, K. France, B.T. Fleming, S. Haas, M. Chambliss, N. DeCicco, M. Steller: The autonomous data reduction pipeline for the Cute mission, *Publ. Astron. Soc. Pac.*, **134**, 114506, doi, 2022.

Stepanova, M., J.E. Borovsky, A. Retino, V. Uritsky, Z. Vörös, G. Zimbardo: Editorial: The role of turbulence in the solar wind, magnetosphere, ionosphere dynamics, *Front. Astron. Space Sci.*, **8**, 763190, doi, 2022.

Strugarek, A., R. Fares, V. Bourrier, A.S. Brun, V. Réville, T. Amari, Ch. Helling, M. Jardine, J. Llama, C. Moutou, A.A. Vidotto, P.J. Wheatley, P. Zarka: MOVES - V. Modelling star-planet magnetic interactions of HD 189733, *MNRAS*, **512**, 4556-4572, doi, 2022.

Sun, J., G. Wang, T.-L. Zhang, H. Hu, H. Yang: Evidence of Alfvén waves generated by mode coupling in the magnetotail lobe, *Geophys. Res. Lett.*, **49**, e2021GL096359, doi, 2022.

Sun, W., D.L. Turner, Q. Zhang, S. Wang, J. Egedal, T. Leonard, J.A. Slavin, Q. Hu, I.J. Cohen, K. Genestreti, G. Poh, D.J. Gershman, A. Smith, G. Le, R. Nakamura, B.L. Giles, R.E. Ergun, J.L. Burch: Properties and acceleration mechanisms of electrons up to 200 keV associated with a flux rope pair and reconnection X-lines around it in Earth's plasma sheet, *J. Geophys. Res.*, **127**, e2022JA030721, doi, 2022.

Sun, W., J.A. Slavin, R. Nakamura, D. Heyner, K.J. Trattner, J.Z.D. Mieth, J. Zhao, Q.-G. Zong, S. Aizawa, N. Andre, Y. Saito: Dayside magnetopause reconnection and flux transfer events under radial Interplanetary Magnetic Field (IMF): BepiColombo Earth-flyby observations, *Ann. Geophys.*, **40**, 217-229, doi, 2022.

Szabó, Gy.M., Z. Garai1, A. Brandeker, D. Gandolfi, T.G. Wilson, A. Deline, G. Olofsson, A. Fortier, D. Queloz, L. Borsato, F. Kiefer, A. Lecavelier des Etangs, M. Lendl, L.M. Serrano, S. Sulis, S. Ulmer Moll, V. Van Grootel, Y. Alibert, R. Alonso, G. Anglada, T. Bárczy, D. Barrado y Navascues, S.C.C. Barros, W. Baumjohann, M. Beck, T. Beck, W. Benz, N. Billot, A. Bonfanti, X. Bonfils, C. Broeg, J. Cabrera, S. Charnoz, A. Collier Cameron, Sz. Csizmadia, M.B. Davies, M. Deleuil, L. Delrez, O. Demangeon, B.-O. Demory, D. Ehrenreich, A. Erikson, L. Fossati, M. Fridlund, M. Gillon, M. Güdel, K. Heng, S. Hoyer, K.G. Isaak, L.L. Kiss, J. Laskar, C. Lovis, D. Magrin, P.F.L. Maxted, M. Mecina, V. Nascimbeni, R. Ottensamer, I. Pagano, E. Pallé, G. Peter, G. Piotto, D. Pollacco, R. Ragazzoni, N. Rando, H. Rauer, I. Ribas, N.C. Santos, M. Sarajlic, G. Scandariato, D. Ségransan, A.E. Simon, A.M.S. Smith, S.G. Sousa, M. Steller, N. Thomas, S. Udry, F. Verrecchia, N. Walton, D. Wolter: Transit timing variations of AU Microscopii b and c, *Astron. Astrophys.*, **659**, L7, doi, 2022.

Tayar, J., F.D. Moyano, M. Soares-Furtado, A. Escorza, M. Joyce, S.L. Martell, R.A. García, S.N. Breton, S. Mathis, S. Mathur, V. Delsanti, S. Kiefer, S. Reffert, D.M. Bowman, T. Van Reeth, S. Shetye, C. Gehan, S.K. Grunblatt: Spinning up the surface: Evidence for planetary engulfment or unexpected angular momentum transport?, *Astrophys. J.*, **940**, 23, doi, 2022.

Telloni, D., L. Adhikari, G.P. Zank, L.Z. Hadid, B. Sánchez-Cano, L. Sorriso-Valvo, L. Zhao, O. Panasenco, C. Shi, M. Velli, R. Susino, D. Verscharen, A. Milillo, T. Alberti, Y. Narita, A. Verdini, C. Grimani, R. Bruno, R. D'Amicis, D. Perrone, R. Marino, F. Carbone, F. Califano, F. Malara, J.E. Stawarz, R. Laker, A. Liberatore, S.D. Bale, J.C. Kasper, D. Heyner, T. Dudok de Wit, K. Goetz, P.R. Harvey, R.J. MacDowall, D.M. Malaspina, M. Pulupa, A.W. Case, K.E. Korreck, D. Larson, R. Livi, M.L. Stevens, P. Whittlesey, H.-U. Auster, I. Richter: Observation and modeling of the solar wind turbulence evolution in the sub-Mercury inner heliosphere, *Astrophys. J. Lett.*, **938**, L8, doi, 2022.

Telloni, D., Z. Vörös, E. Yordanova, R. D'Amicis: Editorial: Magnetic connectivity of the Earth and planetary environments to the Sun in space weather studies, *Front. Astron. Space Sci.*, **9**, 853925, doi, 2022.

Tinoco-Arenas, A., P. Kajdič, L. Preisser, X. Blanco-Cano, D. Trotta, D. Burgess: Parametric study of magnetosheath jets in 2D local hybrid simulations, *Front. Astron. Space Sci.*, **9**, 793195, doi, 2022.

Toepfer, S., I. Oertel, V. Schiron, Y. Narita, K.-H. Glassmeier, D. Heyner, P. Kolhey, U. Motschmann: Reconstruction of Mercury's internal magnetic field beyond the octupole, *Ann. Geophys.*, **40**, 91-105, doi, 2022.

Toepfer, S., Y. Narita, D. Schmid: Reconstruction of the interplanetary magnetic field from the magnetosheath data: A steady-state approach, *Front. Physics*, **10**, 1050859, doi, 2022.

Tsinamdzgvrishvili, T., B.B. Chargeishvili, B.M. Shergelashvili, I. Mghebrishvili: Spatio-temporal bands of coronal bright points and their relation to solar torsional oscillations, *MNRAS*, **509**, 3717-3723, doi, 2022.

Turc, L., K. Takahashi, J.K. Sandhu, M. Volwerk: Editorial: Sources and propagation of ultra-low frequency waves in planetary magnetospheres, *Front. Astron. Space Sci.*, **9**, 1092266, doi, 2022.

Verscharen, D., R.T. Wicks, O. Alexandrova, R. Bruno, D. Burgess, C.H.K. Chen, R. D'Amicis, J. De Keyser, T.D. de Wit, L. Franci, J. He, P. Henri, S. Kasahara, Y. Khotyaintsev, K.G. Klein, B. Lavraud, B.A. Maruca, M. Maksimovic, F. Plaschke, S. Poedts, C.S. Reynolds, O. Roberts, F. Sahraoui, S. Saito, C.S. Salem, J. Saur, S. Servidio, J.E. Stawarz, Š. Štverák, D. Told: A case for electron-astrophysics, *Exp. Astron.*, **54**, 473–519, doi, 2022.

Wang, G.Q., M. Volwerk, S.D. Xiao, M.Y. Wu, Y.Q. Chen, T.L. Zhang: Electron-scale current sheet as the boundary of a linear magnetic hole in the terrestrial current sheet observed by the Magnetospheric Multiscale mission, *J. Geophys. Res.*, **127**, e2021JA029707, doi, 2022.

Wang, L., C. Huang, Y. Ge, A. Du, R. Wang, T.-L. Zhang, G. Chen, J. Fan: Heavy ion escape from Martian wake enhanced by magnetic reconnection, *J. Geophys. Res. Planets*, **127**, e2022JE007181, doi, 2022.

Wang, W., J. Yang, F.R. Toffoletto, R.A. Wolf, R. Nakamura, J. Cui: Current sheet thinning in the wake of a bubble injection, *Geophys. Res. Lett.*, **49**, e2022GL100737, doi, 2022.

Weiss, A.J., T. Nieves-Chinchilla, C. Möstl, M.A. Reiss, T. Amerstorfer, R.L. Bailey: Writhed analytical magnetic flux rope model, *J. Geophys. Res.*, **127**, e2022JA030898, doi, 2022.

Wilson, T.G., E. Goffo, Y. Alibert, D. Gandolfi, A. Bonfanti, C.M. Persson, A. Collier Cameron, M. Fridlund, L. Fossati, J. Korth, W. Benz, A. Deline, H.-G. Floren, P. Guterman, V. Adibekyan, M.J. Hooton, S. Hoyer, A. Leleu, A.J. Mustill, S. Salmon, S.G. Sousa, O. Suarez, L. Abe, A. Agabi, R. Alonso, G. Anglada, J. Asquier, T. Barczy, D. Barrado Navascues, S.C.C. Barros, W. Baumjohann, M. Beck, T. Beck, N. Billot, X. Bonfils, A. Brandeker, C. Broeg, E.M. Bryant, M.R. Burleigh, M. Buttu, J. Cabrera, S. Charnoz, D.R. Ciardi, R. Cloutier, W.D. Cochran, K.A. Collins, K.D. Colon, N. Crouzet, S. Csizmadia, M.B. Davies, M. Deleuil, L. Delrez, O. Demangeon, B.-O. Demory, D. Dragomir, G. Dransfield, D. Ehrenreich, A. Erikson, A. Fortier, T. Gan, S. Gill, M. Gillon, C.L. Gnilka, N. Grieves, S. Grziwa, M. Güdel, T. Guillot, J. Haldemann, K. Heng, K. Horne, S.B. Howell, K.G. Isaak, J.M. Jenkins, E.L.N. Jensen, L. Kiss, G. Lacedelli, K. Lam, J. Laskar, D.W. Latham, A. Lecavelier des Etangs, M. Lendl, K.V. Lester, A.M. Levine, J. Livingston, C. Lovis, R. Luque, D. Magrin, W. Marie-Sainte, P.F.L. Maxted, A.W. Mayo, B. McLean, M. Mecina, D. Mekarnia, V. Nascimbeni, L.D. Nielsen, G. Olofsson, H.P. Osborn, H.L.M. Osborne, R. Ottensamer, I. Pagano, E. Palle, G. Peter, G. Piotto, D. Pollacco, D. Queloz, R. Ragazzoni, N. Rando, H. Rauer, S. Redfield, I. Ribas, G.R. Ricker, M. Rieder, N.C. Santos, G. Scandariato, F.-X. Schmider, R.P. Schwarz, N.J. Scott, S. Seager, D. Segransan, L.M. Serrano, A.E. Simon, A.M.S. Smith, M. Steller, C. Stockdale, G. Szabo, N. Thomas, E.B. Ting, A.H.M.J. Triaud, S. Udry, V. Van Eylen, V. Van Grootel, R.K. Vanderspek, V. Viotto, N. Walton, J.N. Winn: A pair of sub-Neptunes transiting the bright K-dwarf TOI-1064 characterized with CHEOPS, *MNRAS*, **511**, 1043-1071, doi, 2022.

Woitke, P., A.M. Arabhavi, I. Kamp, W.-F. Thi: Mixing and diffusion in protoplanetary disc chemistry, *Astron. Astrophys.*, **668**, A164, doi, 2022.

Wu, S., P. Zarka, L. Lamy, U. Taubenschuss, B. Cecconi, S. Ye, G. Fischer, W.S. Kurth, T. Francez: Observations of the first harmonic of Saturn Kilometric Radiation during Cassini's Grand Finale, *J. Geophys. Res.*, **127**, e2022JA030776, doi, 2022.

Wu, S.Y., S.Y. Ye, G. Fischer, C.M. Jackman, J. Wang, J.D. Menietti, B. Cecconi, M.Y. Long: Reflection and refraction of the L-O mode 5 kHz Saturn narrowband emission by the magnetosheath, *Geophys. Res. Lett.*, **49**, e2021GL096990, doi, 2022.

Wu, S.Y., S.Y. Ye, G. Fischer, U. Taubenschuss, C.M. Jackman, E. O'Dwyer, W.S. Kurth, S. Yao, Z.H. Yao, J.D. Menietti, Y. Xu, M.Y. Long, B. Cecconi: Saturn anomalous myriametric radiation, a new type of Saturn radio emission revealed by Cassini, *Geophys. Res. Lett.*, **49**, e2022GL099237, doi, 2022.

Wurz, P., S. Fatemi, A. Galli, J. Halekas, Y. Harada, N. Jäggi, J. Jasinski, H. Lammer, S. Lindsay, M.N. Nishino, T.M. Orlando, J.M. Raines, M. Scherf, J. Slavin, A. Vorburger, R.Winslow: Particles and photons as drivers for particle release from the surfaces of the Moon and Mercury, *Space Sci. Rev.*, **218**, 10, doi, 2022.

Xu, Y.-B., L. Zhou, C. Lhotka, L.-Y. Zhou, W.-H. Ip: Trojan asteroids and the co-orbital dust ring of Venus, *Astron. Astrophys.*, **666**, A88, doi, 2022.

Zhang, L.Q., C. Wang, L. Dai, W. Baumjohann, A.T.Y. Lui, J.L. Burch, Yu.V. Khotyaintsev, Y. Ren: Vorticity within bursty bulk flows: Convective versus kinetic, *J. Geophys. Res.*, **127**, e2020JA028934, doi, 2022.

Zhang, L.Q., C. Wang, L. Dai, W. Baumjohann, J.L. Burch, Yu.V. Khotyaintsev, J.Y. Wang: Turbulent current sheet frozen in bursty bulk flow: Observation and model, *Sci. Rep.*, **12**, 15547, doi, 2022.

Zhang, M., H.A. Knutson, L. Wang, F. Dai, L.A. dos Santos, L. Fossati, G.W. Henry, D. Ehrenreich, Y. Alibert, S. Hoyer, T.G. Wilson, A. Bonfanti: Detection of ongoing mass loss from HD 63433c, a young mini-Neptune, *Astron. J.*, **163**, 68, doi, 2022.

BOOKS

Baumjohann, W., R. Treumann: Basic Space Plasma Physics, 3rd Edition, World Scientific, Singapore, 530 pages, 2022.

Forget, F., O. Korablev, J. Venturini, T. Imamura, H. Lammer, M. Blanc (Eds.): Understanding the Diversity of Planetary Atmospheres, Springer, Berlin, 591 pages, 2022.

PROCEEDINGS & BOOK CHAPTERS

Cosentino, R., M. Focardi, E. Galli, M. Steller, C. Del Vecchio Blanco, S. Pezzuto, G. Giusi, A.M. Di Giorgio, D. Biondi, H. Jeszenszky, H. Ottacher, G. Laky, L. Serafini, D. Loidolt, R. Ottensamer, A. Russi, M. Vela Nuñez, A. Luntzer, F. KerschbaumAuthor Affiliations +: PLATO: The status of the instrument control unit following its critical design review. In: *Proc. SPIE 12180, Space Telescopes and Instrumentation 2022: Optical, Infrared, and Millimeter Wave*, Eds. Coyle, L.E., S. Matsuura, M.D. Perrin, SPIE, Bellingham WA, USA, 121801B, doi, 2022.

de Andres Tirado, A., M. Viturro Balufo, J. Carro, V. Morand, M. Steindorfer, G. Kirchner: An advanced tool to determine the apparent rotation period of a space object from a fusion of measurements. In: *73rd International Astronautical Congress, Paris, 18-22 September 2022*, Ed. International Astronautical Federation, International Astronautical Federation, Paris, 10 p., 2022.

Liu, Y.J., Z. Hatab, E. Leitgeb, P.Y. Wang: Experimental coupling loss analysis of free space optical link under different weather conditions. In: *Proceedings, 4th International Conference on Broadband Communications for Next Generation Networks and Multimedia Applications (CoBCom)*, Eds. Leitgeb, E., W, Gappmair, F. Tesch, IEEE, Piscataway, NJ, 4 pp., doi, 2022.

Scherzer, M., M. Auer: A digitally-controlled fully differential low noise current source. In: *2022 IEEE International Symposium on Circuits and Systems (ISCAS)*, IEEE, Piscataway, NJ, 4 pp., doi, 2022.

Scherzer, M., M. Auer, A. Valavanoglou, W. Magnes: Implementation of a fully differential low noise current source for fluxgate sensors. In: *2022 IEEE 13th Latin America Symposium on Circuits and System (LASCAS)*, IEEE, Piscataway, NJ, 4 pp., doi, 2022.

Shi, J.K., Z. Wang, Z.W. Cheng, M.N.S. Qureshi, K. Torkar: A theoretical model for nonlinear waves observed in space plasmas. In: *Proceedings 2022 Photonics & Electromagnetics Research Symposium (PIERS)*, Ed. IEEE, IEEE, Piscataway, NJ, 718-724, doi, 2022.

Steindorfer, M., F. Koidl, S. Schneider, P. Wang, C. Jonglez, M. Barschke, T. Soares, E. Padilla Gutierrez, A. Cipriano: Reflector-based attitude detection system. In: *73rd International Astronautical Congress, Paris, 18-22 September 2022*, Ed. International Astronautical Federation, International Astronautical Federation, Paris, 6 p., 2022.

PERSONNEL

Agú, Martín A., Dipl.-Ing.
Bach-Møller, Nanna, MSc
Balduin, Thorsten, MSc
Bangera, Nidhi R., Msc
Barth, Patrick, MSc
Berghofer, Gerhard, Ing.
Besser, Bruno P., Dr.
Betzler Alexander-Pieter, Dipl.-Ing.
Blasl, Kevin-Alexander, MSc
Bonfanti, Andrea, Dr.
Boudjada, Mohammed Y., Dr.
Carone, Ludmila, Dr.
Delva, Magda, Dr.
Eichelberger, Hans U., Dr.
Fabian, Peter
Fauland, Daniel, Ing.
Fischer, David, Dipl.-Ing.
Fischer, Georg, Dr.
Fleck, Nina, BSc
Flock, Barbara, Mag.
Fossati, Luca, Doz.
Fremuth, Gerhard, Dipl.-Ing.
Giner, Franz, Dipl.-Ing.
Graf, Christian, Ing.
Gratzer, Alexander J.
Grill, Claudia
Hasiba, Johann, Dipl.-Ing.
Helling, Christiane, Prof. Dr.
Höck, Eduard, Dipl.-Ing.
Hofmann, Karl, Dipl.-Ing.
Hosner, Martin, MSc
Hradecky, Doris
Jernej, Irmgard, Ing.
Jeszenszky, Harald, Dipl.-Ing.
Kadam, Kundan V., Dr.
Kargl, Günter, Dr.
Käufer, Till F., MSc
Khodachenko, Maxim L., Dr.
Koidl, Franz, Ing.
Krenn, Andreas F., MSc
Kubyshkina, Daria, Dr.
Kürbisch, Christoph, Ing.
Laky, Gunter, Dipl.-Ing.
Lammer, Helmut, Doz.
Lecoq Molinos, Helena, MSc
Leichtfried, Mario, Ing.
Lentz, Constant M. F., Dipl.-Ing.
Lewis, David A., MSc
Macher, Wolfgang, Dr.
Magnes, Werner, Dr.
Muck, Cosima
Nakamura, Rumi, Doz.
Narita, Yasuhito, Doz.
Neukirchner, Sonja, Ing.
Nischelwitzer-Fennes, Ute, Ing.
Ottacher, Harald, Dipl.-Ing.
Panov, Evgeny, Dr.
Pitterle, Martin
Pollinger, Andreas, Dr.
Posch, Oliver F.
Preisser Renteria, Luis F., Dr.
Reisinger, Nadja, BSc
Roberts, Owen W., Dr.
Samra, Dominic B. S., Dr.
Scherf, Manuel, Dr.
Scherr, Alexandra, Mag.
Schmid, Daniel, Dr.
Schneider, Sebastian, BSc
Settino, Adriana, Dr.
Simon Wedlund, Cyril Laurent, Dr.
Sindel, Jan P., Dr.
Stachel, Manfred, Dipl.-Ing.
Steinberger, Michael, Dipl.-Ing.
Steindorfer, Michael, Dr.
Steller, Manfred B., Dr.
Stieninger, Reinhard, Ing.
Suslina, Elena, MSc
Taubner, Ruth-Sophie, Dr.
Teubenbacher, Daniel, Dipl.-Ing.
Tonfat Seclen, Jorge L., Dr.
Trummer, Nadine M., BSc
Tschachler, Elvira, Mag.
Valavanoglou, Aris, Dipl.-Ing.
Varsani, Ali, Dr.
Voller, Wolfgang G., Mag.
Volwerk, Martin, Dr.
Vörös, Zoltan, Dr.
Wallner, Robert, Ing.
Wang, Peiyuan, MSc
Weichbold, Fabian, BSc
Wilfinger, Josef, BSc
Woitke, Peter, Dr.
Zhang, Tie-Long, Prof.
Zivithal, Stephan, BSc

As of 31 December 2022

IMPRESSUM

PUBLISHER

Prof. Dr. Christiane Helling, Director
Institut für Weltraumforschung (IWF)
Österreichische Akademie der Wissenschaften (OeAW)
Schmiedlstraße 6, 8042 Graz, Austria
www.oeaw.ac.at/iwf
Twitter: @IWF_oeaw

EDITORS

Bruno Besser, Alexandra Scherr, Martin Volwerk

DESIGN

Alexandra Scherr
pr.iwf@oeaw.ac.at

PRINT

Servicebetrieb ÖH-Uni Graz GmbH